Radiation Pressure Acceleration of Ions and the Role of Hydrodynamical Breaking

Andrea Macchi

www.df.unipi.it/∼macchi

polyLAB, CNR-INFM, University of Pisa and INFN, Italy

PHELIX Theory Workshop, Darmstadt, October 15, 2007

Coworkers

Coworkers

Alessandra Bigongiari, Francesco Ceccherini, Fulvio Cornolti,Tatiana V. Liseikina[1], Domenico Prellino

Department of Physics, University of Pisa, Italy

Coworkers

Alessandra Bigongiari, Francesco Ceccherini, Fulvio Cornolti, Tatiana V. Liseikina[1], Domenico Prellino

Department of Physics, University of Pisa, Italy

[1]*On leave from Institute for Computational Technologies, Novosibirsk, Russia*

Coworkers

Alessandra Bigongiari, Francesco Ceccherini, Fulvio Cornolti,Tatiana V. Liseikina[1], Domenico Prellino

Department of Physics, University of Pisa, Italy

[1]*On leave from Institute for Computational Technologies, Novosibirsk, Russia*

Marco Borghesi and Satyabrata Kar

IRCEP and School of Mathematics and Physics, Queen's University of Belfast, UK

Outlook

- We consider two cases of ion acceleration driven by the steady ponderomotive force (i.e. by radiation pressure):

Outlook

- We consider two cases of ion acceleration driven by the steady ponderomotive force (i.e. by radiation pressure):

1. Radial acceleration after self-channeling in underdense plasma ($\omega_p < \omega$)

   S. Kar, M. Borghesi, C. Cecchetti, F. Ceccherini, T. V. Liseikina, A. Macchi et al, arXiv:physics/0701332, New J. Phys. (in press)

   A.Macchi, F.Ceccherini, F.Cornolti, S.Kar, M.Borghesi, arXiv:physics/0701139

Outlook

- We consider two cases of ion acceleration driven by the steady ponderomotive force (i.e. by radiation pressure):

1. Radial acceleration after self-channeling in underdense plasma ($\omega_p < \omega$)
   S. Kar, M. Borghesi, C. Cecchetti, F. Ceccherini, T. V. Liseikina, A. Macchi et al, arXiv:physics/0701332, New J. Phys. (in press)
   A.Macchi, F.Ceccherini, F.Cornolti, S.Kar, M.Borghesi, arXiv:physics/0701139
2. Longitudinal acceleration by circularly polarized pulses in overdense plasma ($\omega_p < \omega$)
   A. Macchi, F. Cattani, T. V. Liseikina, F. Cornolti, Phys. Rev. Lett. **94**, 165003 (2005);
   T. V. Liseikina and A. Macchi, arXiv:0705.4019, Appl. Phys. Lett. (in press).

Outlook

- We consider two cases of ion acceleration driven by the steady ponderomotive force (i.e. by radiation pressure):

1. Radial acceleration after self-channeling in underdense plasma ($\omega_p < \omega$)
   S. Kar, M. Borghesi, C. Cecchetti, F. Ceccherini, T. V. Liseikina, A. Macchi et al, arXiv:physics/0701332, New J. Phys. (in press)

   A.Macchi, F.Ceccherini, F.Cornolti, S.Kar, M.Borghesi, arXiv:physics/0701139
2. Longitudinal acceleration by circularly polarized pulses in overdense plasma ($\omega_p < \omega$)
   A. Macchi, F. Cattani, T. V. Liseikina, F. Cornolti, Phys. Rev. Lett. **94**, 165003 (2005);

   T. V. Liseikina and A. Macchi, arXiv:0705.4019, Appl. Phys. Lett. (in press).

- We emphasize similiarities in the physical mechanisms of ion acceleration, in particular the role of hydrodynamical “breaking” in the ion fluid.

PART 1: RADIAL ION ACCELERATION AFTER SELF-CHANNELING IN AN UNDERDENSE PLASMA

Channeling in underdense plasma

Channeling in underdense plasma

The interaction of a 1 ps, $10^{18} \div 10^{19}$ W/cm^2 pulse with a gas jet has been investigated at RAL using the proton imaging technique

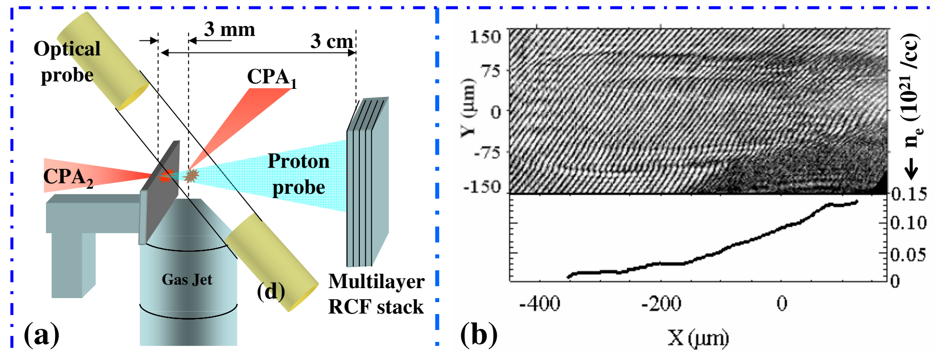

S.Kar et al, NJP, in press [arxiv:physics/0701332]

Channeling in underdense plasma

The interaction of a 1 ps, $10^{18} \div 10^{19}$ W/cm^2 pulse with a gas jet has been investigated at RAL using the proton imaging technique

Experimental data show that a charge-displacement channel is produced by the laser pulse

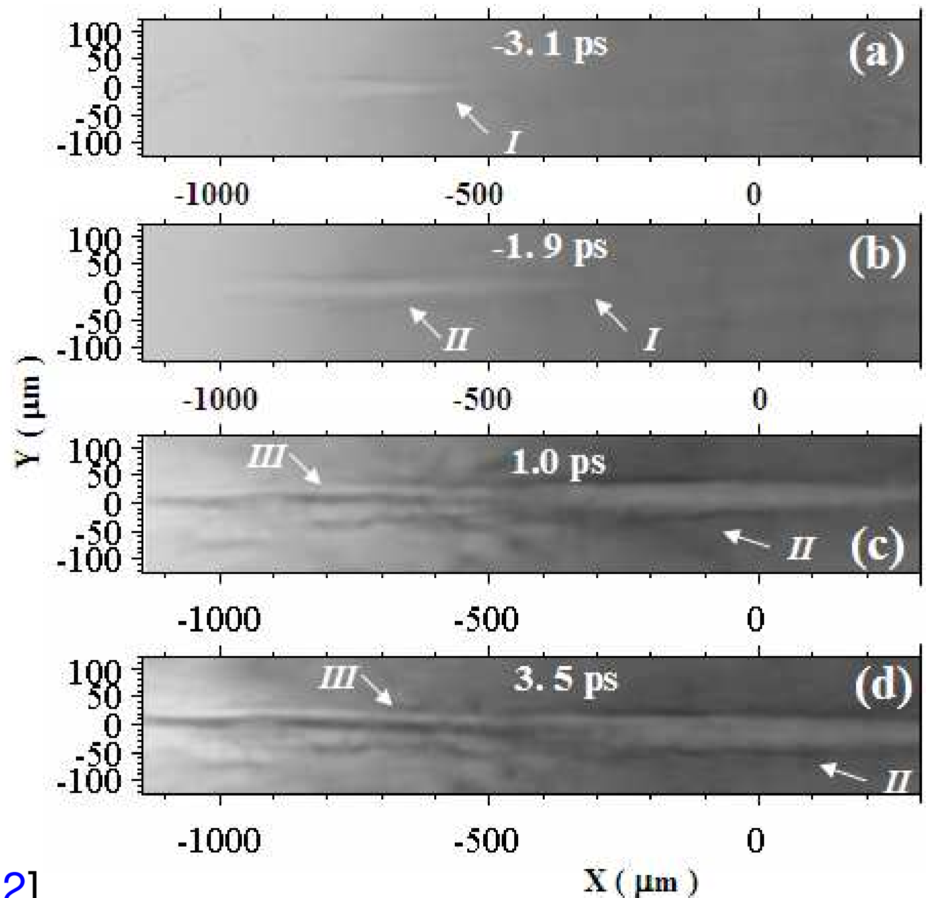

S.Kar et al, NJP, in press [arxiv:physics/0701332]

Channeling in underdense plasma

The interaction of a 1 ps, $10^{18} \div 10^{19}$ W/cm^2 pulse with a gas jet has been investigated at RAL using the proton imaging technique

Experimental data show that a charge-displacement channel is produced by the laser pulse

In the trail of the channel a reversal of the radial field is inferred

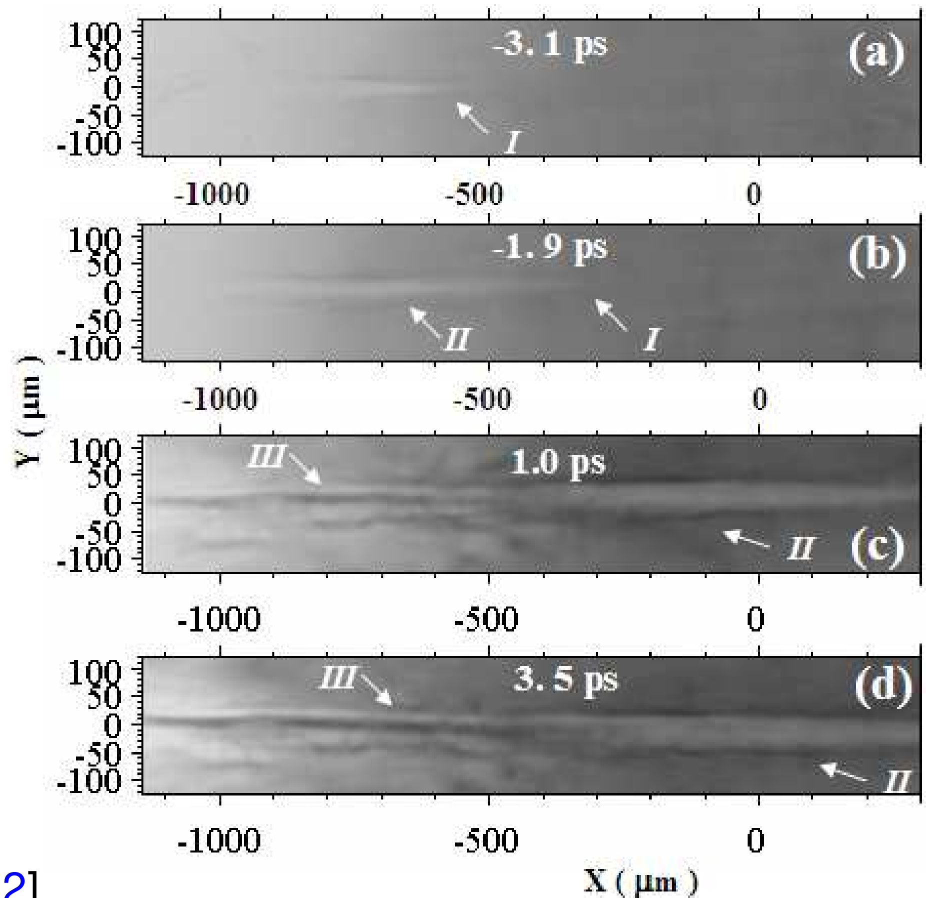

S.Kar et al, NJP, in press [arxiv:physics/0701332]

Simulations of the experiment

Simulations of the experiment

Particle-in-Cell (PIC) simulations in 2D cartesian geometry

Simulations of the experiment

Particle-in-Cell (PIC) simulations in 2D cartesian geometry

Laser amplitude $a_L = 1.7 \div 2.7$
duration $\tau_L = 150 \div 300 T_L$ ($T_L = \lambda/c$)
$\Rightarrow \; I = 10^{18} \div 10^{19}$ W/cm^2,
$\tau_L = 0.5 \div 1$ ps for $\lambda = 1 \; \mu$m.
S-polarization (E_z)

Simulations of the experiment

Particle-in-Cell (PIC) simulations in 2D cartesian geometry

Laser amplitude $a_L = 1.7 \div 2.7$
duration $\tau_L = 150 \div 300 T_L$ $\quad (T_L = \lambda/c)$
$\Rightarrow \; I = 10^{18} \div 10^{19}$ W/cm^2,
$\tau_L = 0.5 \div 1$ ps for $\lambda = 1\ \mu$m.
S-polarization (E_z)

Inhomogenous plasma
Peak density $n_e = 0.1 n_c$
Size $S = 500\ \lambda$
Scalelength $L = 400\ \lambda$

Simulations of the experiment

Particle-in-Cell (PIC) simulations in 2D cartesian geometry

Laser amplitude $a_L = 1.7 \div 2.7$
duration $\tau_L = 150 \div 300 T_L$ $\qquad (T_L = \lambda/c)$
$\Rightarrow \; I = 10^{18} \div 10^{19}$ W/cm^2,
$\tau_L = 0.5 \div 1$ ps for $\lambda = 1\ \mu$m.
S-polarization (E_z)

Inhomogenous plasma
Peak density $n_e = 0.1 n_c$
Size $S = 500\ \lambda$
Scalelength $L = 400\ \lambda$

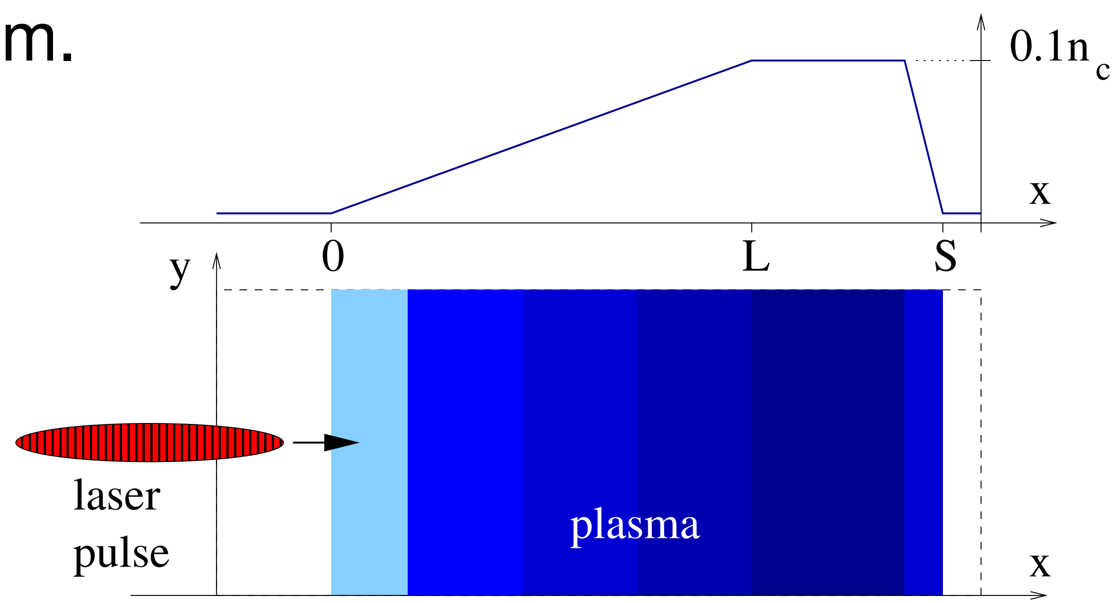

Self-channeling and radial field evolution

Self-channeling and radial field evolution

2D PIC simulations show that the laser pulse drills a regular charge-displacement channel in the low-density region

Self-channeling and radial field evolution

2D PIC simulations show that the laser pulse drills a regular charge-displacement channel in the low-density region

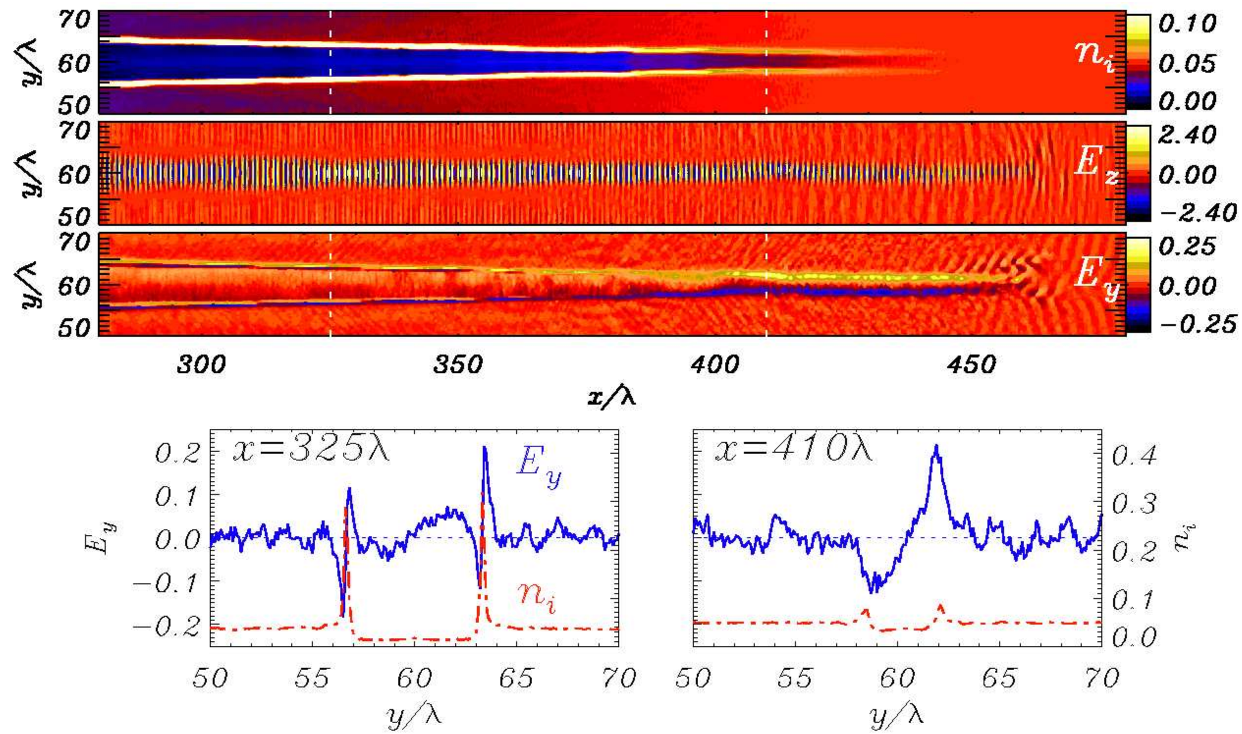

Self-channeling and radial field evolution

2D PIC simulations show that the laser pulse drills a regular charge-displacement channel in the low-density region

The profile of the "radial" space-charge field (E_y) changes in the trailing part of the pulse where field reversal occurs

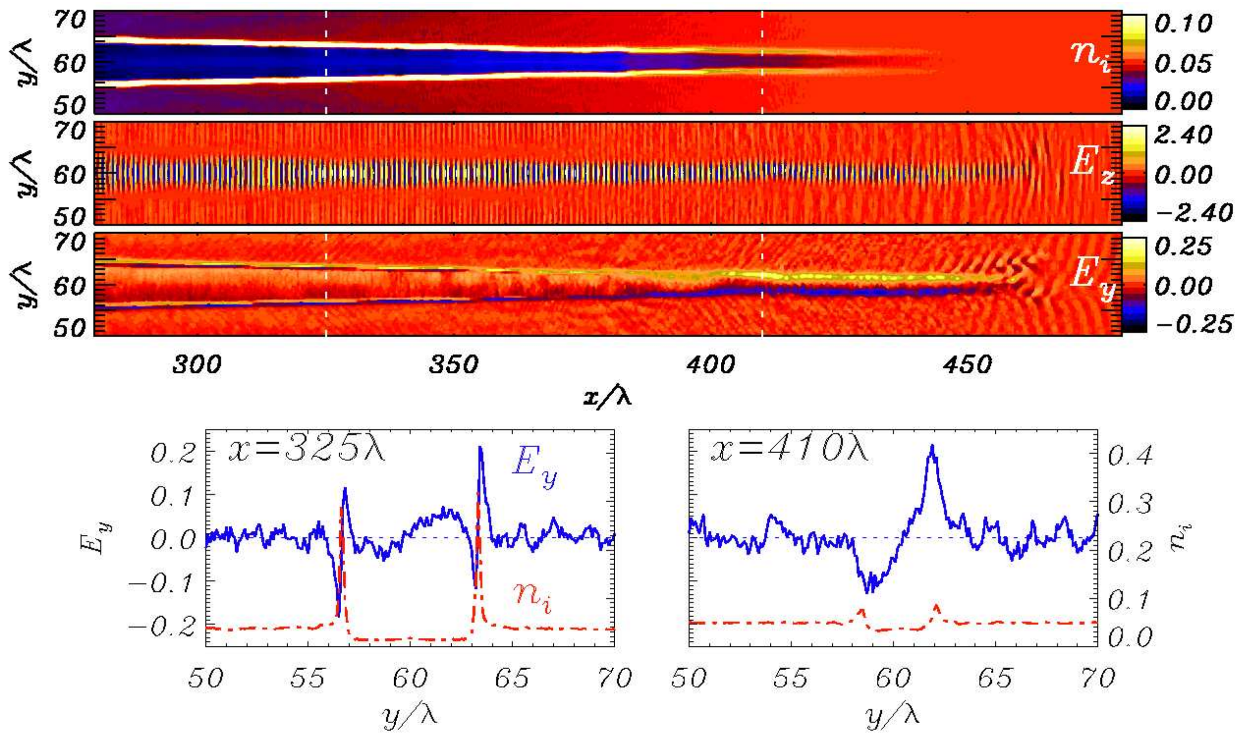

S.Kar et al., NJP, in press [arXiv:physics/0702177]

Ponderomotive electrostatic 1D model

Ponderomotive electrostatic 1D model

- 1D electrostatic PIC simulation, cylindrical geometry

Ponderomotive electrostatic 1D model

- 1D electrostatic PIC simulation, cylindrical geometry
- Laser pulse action is included via the radial ponderomotive force on electrons (as an "external" driver)

$$F_p = -m_e c^2 \nabla \sqrt{1 + a^2(r,t)/2}$$
$$a^2(r,t) = a_L^2 e^{-(r/r_0)^2 - (t/\tau)^2}$$

Ponderomotive electrostatic 1D model

- 1D electrostatic PIC simulation, cylindrical geometry
- Laser pulse action is included via the radial ponderomotive force on electrons (as an "external" driver)

$$F_p = -m_e c^2 \nabla \sqrt{1 + a^2(r,t)/2}$$
$$a^2(r,t) = a_L^2 e^{-(r/r_0)^2 - (t/\tau)^2}$$

- Model equations

$$\frac{dp_e}{dt} = -eE_r + F_p, \qquad \frac{dp_i}{dt} = ZeE_r$$
$$\frac{1}{r}\frac{\partial}{\partial r}(rE_r) = 4\pi\rho = e(Zn_i - n_e).$$

Ponderomotive electrostatic 1D model

- 1D electrostatic PIC simulation, cylindrical geometry
- Laser pulse action is included via the radial ponderomotive force on electrons (as an "external" driver)

$$F_p = -m_e c^2 \nabla \sqrt{1 + a^2(r,t)/2}$$
$$a^2(r,t) = a_L^2 e^{-(r/r_0)^2 - (t/\tau)^2}$$

- Model equations

$$\frac{dp_e}{dt} = -eE_r + F_p, \qquad \frac{dp_i}{dt} = ZeE_r$$
$$\frac{1}{r}\frac{\partial}{\partial r}(rE_r) = 4\pi\rho = e(Zn_i - n_e).$$

[A. Macchi et al, arXiv:physics/0701139]

Comparison with experimental results

Comparison with experimental results

The simple 1D model has been integrated with a particle tracing code (developed by A. Schiavi) to simulate the proton projection images: very good agreement is found

Comparison with experimental results

The simple 1D model has been integrated with a particle tracing code (developed by A. Schiavi) to simulate the proton projection images: very good agreement is found

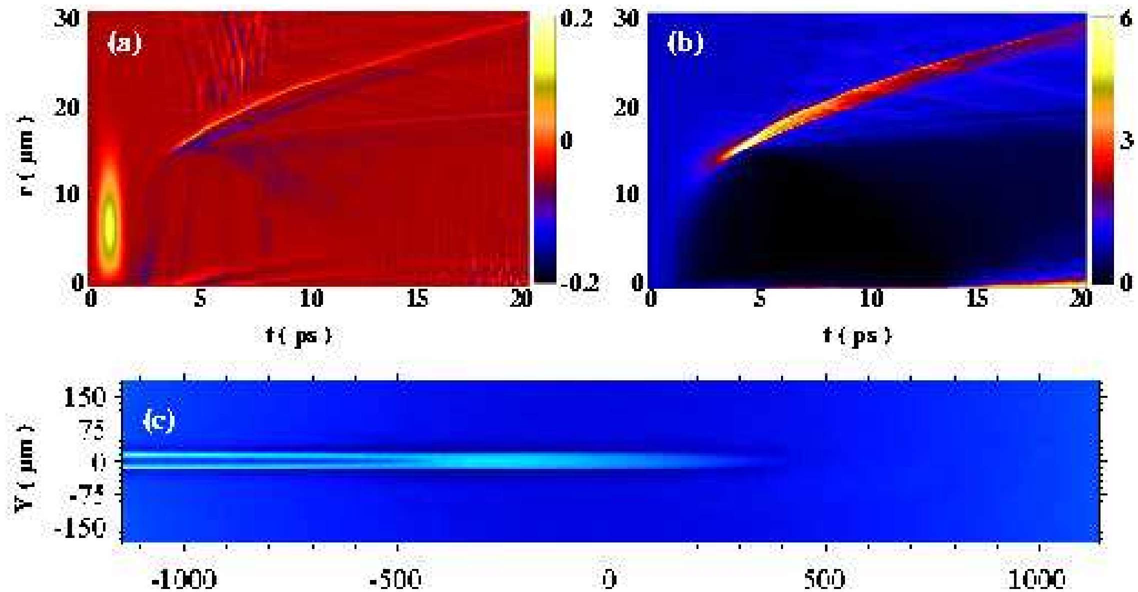

Comparison with experimental results

The simple 1D model has been integrated with a particle tracing code (developed by A. Schiavi) to simulate the proton projection images: very good agreement is found

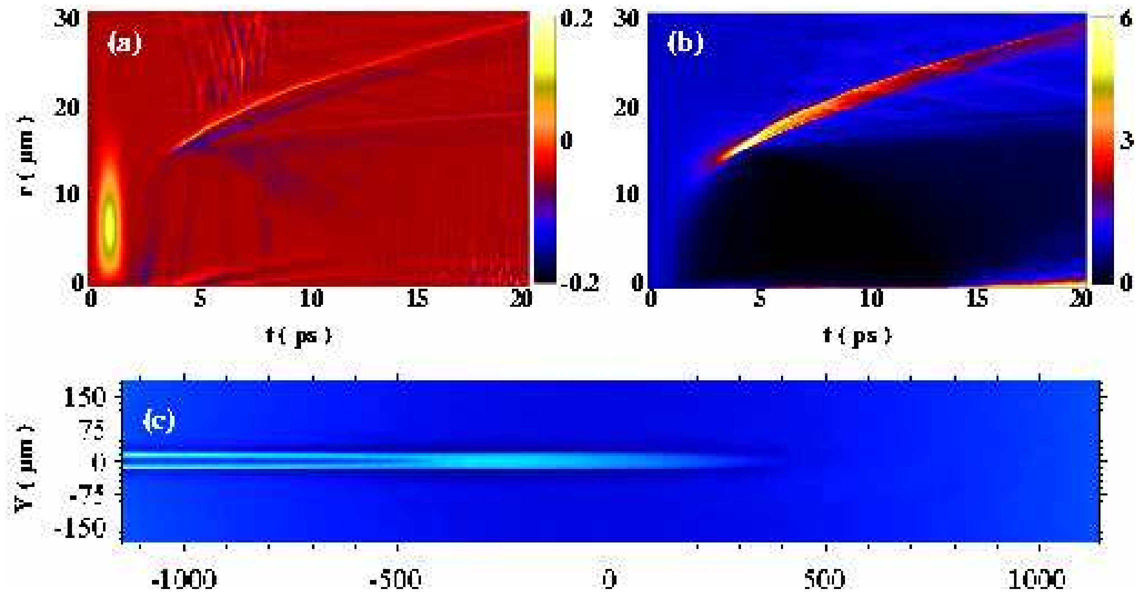

The model reproduces fairly experimental and numerical results of radial ion acceleration in similar conditions

[see e.g. Sarkisov et al, JETP **66**, 828 (1997);Krushelnick et al, PRL **83**, 737 (1999); Fritzler et al, PRL **89**, 165004 (2002).]

Echo effect in the radial field

Echo effect in the radial field

1D electrostatic PIC simulation

$a_L = 2.7$, $\tau_L = 300T_L$, $r_L = 7.5\lambda$

Echo effect in the radial field

1D electrostatic PIC simulation

$a_L = 2.7$, $\tau_L = 300T_L$, $r_L = 7.5\lambda$

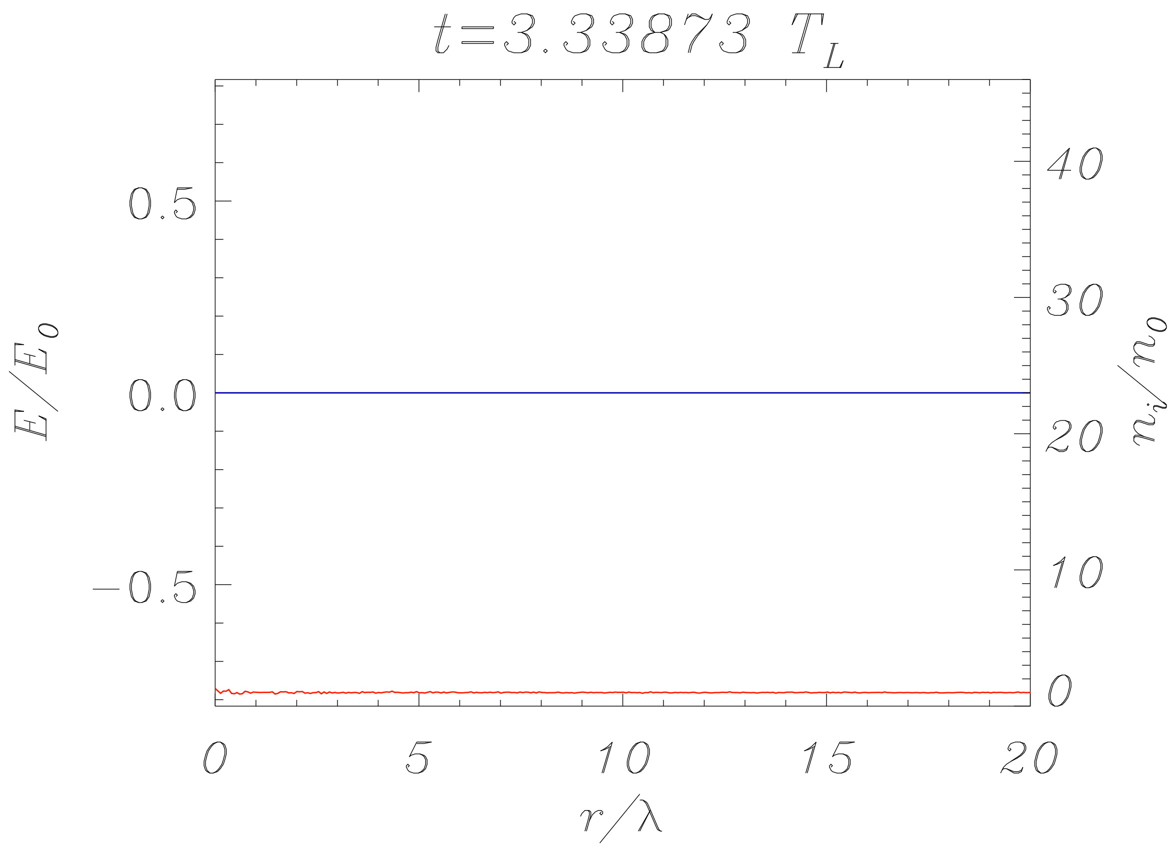

During the laser pulse the space-charge field E_r created by electron depletion in the channel exactly balances the PM force F_p

Echo effect in the radial field

1D electrostatic PIC simulation

$a_L = 2.7$, $\tau_L = 300T_L$, $r_L = 7.5\lambda$

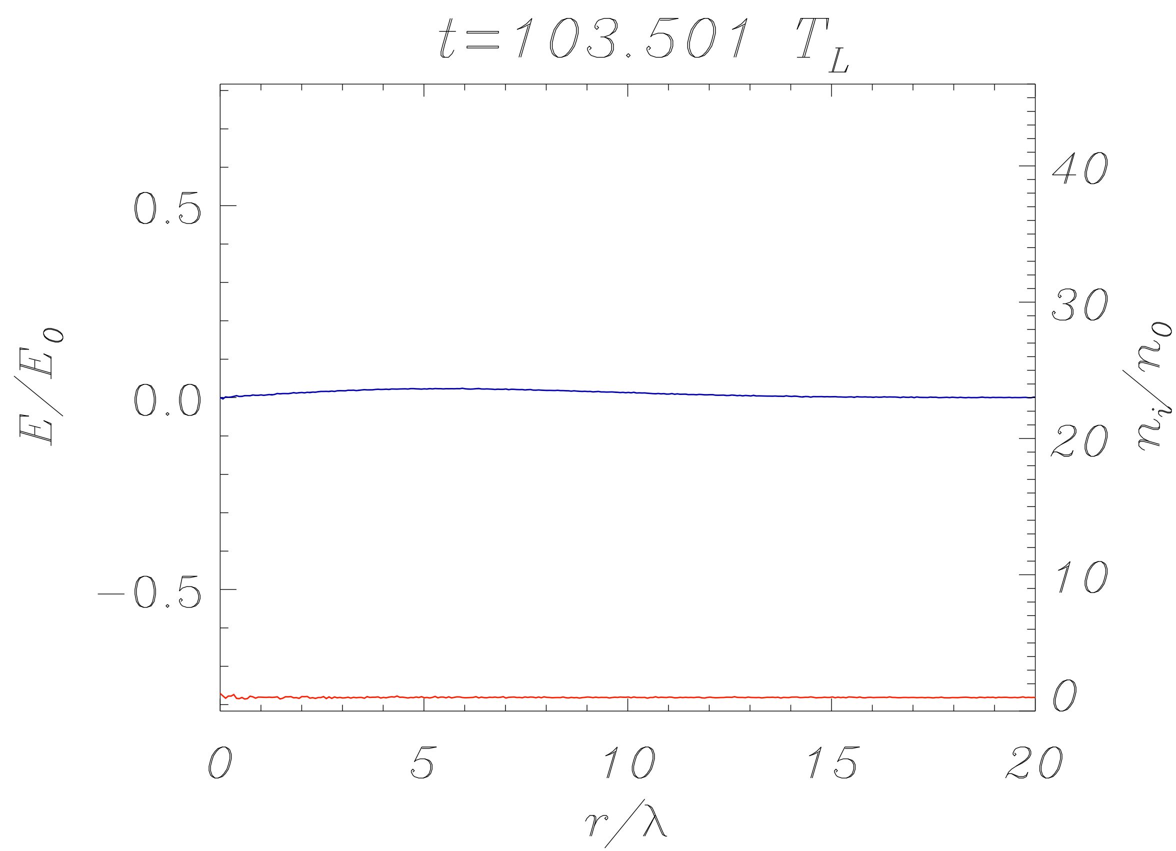

During the laser pulse the space-charge field E_r created by electron depletion in the channel exactly balances the PM force F_p

Echo effect in the radial field

1D electrostatic PIC simulation

$a_L = 2.7$, $\tau_L = 300T_L$, $r_L = 7.5\lambda$

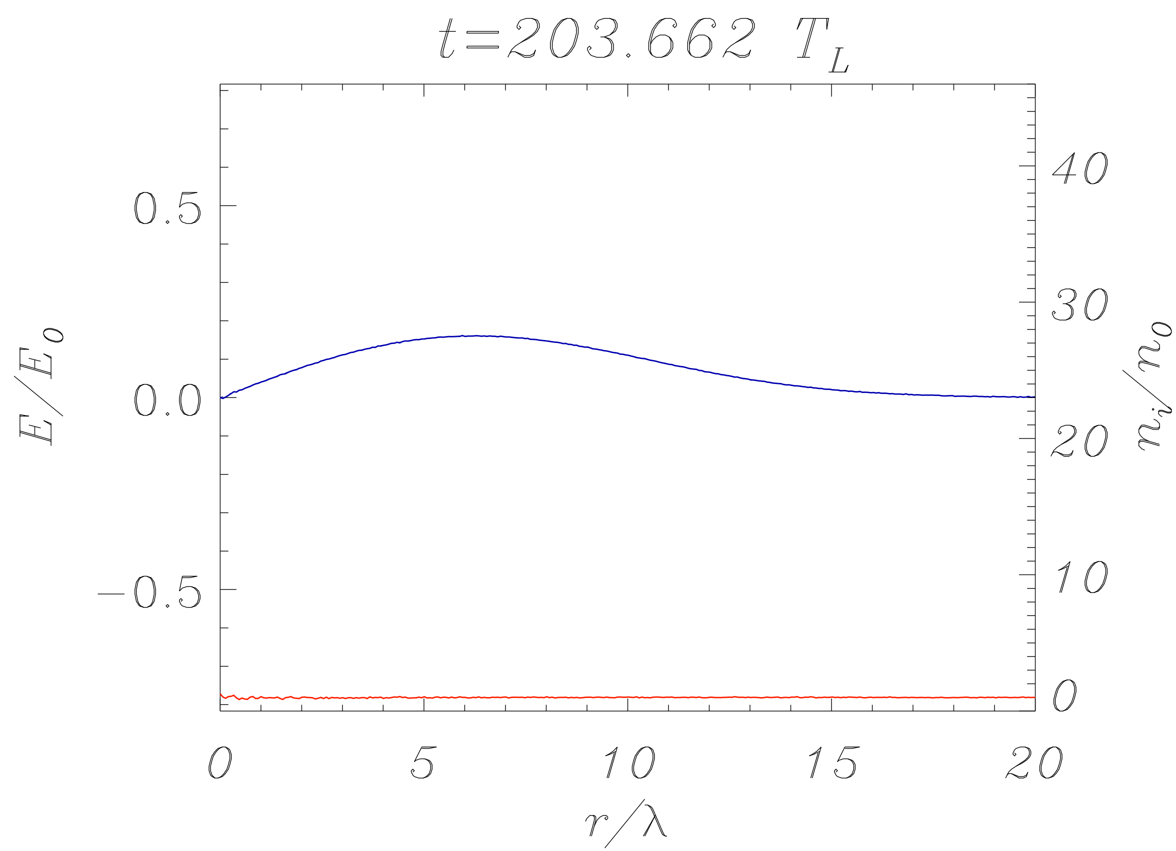

During the laser pulse the space-charge field E_r created by electron depletion in the channel exactly balances the PM force F_p

Echo effect in the radial field

1D electrostatic PIC simulation

$a_L = 2.7$, $\tau_L = 300T_L$, $r_L = 7.5\lambda$

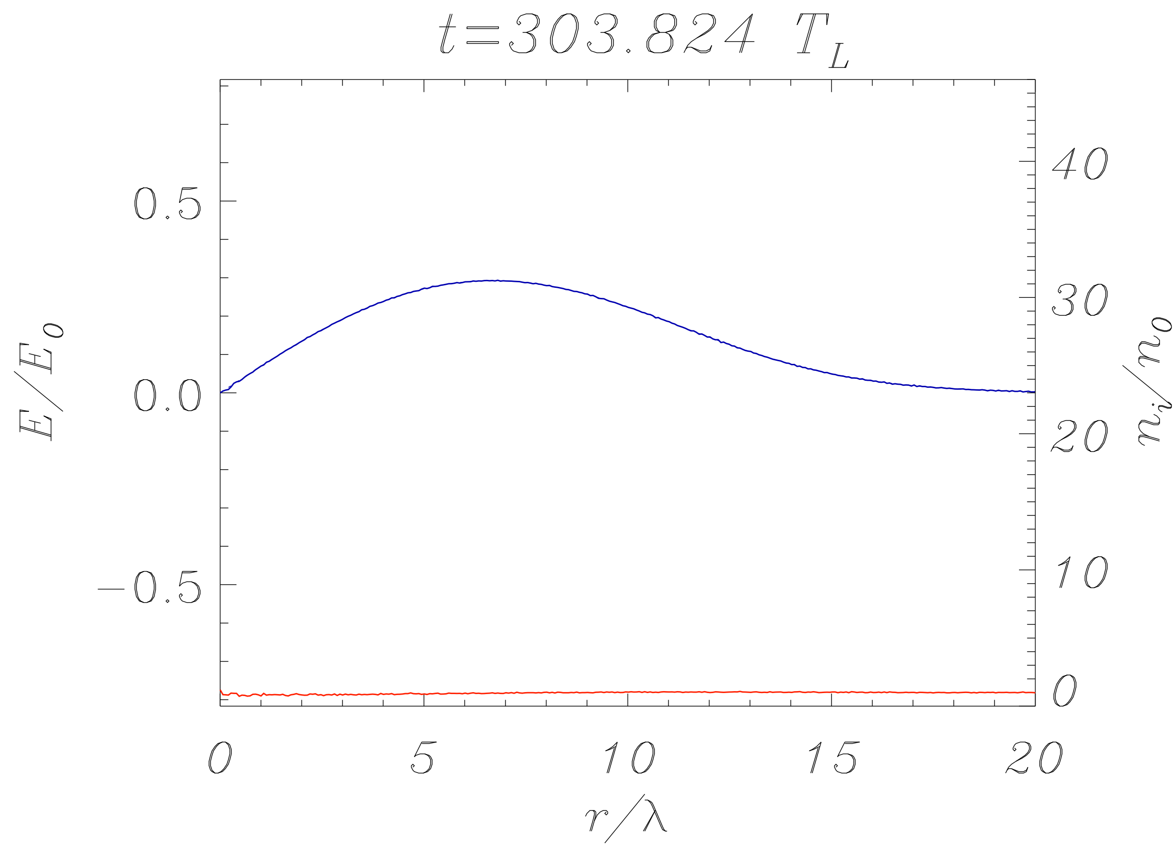

During the laser pulse the space-charge field E_r created by electron depletion in the channel exactly balances the PM force F_p

Echo effect in the radial field

1D electrostatic PIC simulation

$a_L = 2.7$, $\tau_L = 300T_L$, $r_L = 7.5\lambda$

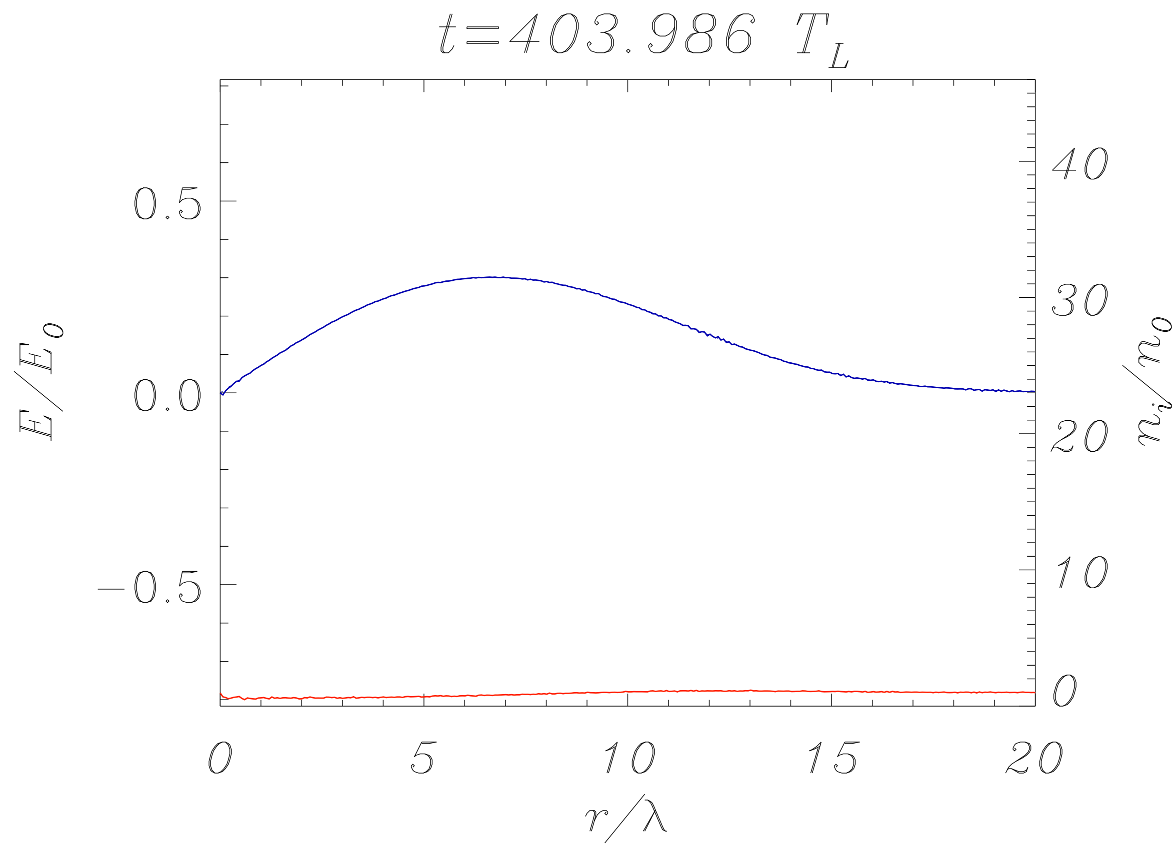

During the laser pulse the space-charge field E_r created by electron depletion in the channel exactly balances the PM force F_p

Echo effect in the radial field

1D electrostatic PIC simulation

$a_L = 2.7$, $\tau_L = 300 T_L$, $r_L = 7.5\lambda$

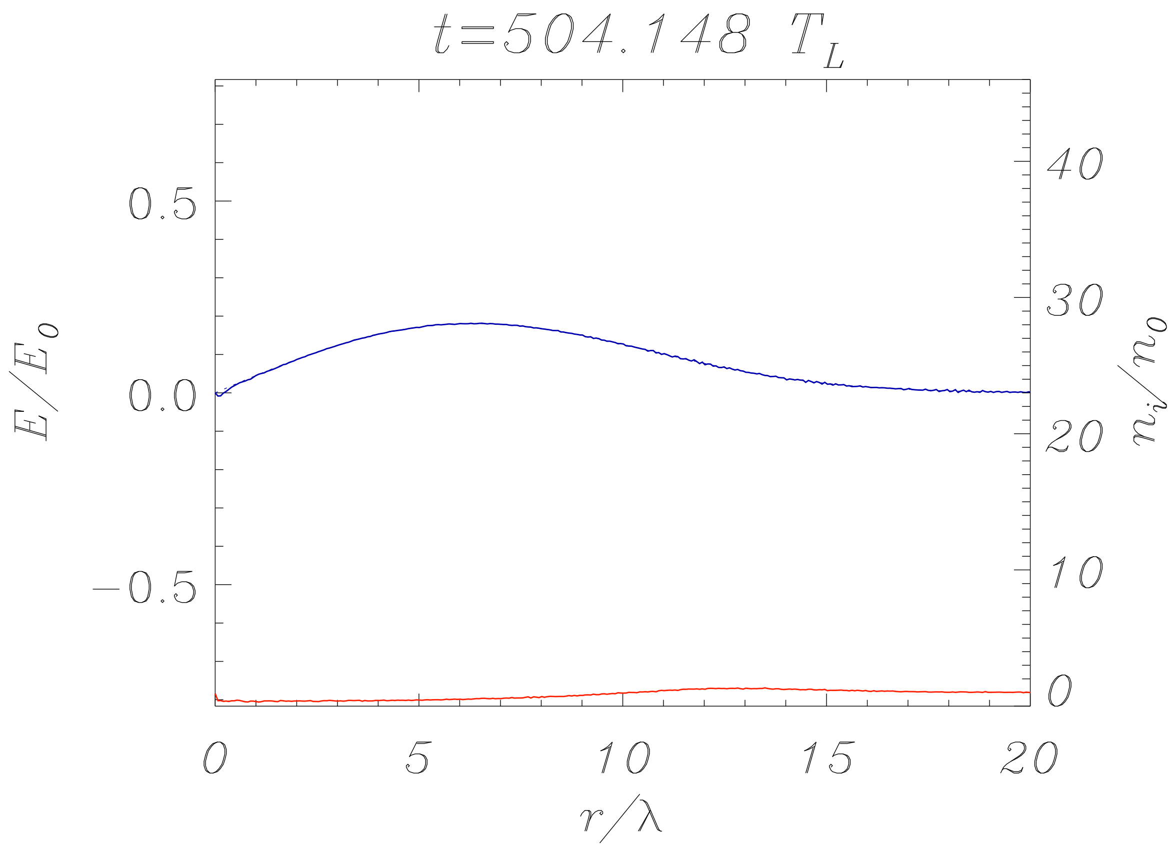

During the laser pulse the space-charge field E_r created by electron depletion in the channel exactly balances the PM force F_p

Echo effect in the radial field

1D electrostatic PIC simulation
$a_L = 2.7$, $\tau_L = 300T_L$, $r_L = 7.5\lambda$

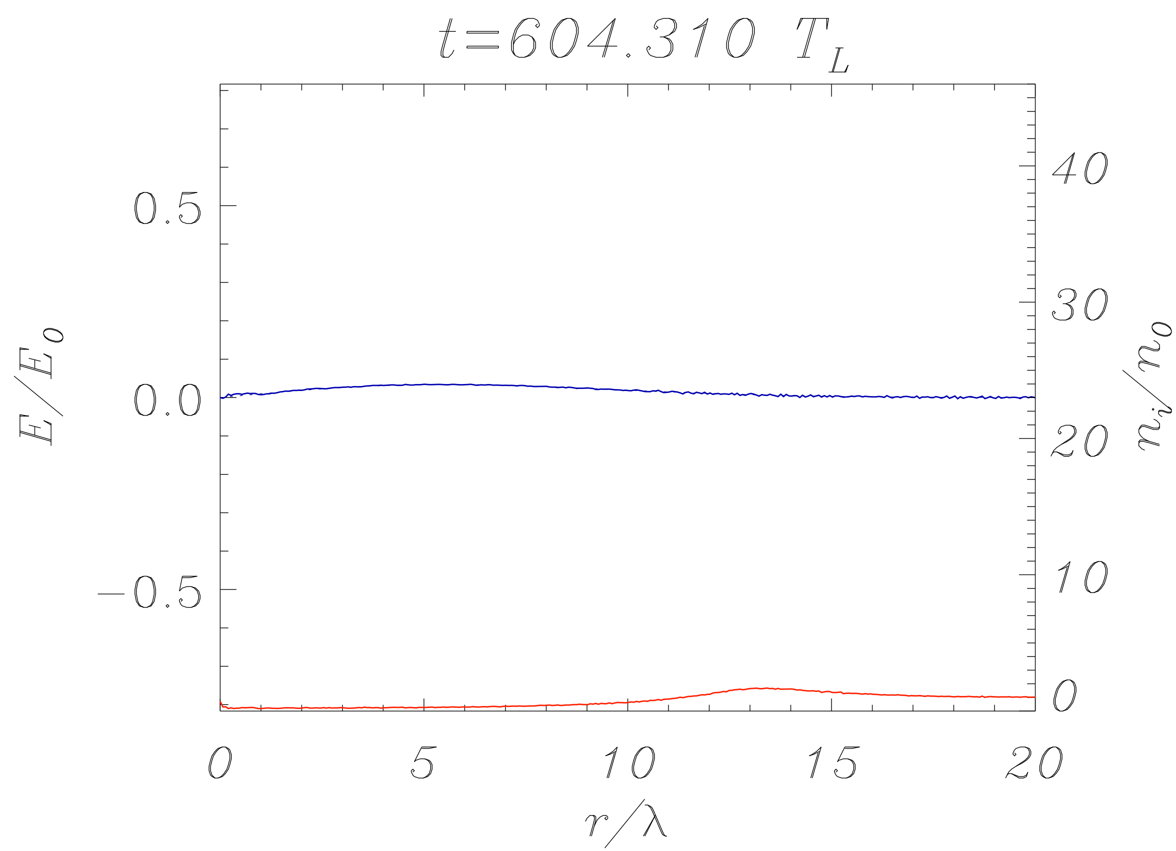

During the laser pulse the space-charge field E_r created by electron depletion in the channel exactly balances the PM force F_p

Echo effect in the radial field

1D electrostatic PIC simulation
$a_L = 2.7$, $\tau_L = 300 T_L$, $r_L = 7.5\lambda$

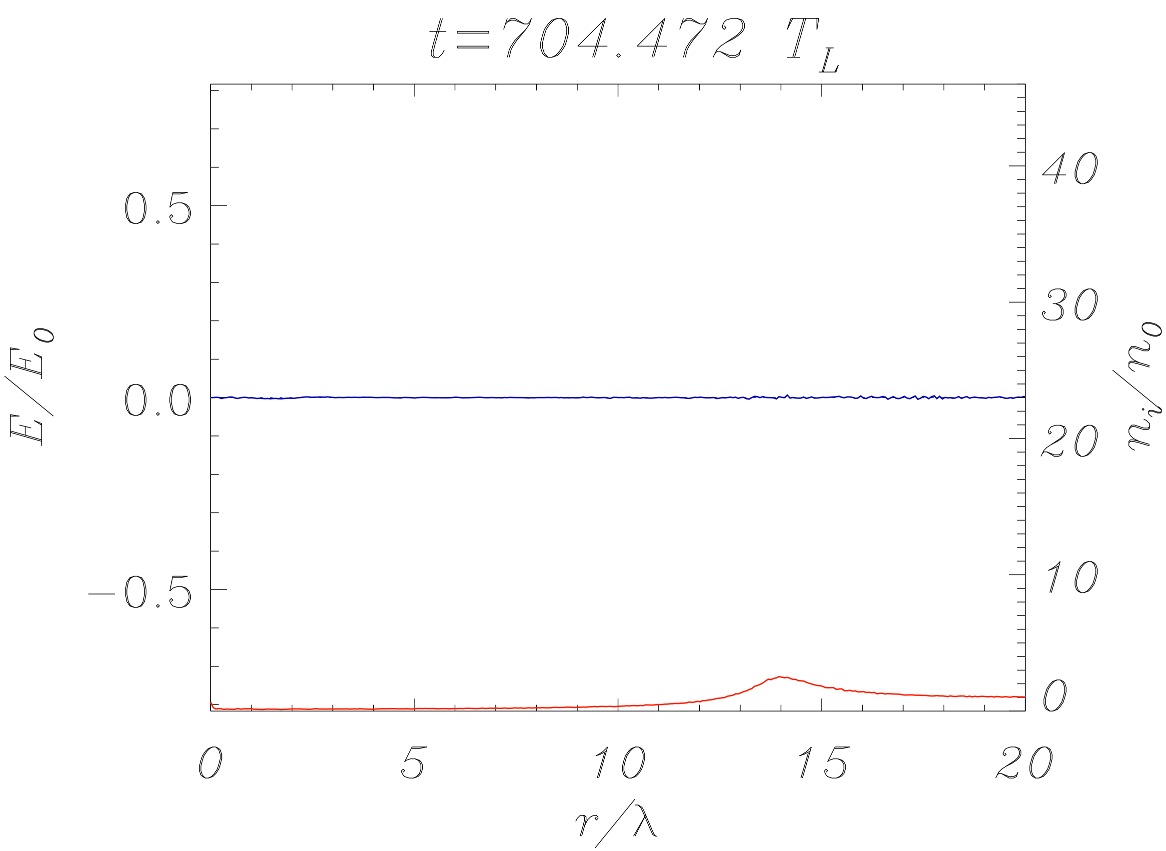

After the laser pulse E_r has almost vanished

Echo effect in the radial field

1D electrostatic PIC simulation

$a_L = 2.7$, $\tau_L = 300T_L$, $r_L = 7.5\lambda$

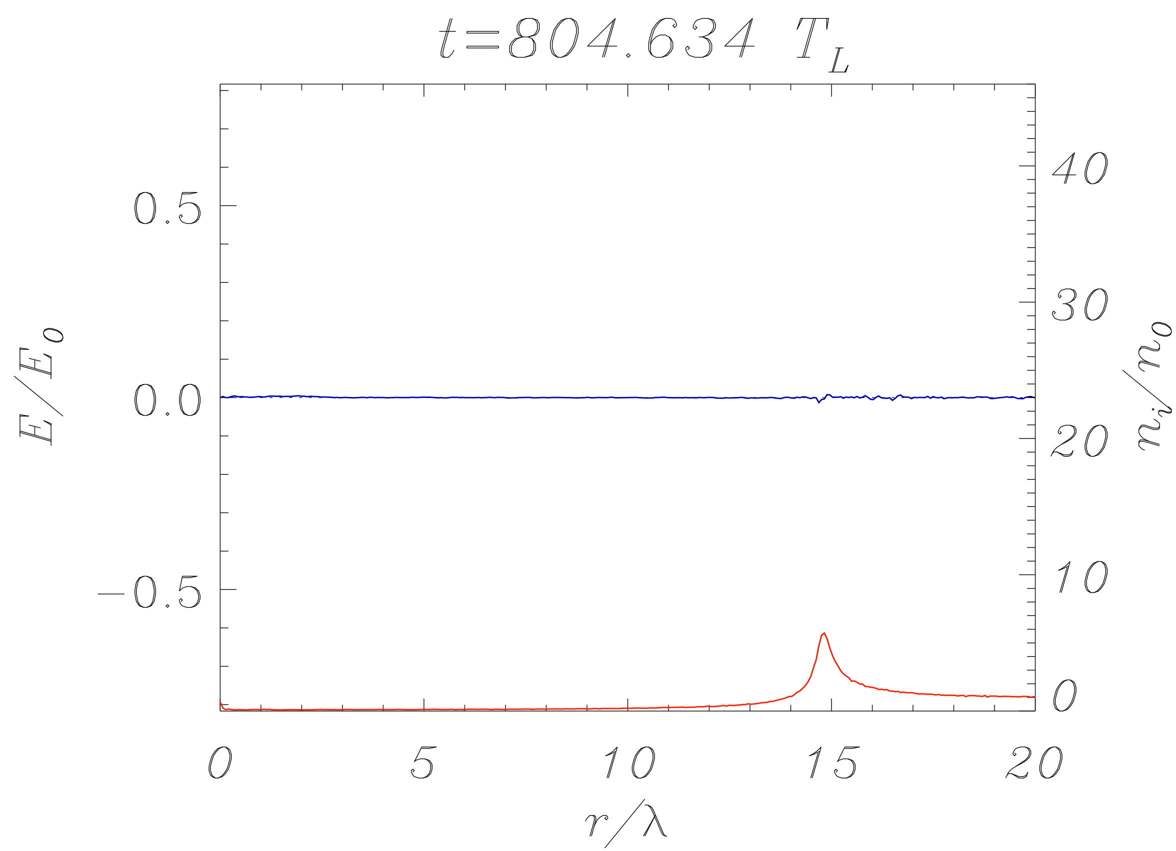

After the laser pulse E_r has almost vanished

Echo effect in the radial field

1D electrostatic PIC simulation

$a_L = 2.7$, $\tau_L = 300T_L$, $r_L = 7.5\lambda$

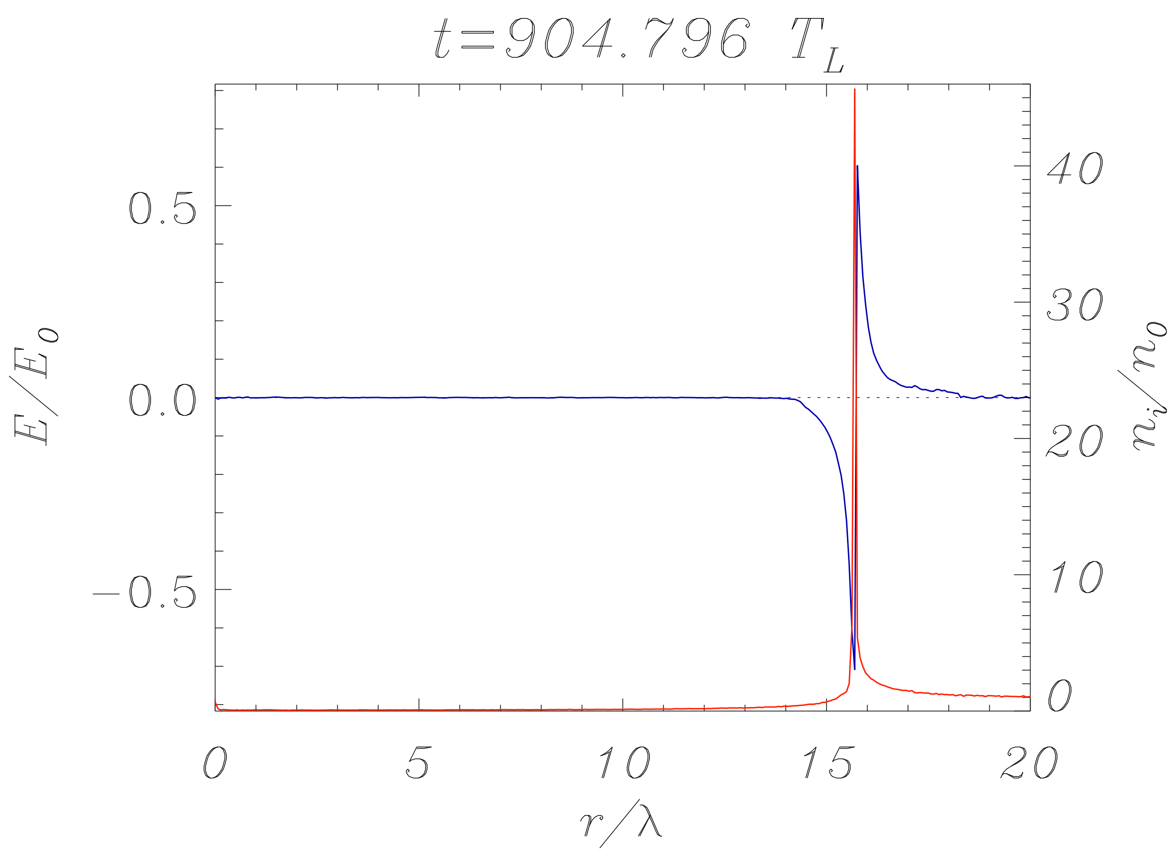

E_r appears back ("echo") where a sharp spike of n_i is produced;
the spike then "breaks" producing a fast bunch of ions

Echo effect in the radial field

1D electrostatic PIC simulation

$a_L = 2.7$, $\tau_L = 300T_L$, $r_L = 7.5\lambda$

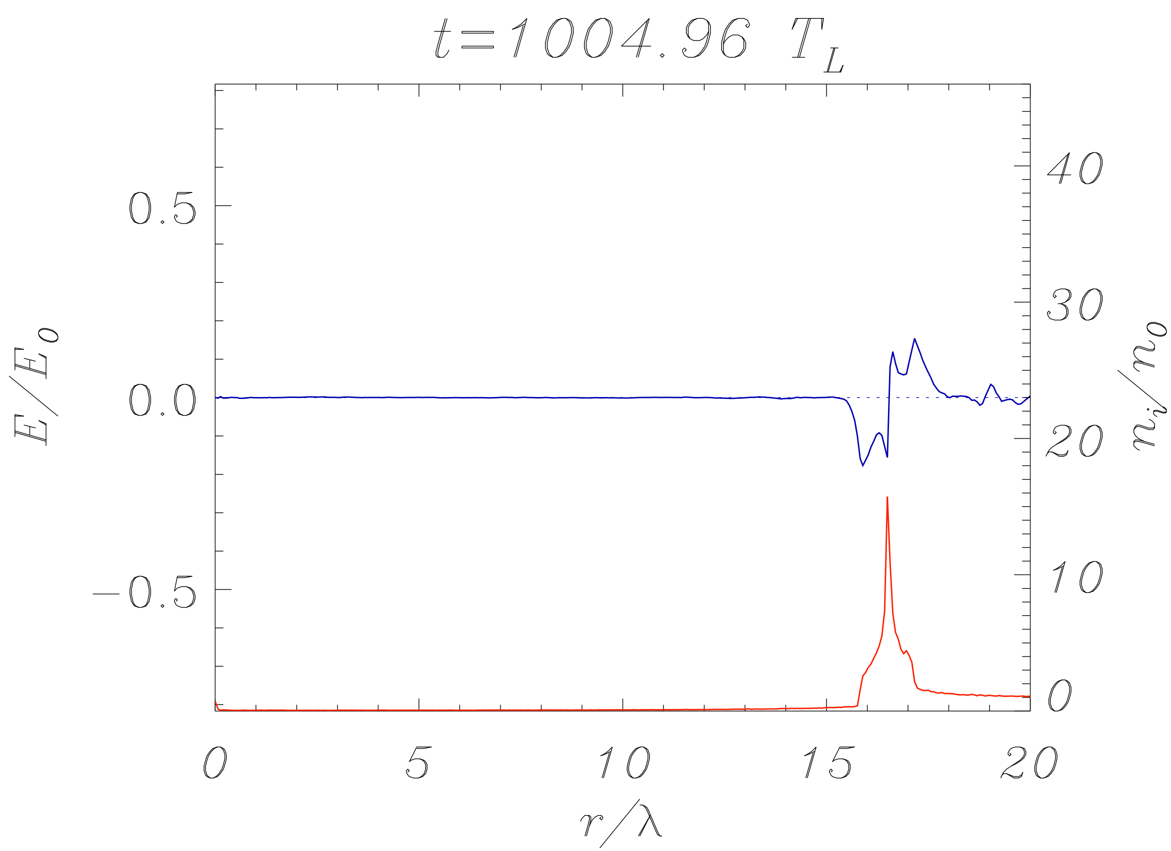

E_r appears back ("echo") where a sharp spike of n_i is produced;
the spike then "breaks" producing a fast bunch of ions

Echo effect in the radial field

1D electrostatic PIC simulation

$a_L = 2.7$, $\tau_L = 300T_L$, $r_L = 7.5\lambda$

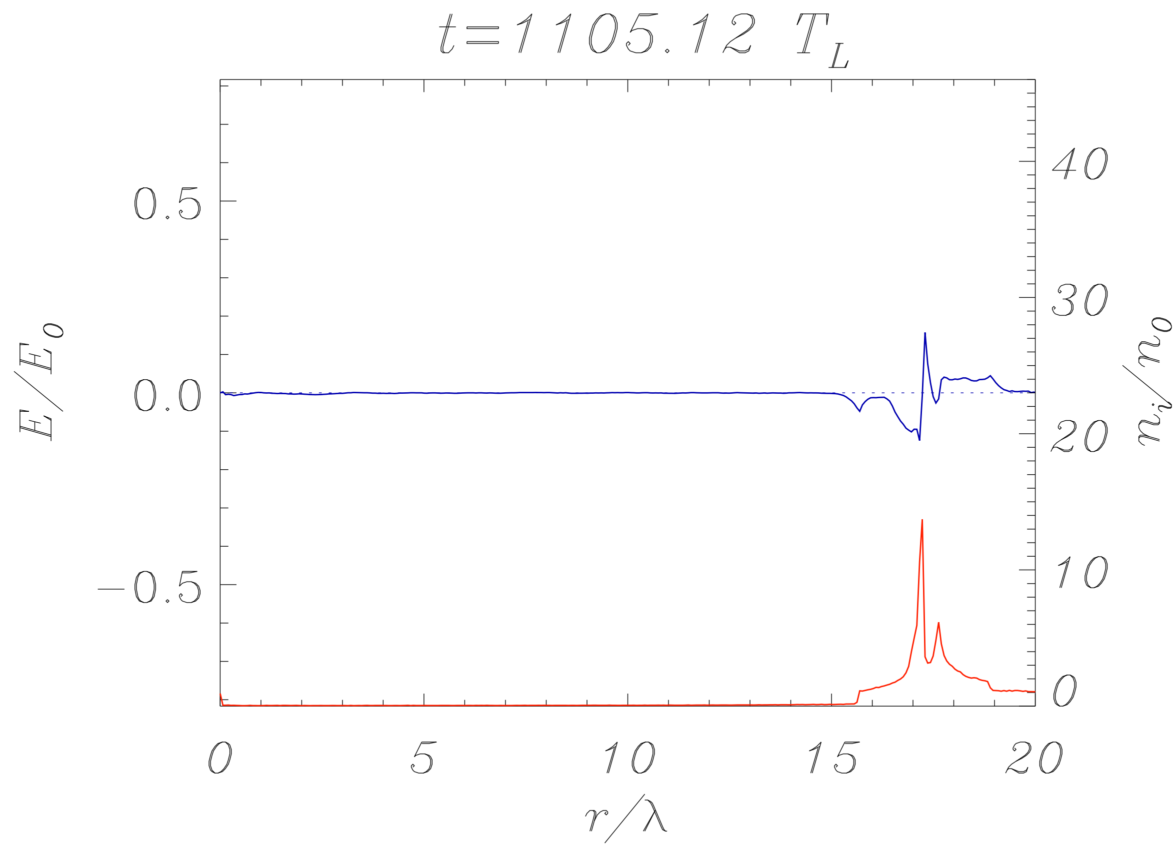

E_r appears back ("echo") where a sharp spike of n_i is produced;
the spike then "breaks" producing a fast bunch of ions

Echo effect in the radial field

1D electrostatic PIC simulation

$a_L = 2.7$, $\tau_L = 300T_L$, $r_L = 7.5\lambda$

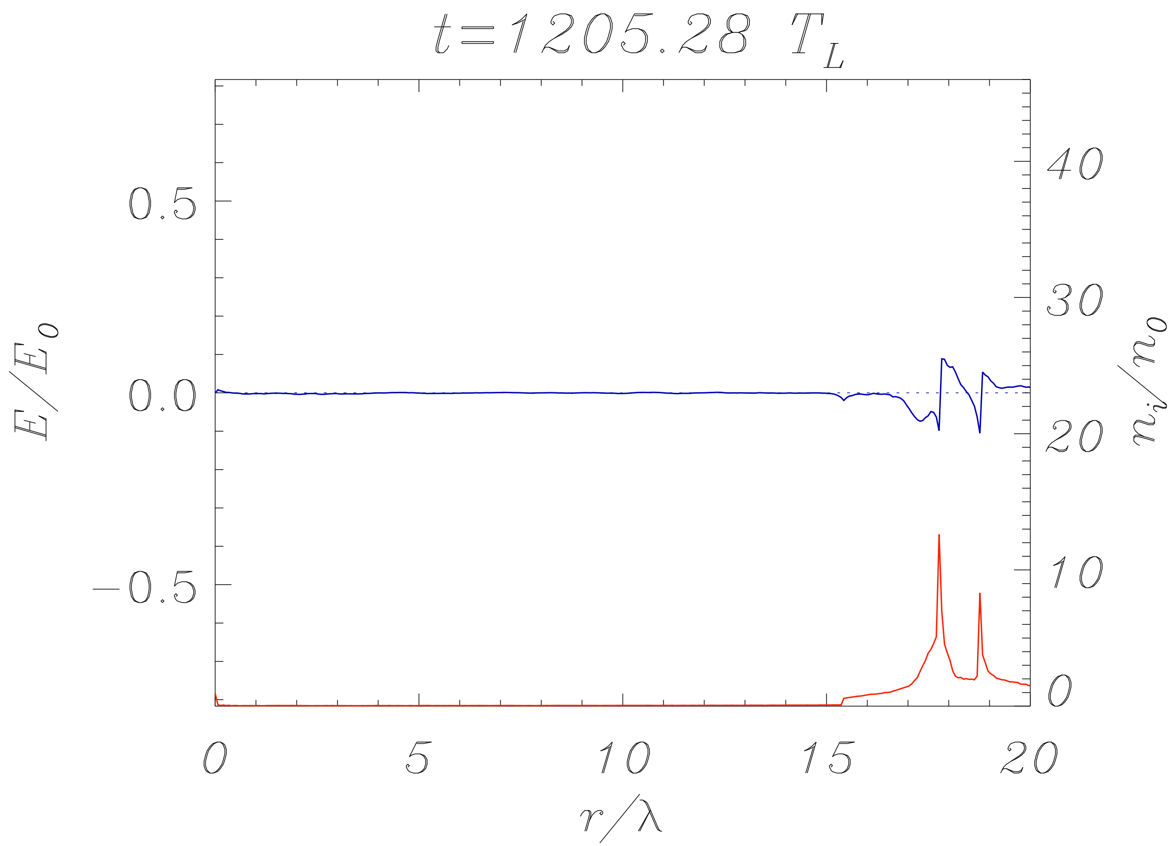

E_r appears back ("echo") where a sharp spike of n_i is produced;
the spike then "breaks" producing a fast bunch of ions

Echo effect in the radial field

1D electrostatic PIC simulation
$a_L = 2.7$, $\tau_L = 300 T_L$, $r_L = 7.5\lambda$

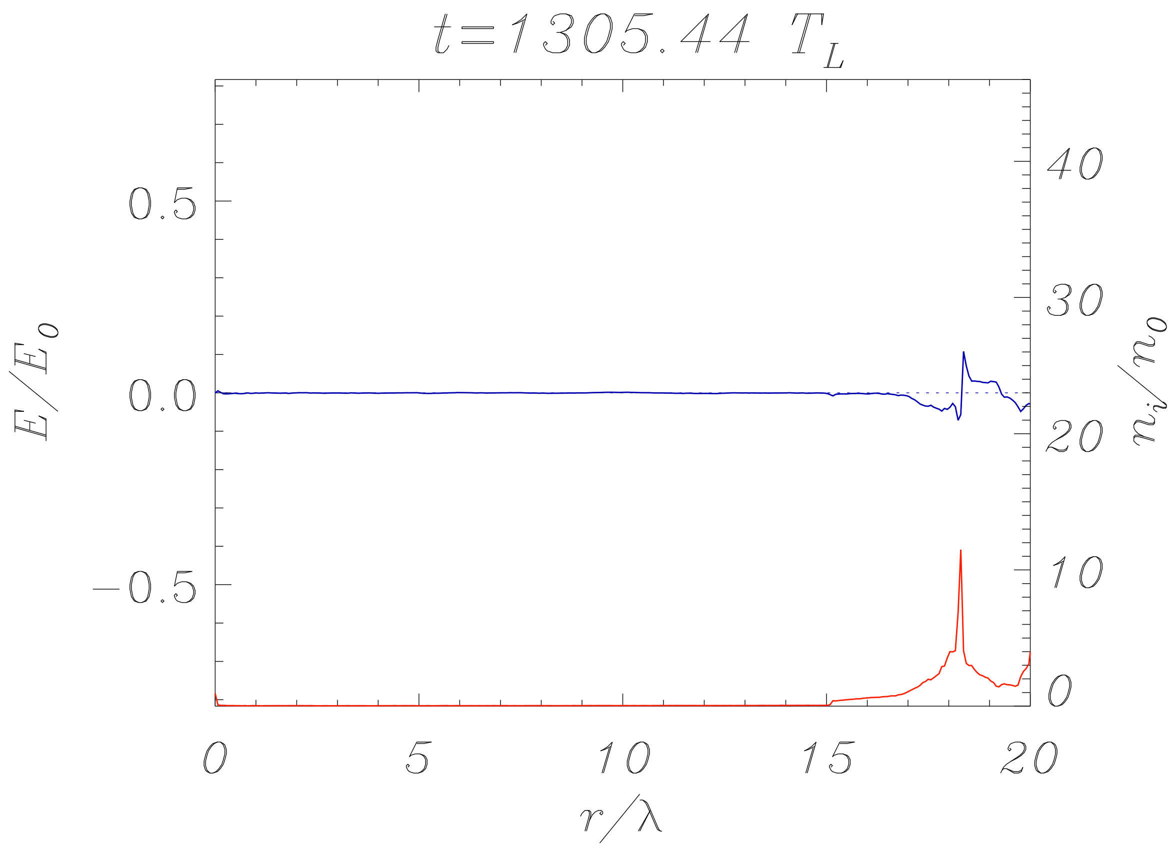

E_r appears back ("echo") where a sharp spike of n_i is produced;
the spike then "breaks" producing a fast bunch of ions

Echo effect is due to “breaking”

Echo effect is due to “breaking”

Analysis of ion phase space show that hydrodynamical breaking occurs when faster ions overlap the slowest ones

Echo effect is due to "breaking"

Analysis of ion phase space show that hydrodynamical breaking occurs when faster ions overlap the slowest ones

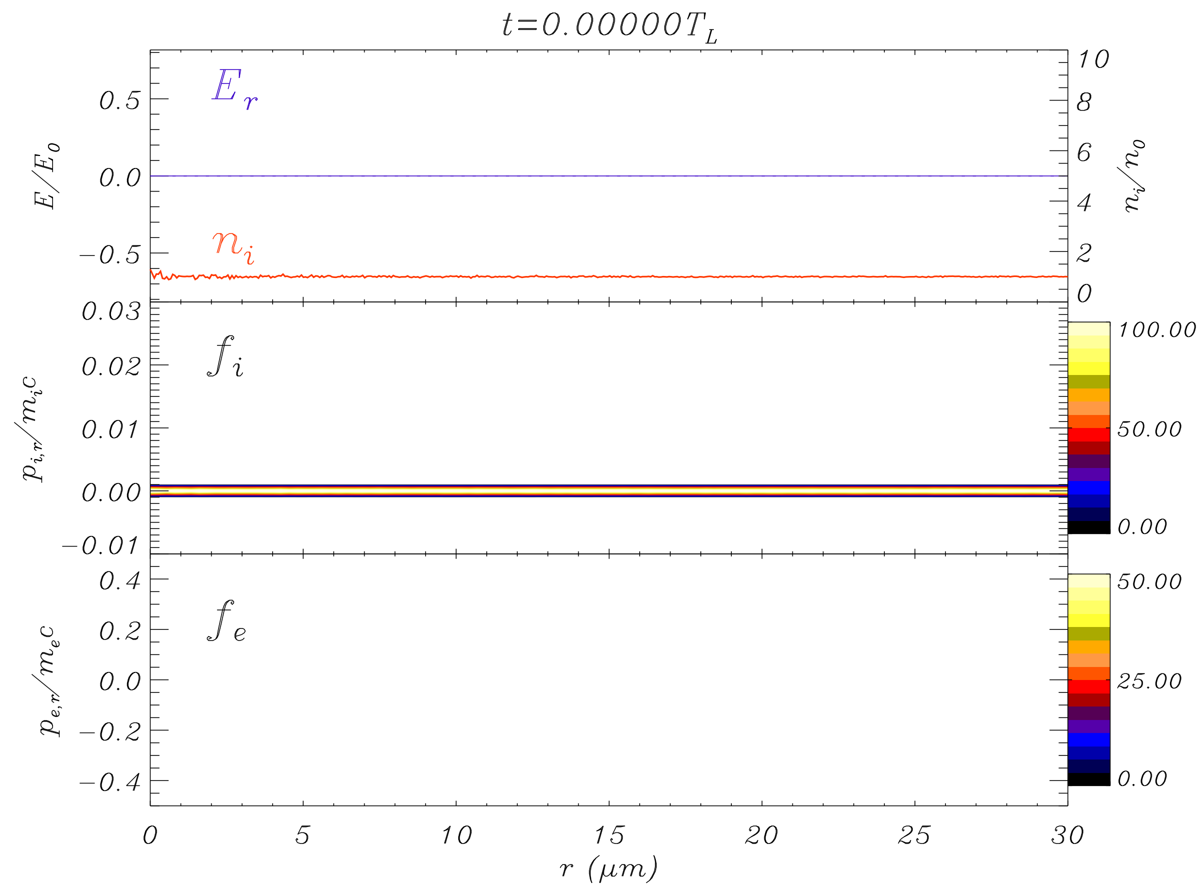

Echo effect is due to “breaking”

Analysis of ion phase space show that hydrodynamical breaking occurs when faster ions overlap the slowest ones

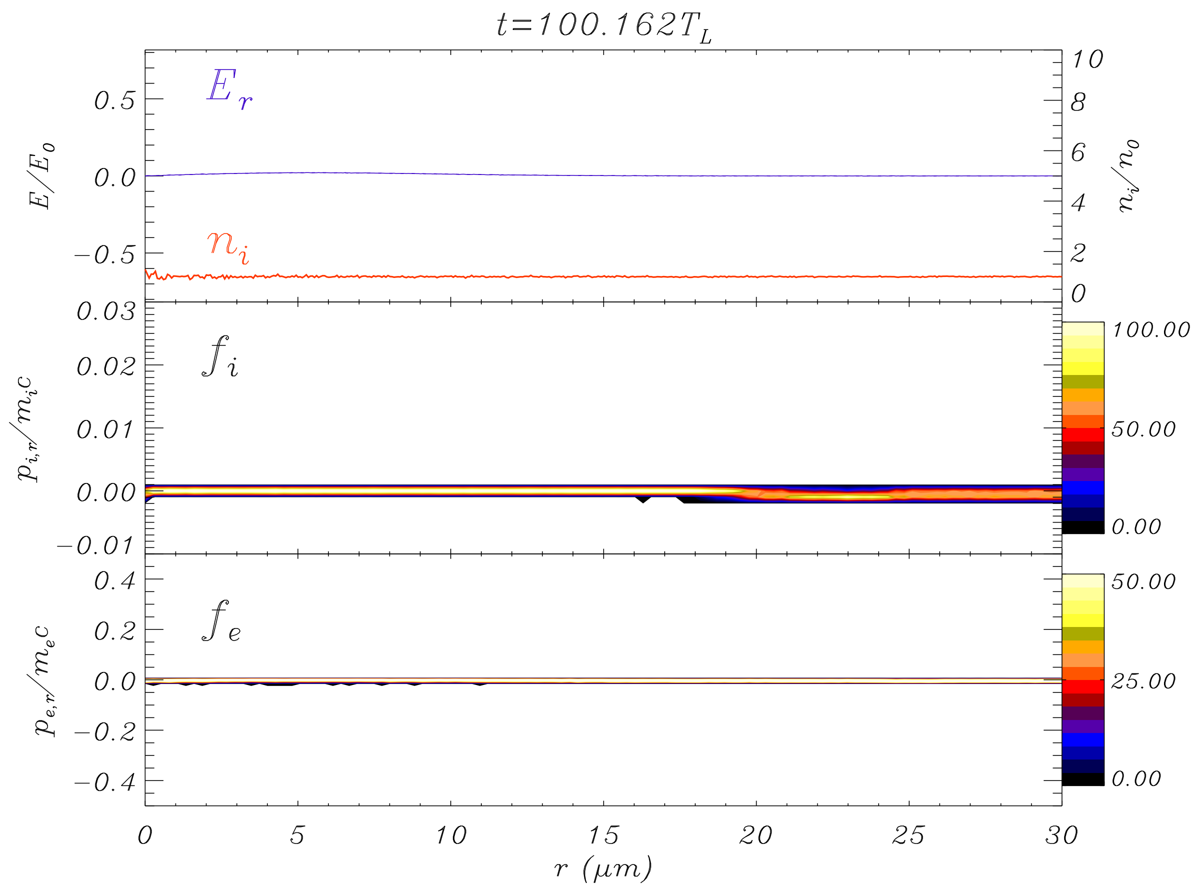

Echo effect is due to “breaking”

Analysis of ion phase space show that hydrodynamical breaking occurs when faster ions overlap the slowest ones

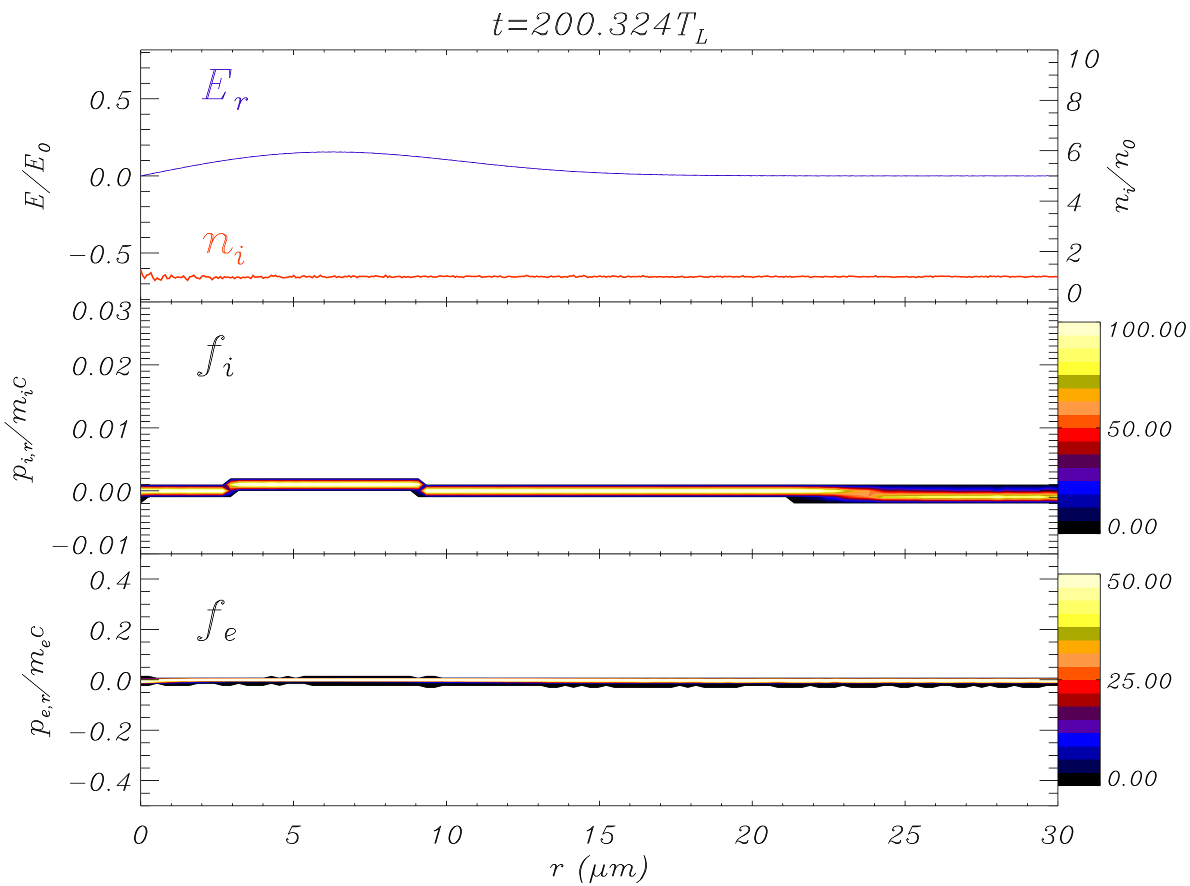

Echo effect is due to "breaking"

Analysis of ion phase space show that hydrodynamical breaking occurs when faster ions overlap the slowest ones

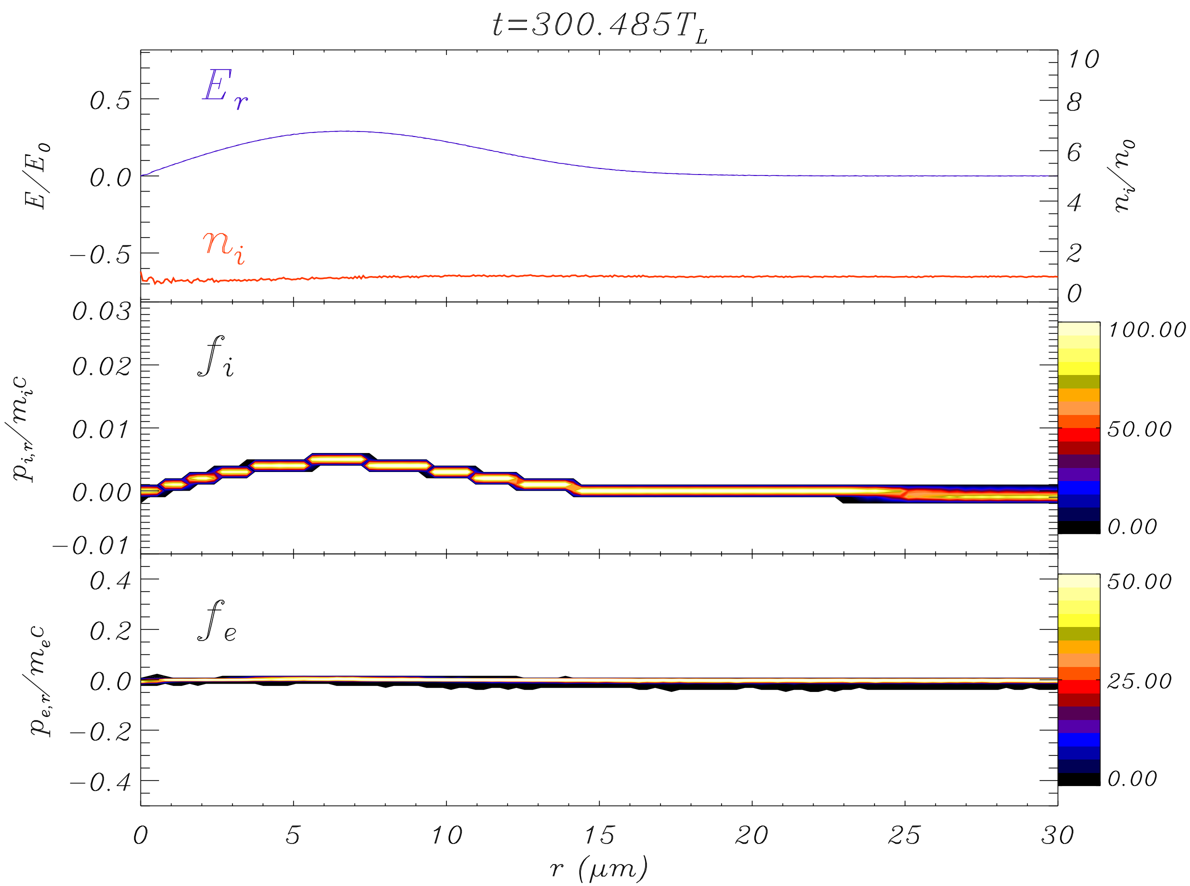

Echo effect is due to "breaking"

Analysis of ion phase space show that hydrodynamical breaking occurs when faster ions overlap the slowest ones

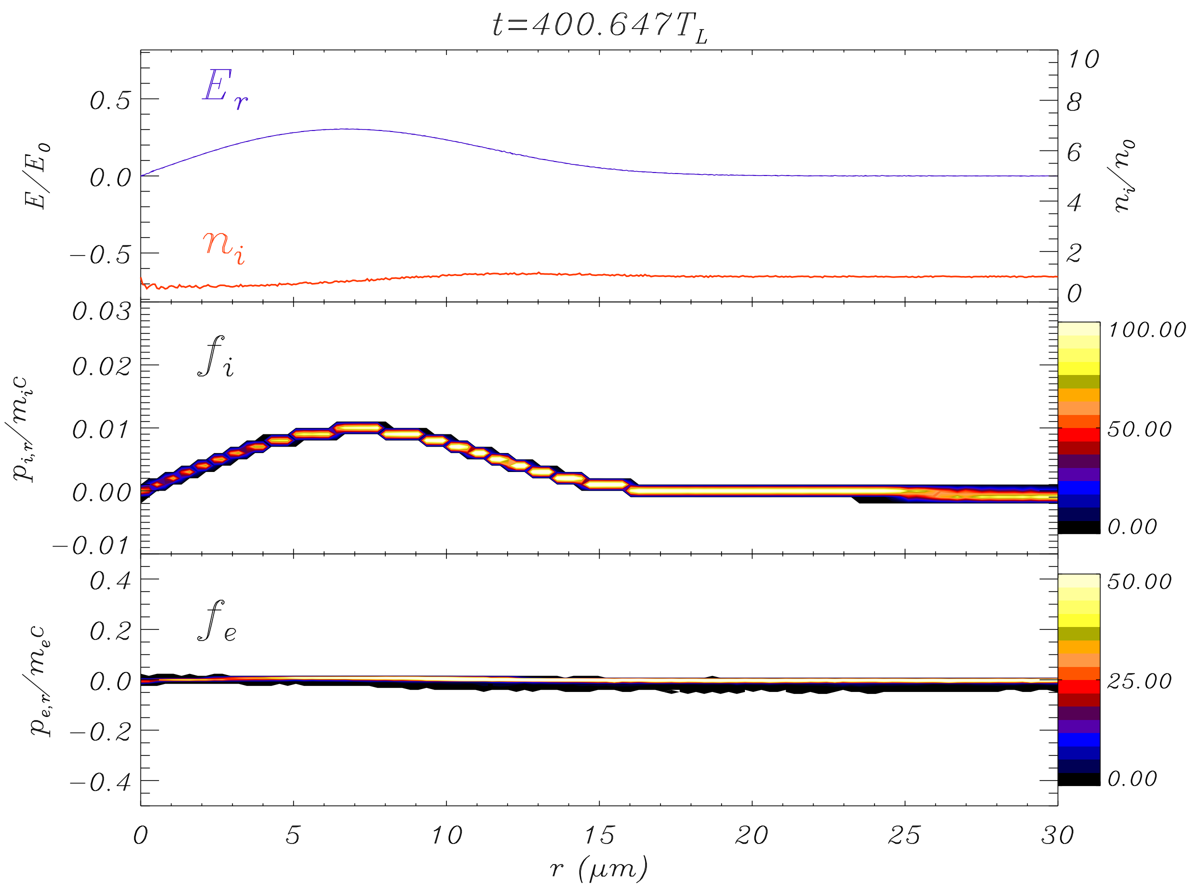

Echo effect is due to “breaking”

Analysis of ion phase space show that hydrodynamical breaking occurs when faster ions overlap the slowest ones

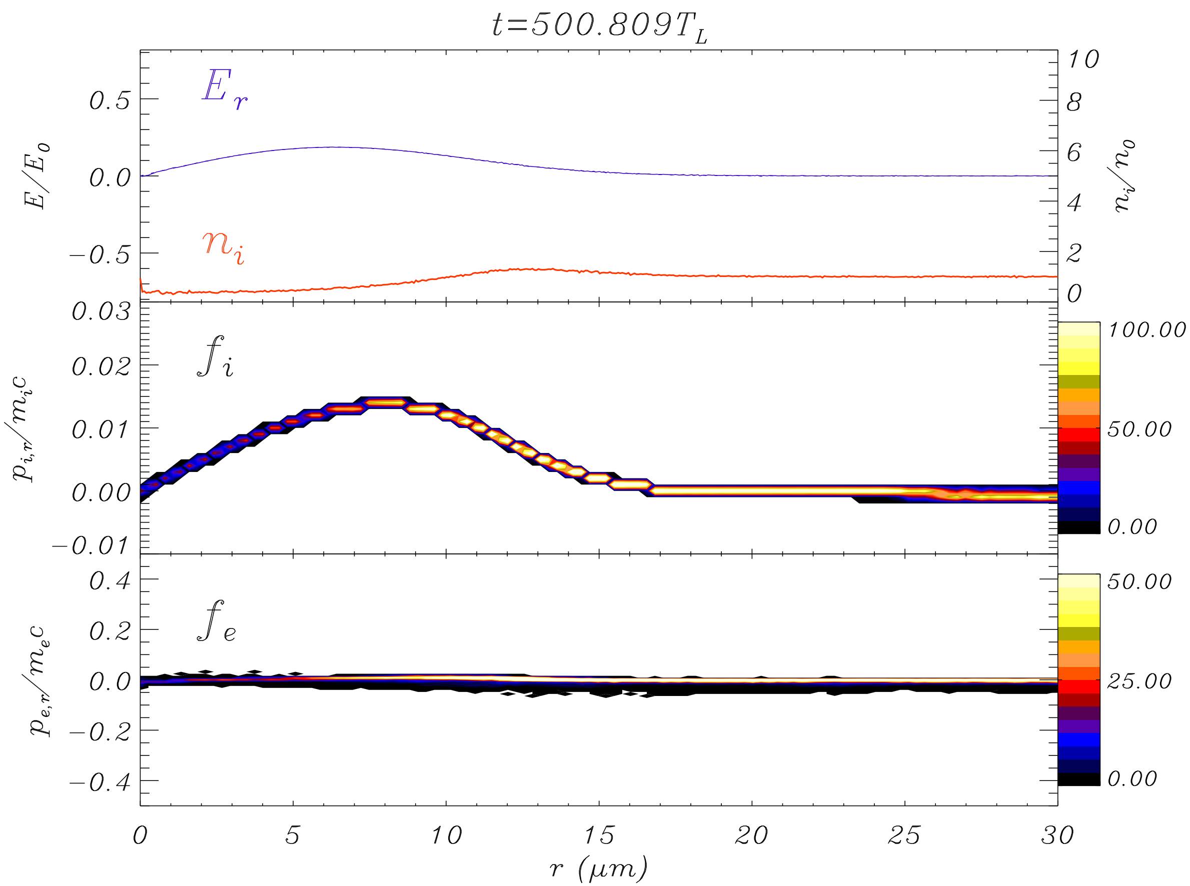

Echo effect is due to “breaking”

Analysis of ion phase space show that hydrodynamical breaking occurs when faster ions overlap the slowest ones

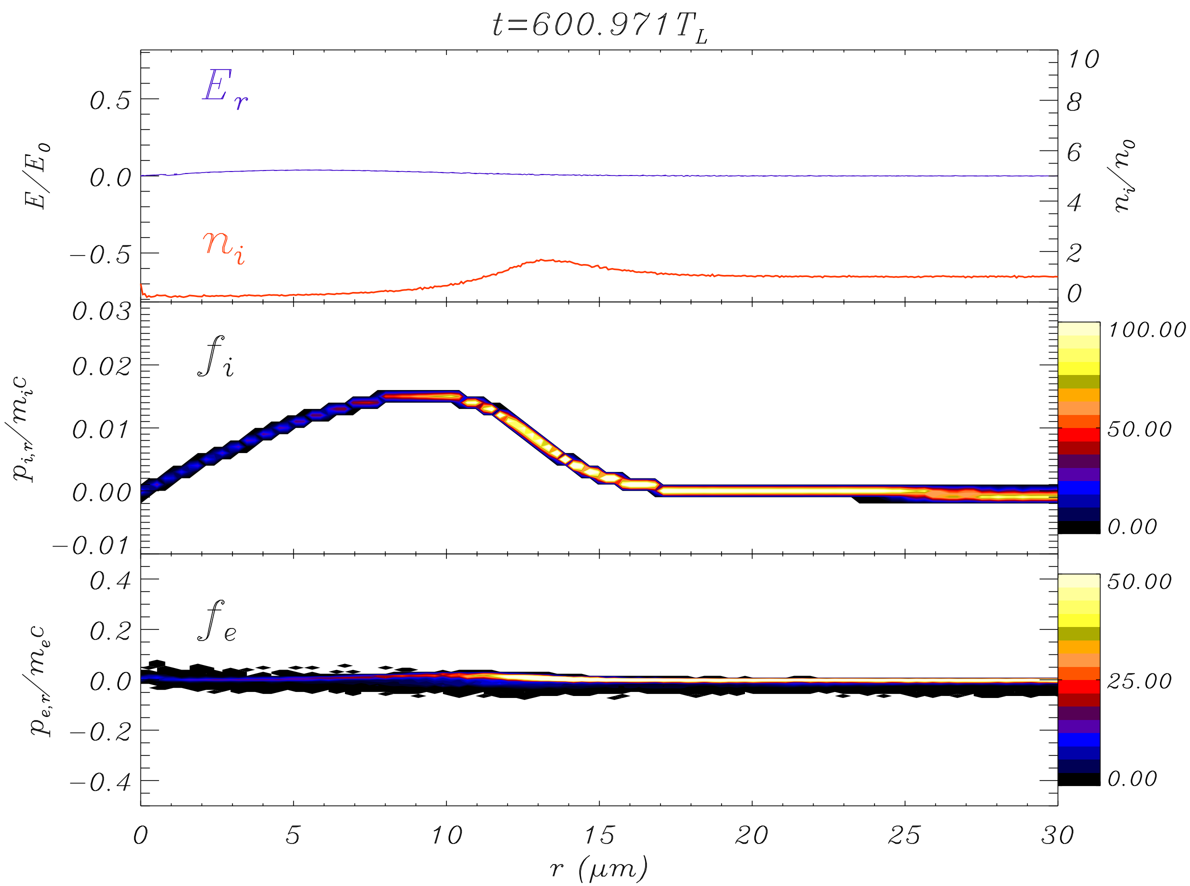

Echo effect is due to "breaking"

Analysis of ion phase space show that hydrodynamical breaking occurs when faster ions overlap the slowest ones

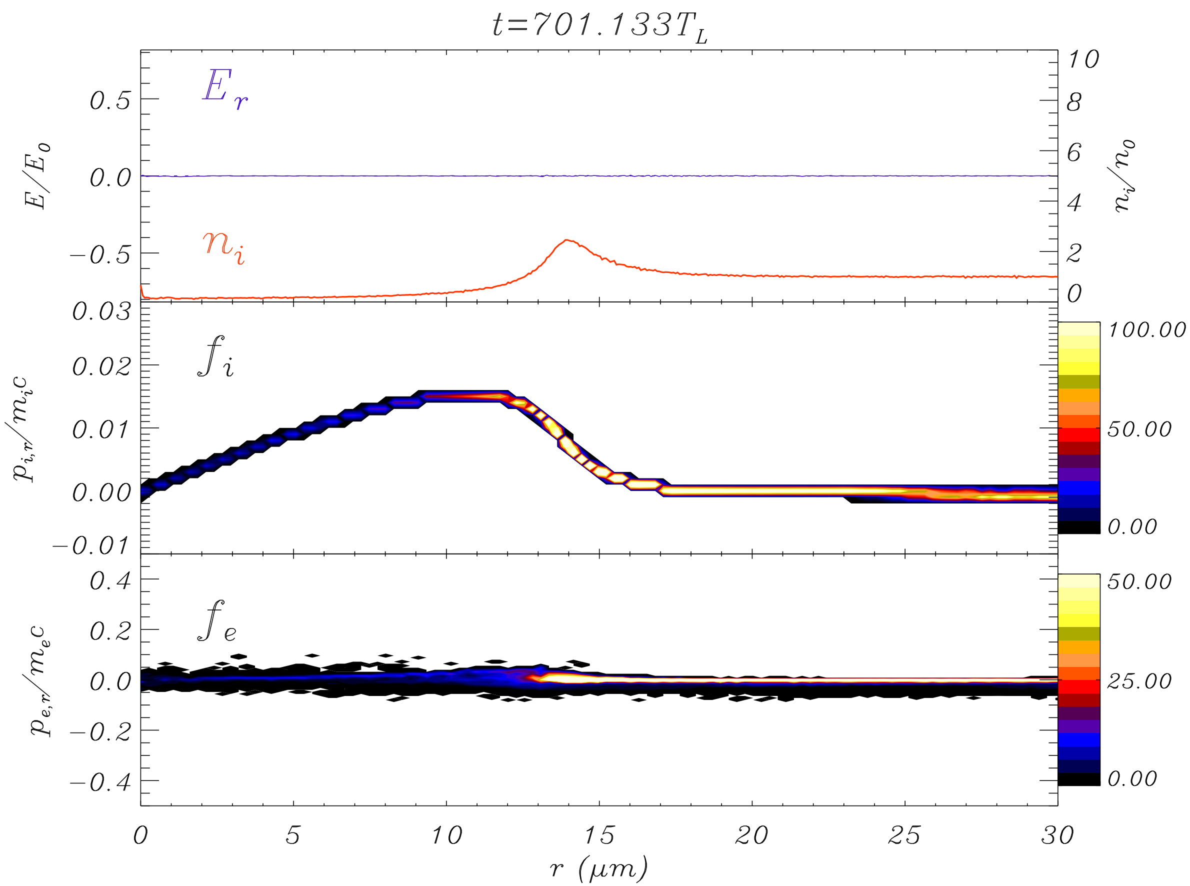

Echo effect is due to "breaking"

Analysis of ion phase space show that hydrodynamical breaking occurs when faster ions overlap the slowest ones

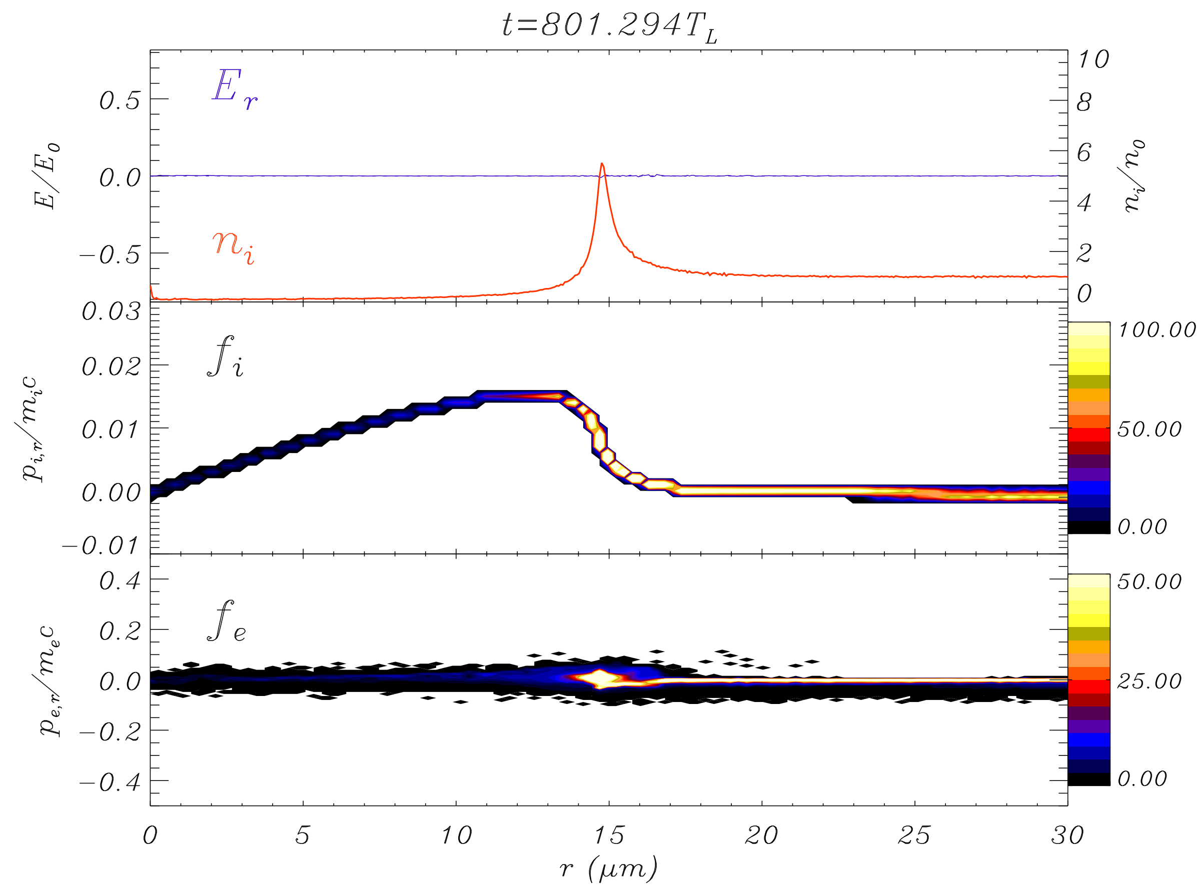

Echo effect is due to “breaking”

Analysis of ion phase space show that hydrodynamical breaking occurs when faster ions overlap the slowest ones

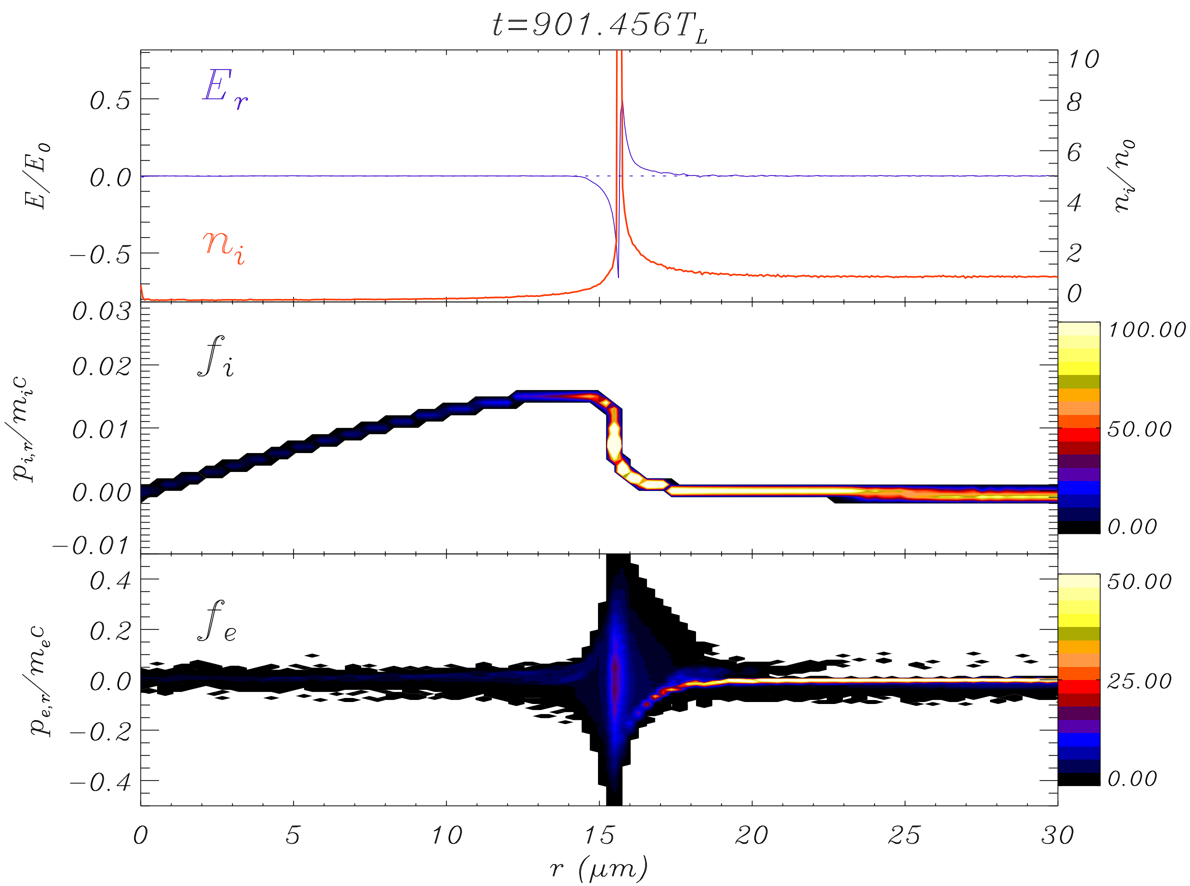

At breaking, strong electron heating occurs

An ambipolar electric field is generated around the density spike

Echo effect is due to “breaking”

Analysis of ion phase space show that hydrodynamical breaking occurs when faster ions overlap the slowest ones

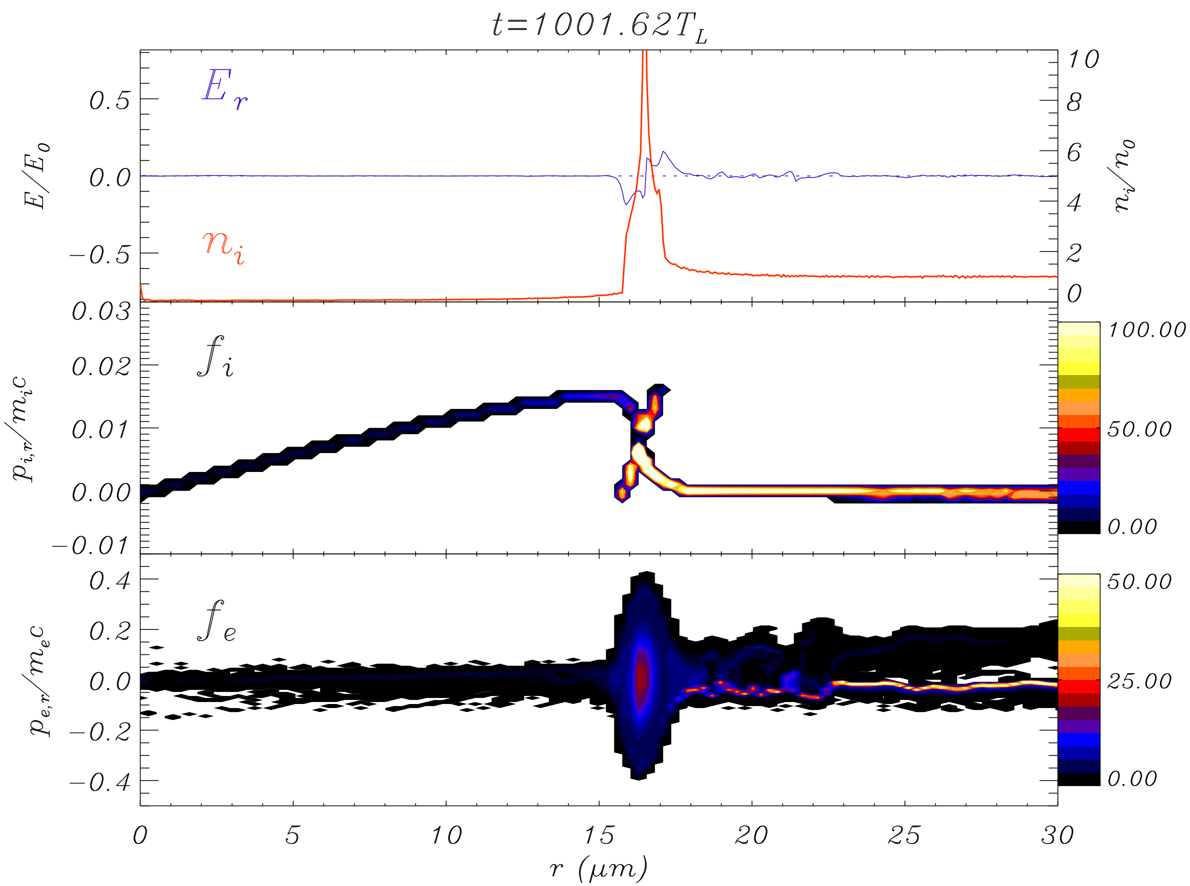

At breaking, strong electron heating occurs

An ambipolar electric field is generated around the density spike

Echo effect is due to "breaking"

Analysis of ion phase space show that hydrodynamical breaking occurs when faster ions overlap the slowest ones

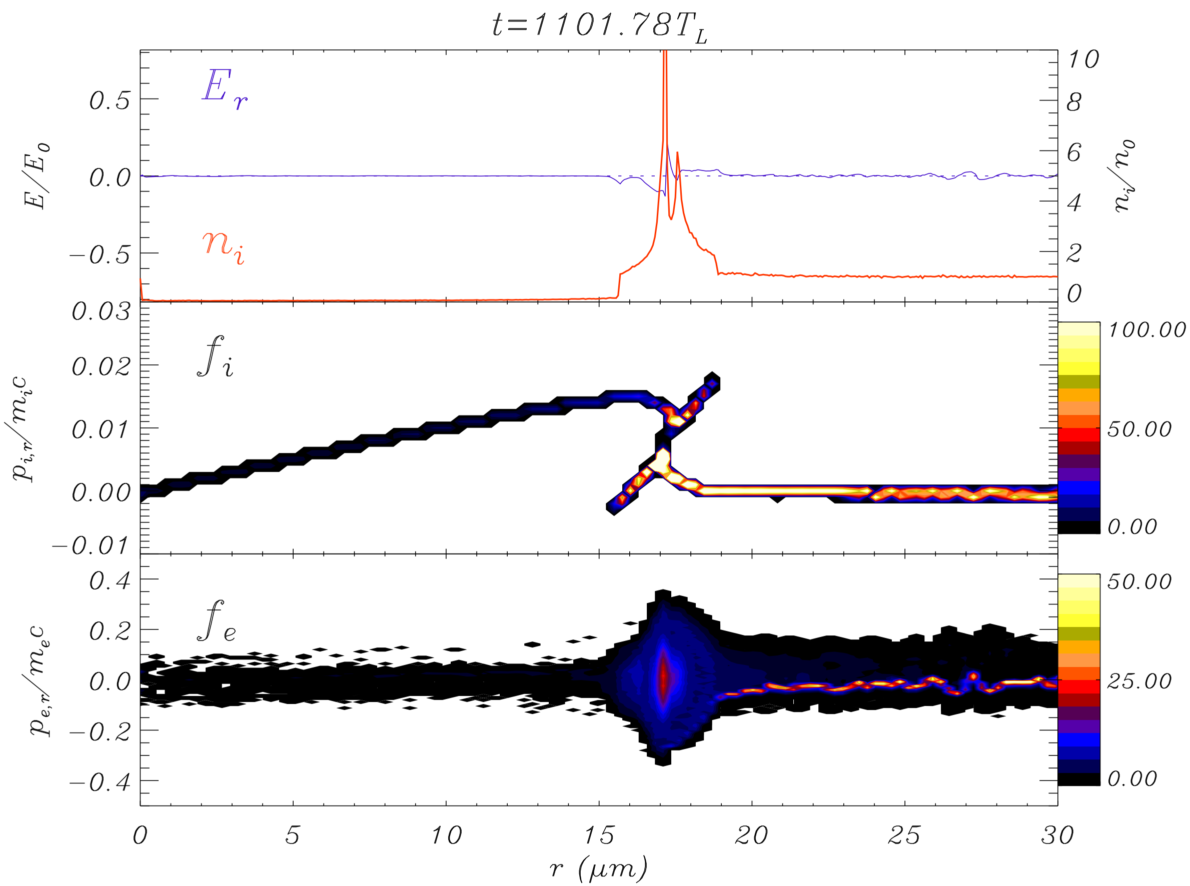

At breaking, strong electron heating occurs

An ambipolar electric field is generated around the density spike

Echo effect is due to “breaking”

Analysis of ion phase space show that hydrodynamical breaking occurs when faster ions overlap the slowest ones

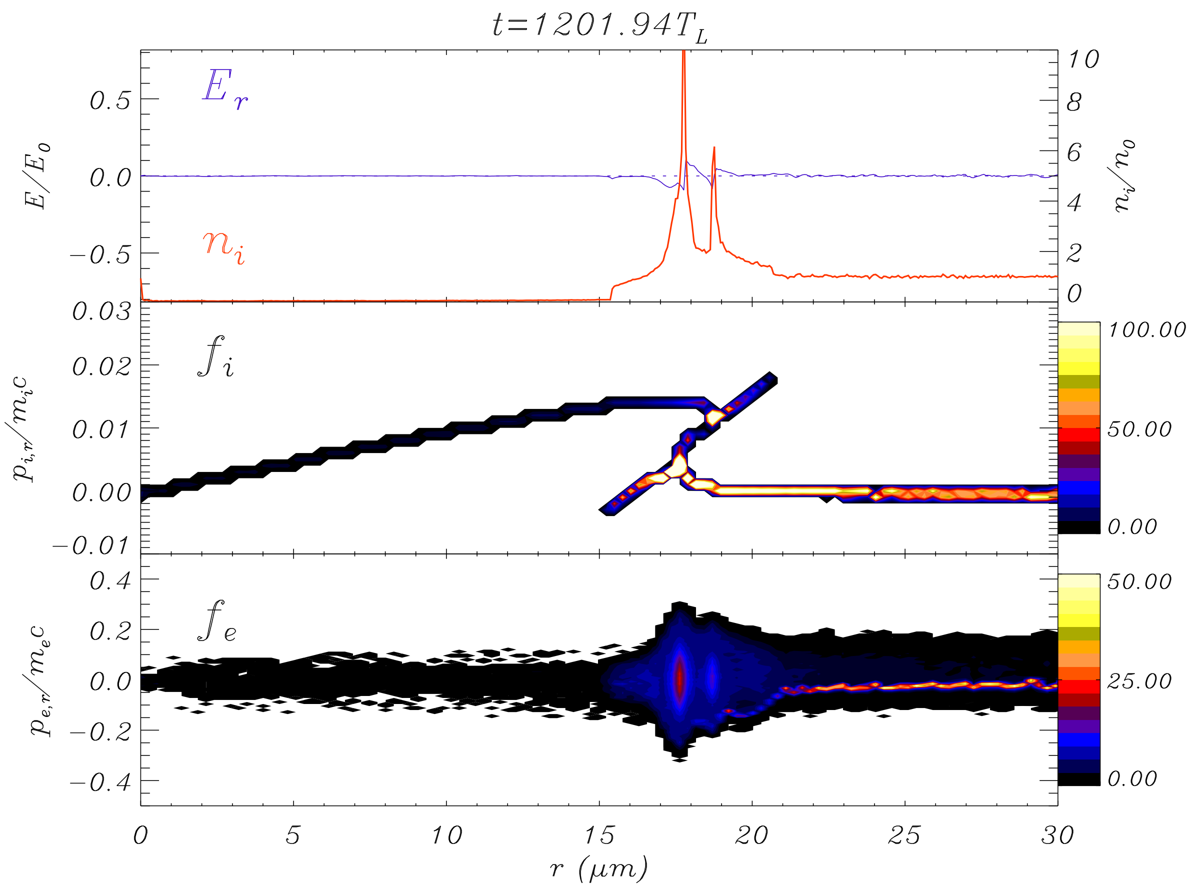

At breaking, strong electron heating occurs

An ambipolar electric field is generated around the density spike

Echo effect is due to “breaking”

Analysis of ion phase space show that hydrodynamical breaking occurs when faster ions overlap the slowest ones

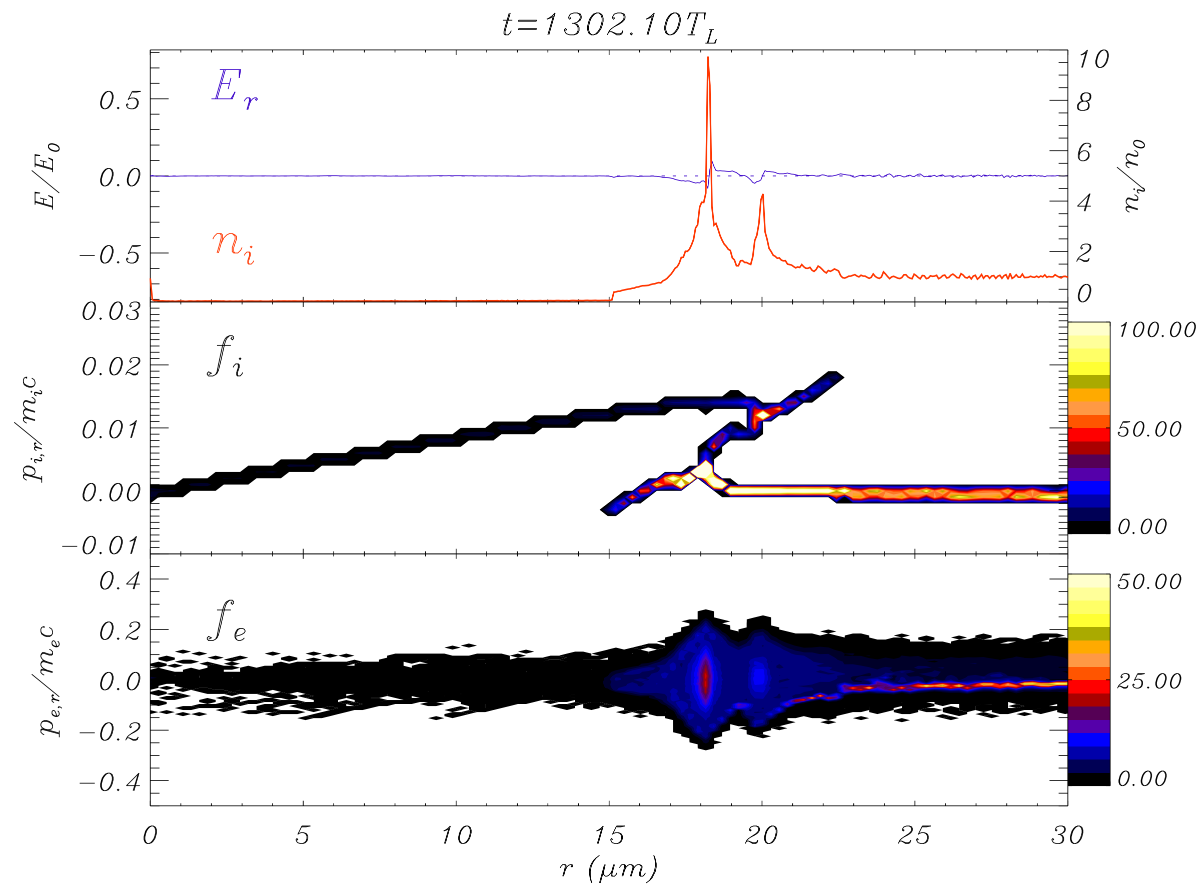

At breaking, strong electron heating occurs

An ambipolar electric field is generated around the density spike

Breaking time and place

Breaking time and place

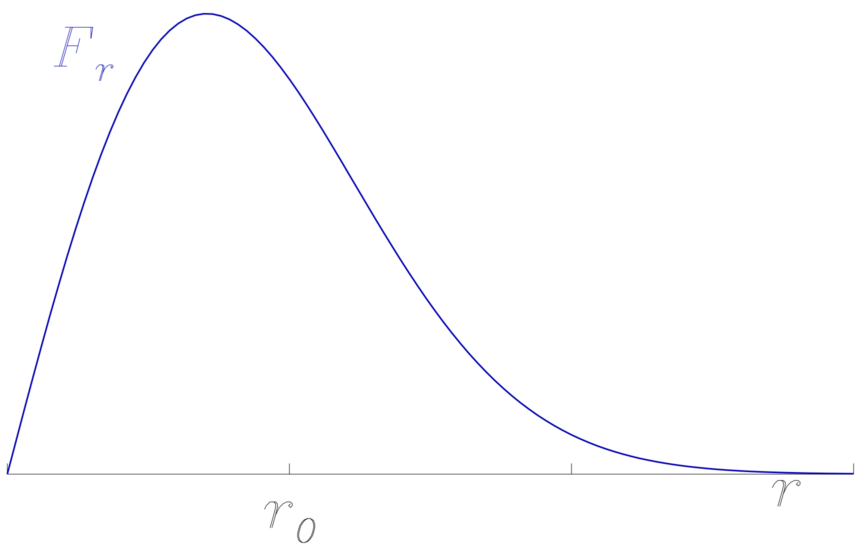

Ions are accelerated by $ZeE_r \simeq ZF_r$.
For $r > r_{max} \simeq r_0$, $dF_r/dr < 0 \Rightarrow$ ions tend to pile up at the edge of the pulse profile

A. Macchi et al, arXiv:physics/0701139

Breaking time and place

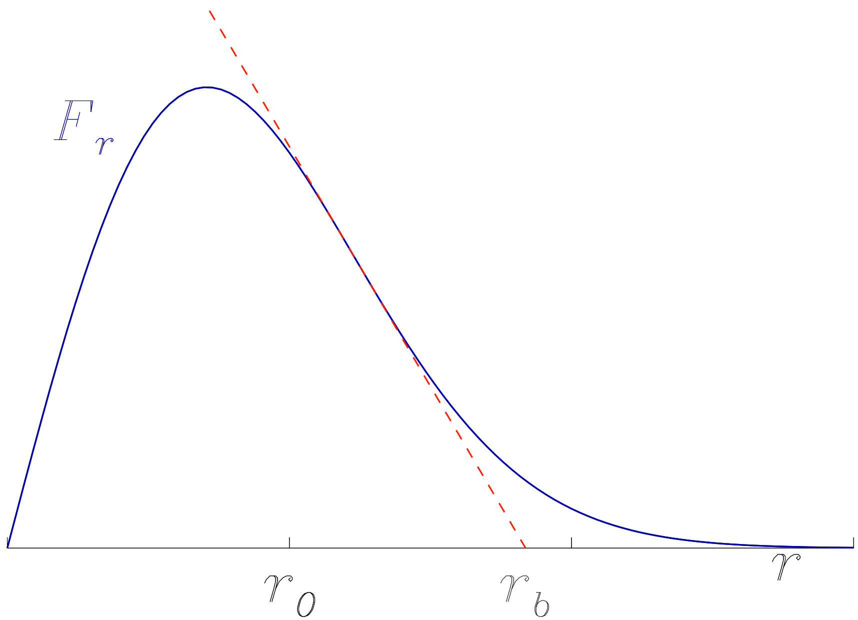

If F_r was a linear function, all ions would get to a same point r_b at the same time t_b.

$$ZF_r \simeq -k(r - r_b)$$

A. Macchi et al, arXiv:physics/0701139

Breaking time and place

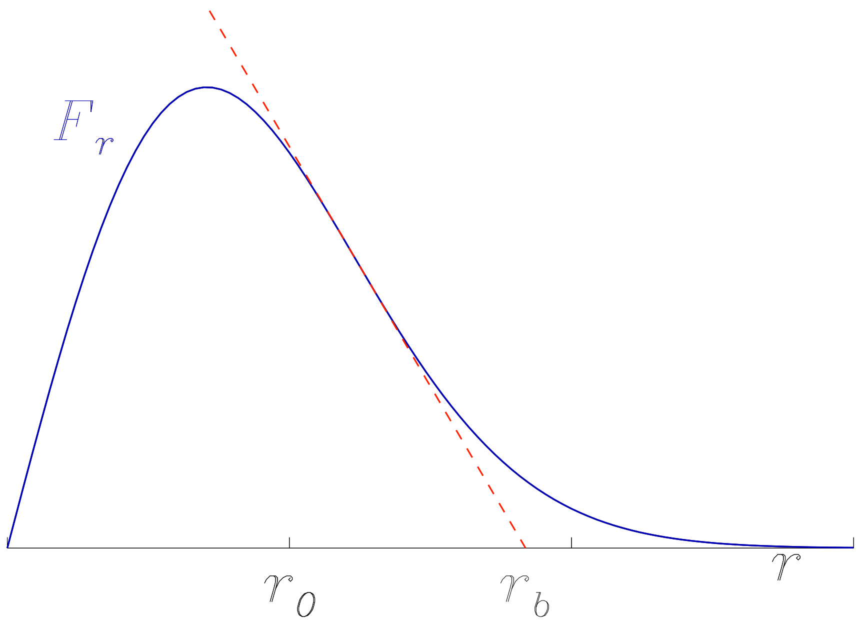

If F_r was a linear function, all ions would get to a same point r_b at the same time t_b.

$$ZF_r \simeq -k(r - r_b)$$

By performing a linear approximation of F_r we obtain

$$r_b = (3/2)^{3/2} r_0 \qquad t_b = \frac{\pi}{2}\sqrt{\frac{k}{m_i}} = \frac{\pi}{2} e^{3/4} \sqrt{\frac{A}{Z}\frac{m_p}{m_e}\frac{r_0}{a_0 c}}$$

A. Macchi et al, arXiv:physics/0701139

Electric field generation after breaking

Electric field generation after breaking

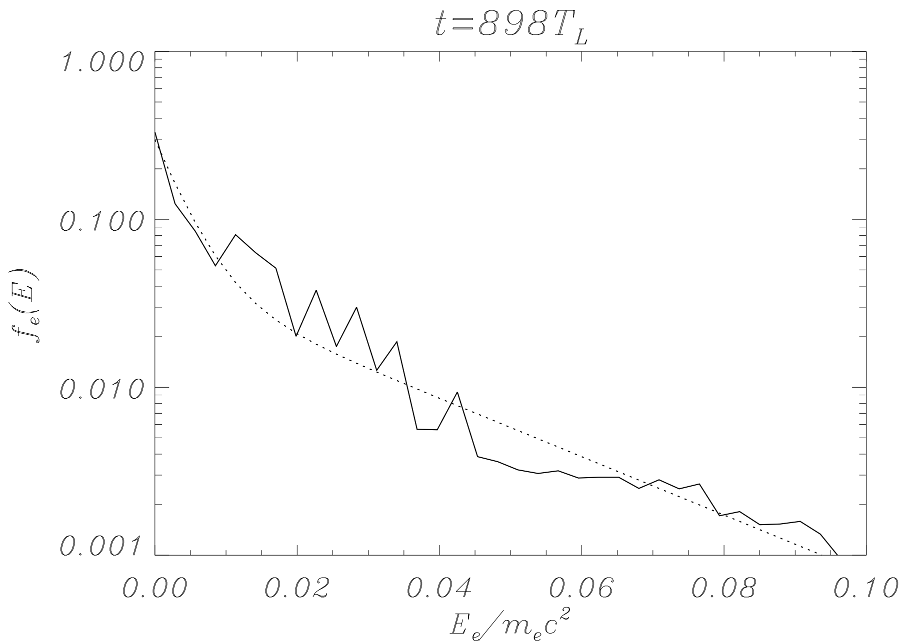

A “hot” electron tail is generated near the breaking point

$T_{hot} \simeq 12.8$ keV $\simeq 6T_{cold}$

A. Macchi et al, arXiv:physics/0701139

Electric field generation after breaking

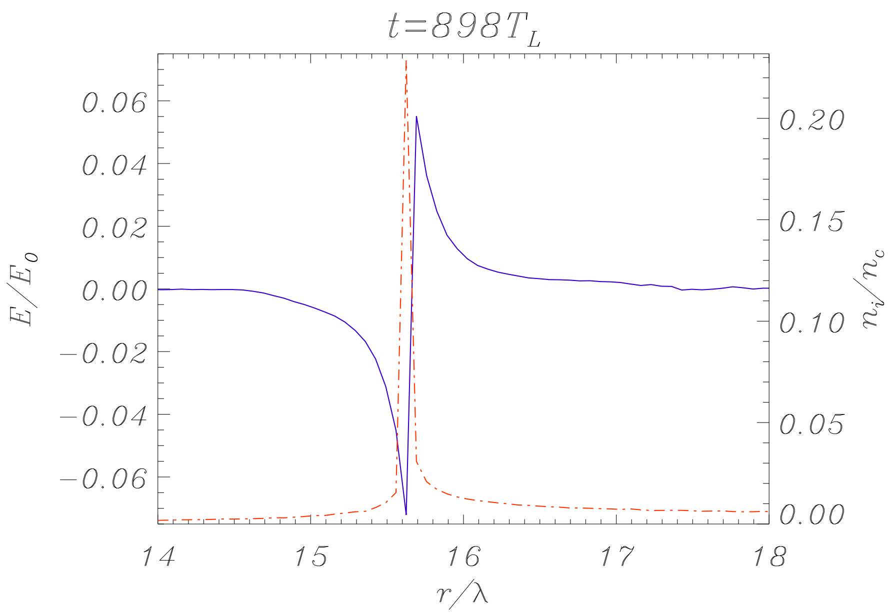

Hot electrons (density n_h) generate an antisymmetrical sheath field (extension ℓ_s, peak field E_s) around the density spike (thickness d)

$$E_s = 2\pi e n_h d \qquad \ell_s = \frac{8\lambda_D^2}{d}$$

A. Macchi et al, arXiv:physics/0701139

Electric field generation after breaking

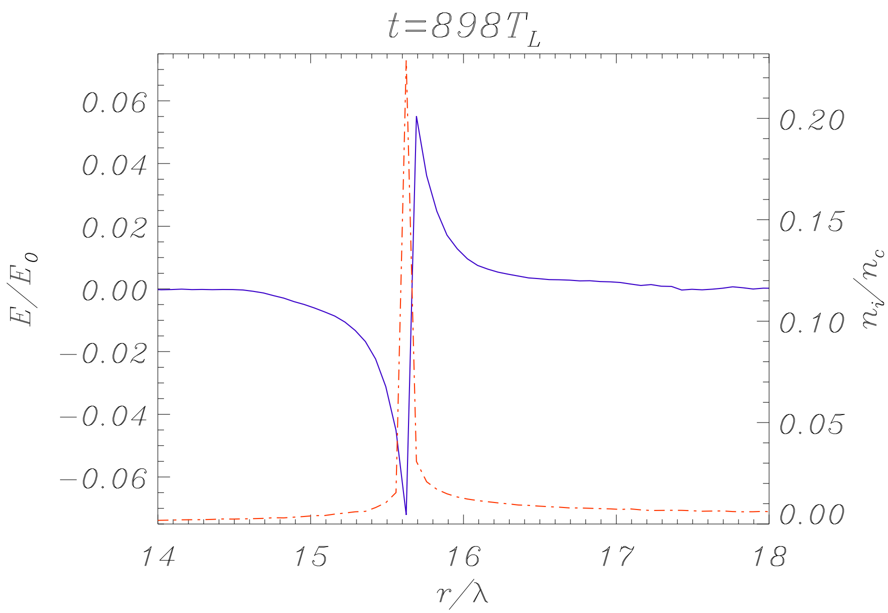

Hot electrons (density n_h) generate an antisymmetrical sheath field (extension ℓ_s, peak field E_s) around the density spike (thickness d)

$$E_s = 2\pi e n_h d \qquad \ell_s = \frac{8\lambda_{\mathsf{D}}^2}{d}$$

Hot electron generation might be ascribed to non-adiabatic electron oscillations across the sharp density gradient or to local two-stream-like instabilities

A. Macchi et al, arXiv:physics/0701139

Ion dynamics after breaking

Ion dynamics after breaking

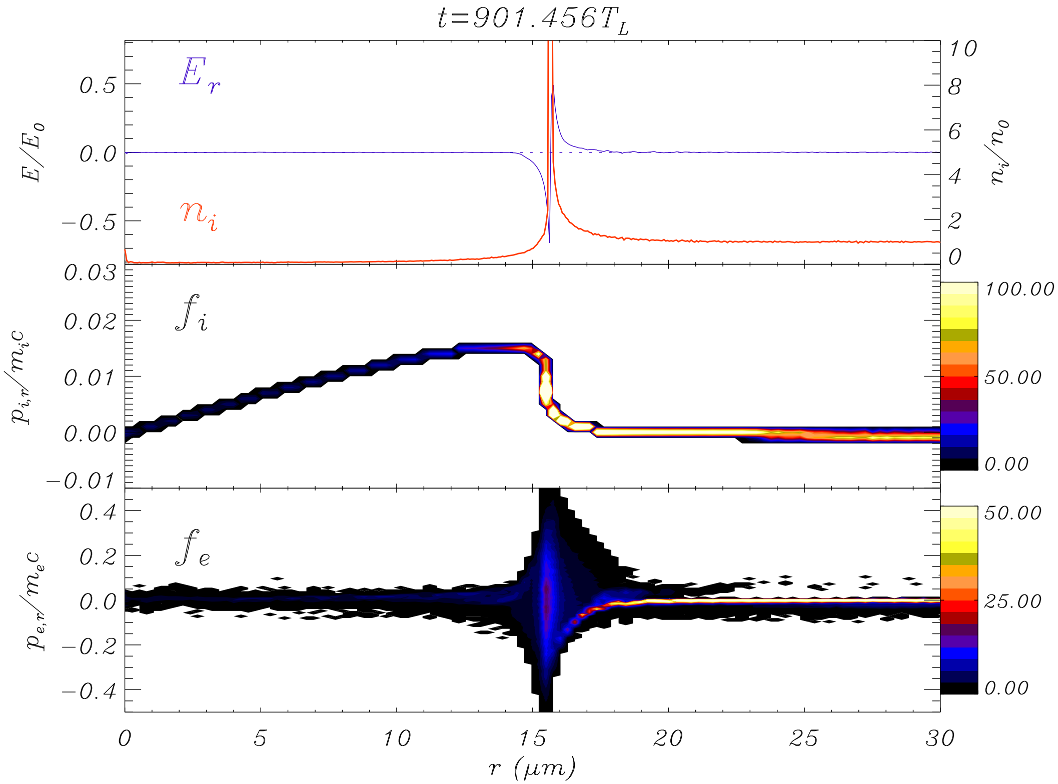

Ion dynamics after breaking

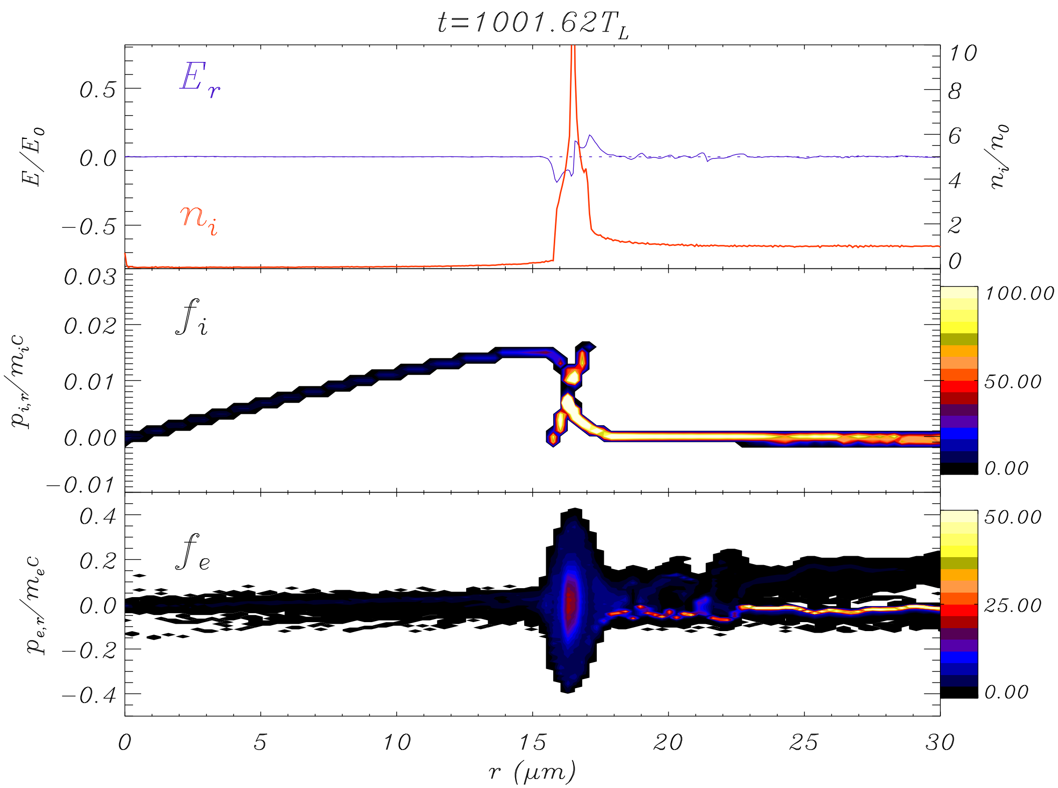

After breaking the ion spectrum “splits”: only faster ions are injected outside the channel

Ion dynamics after breaking

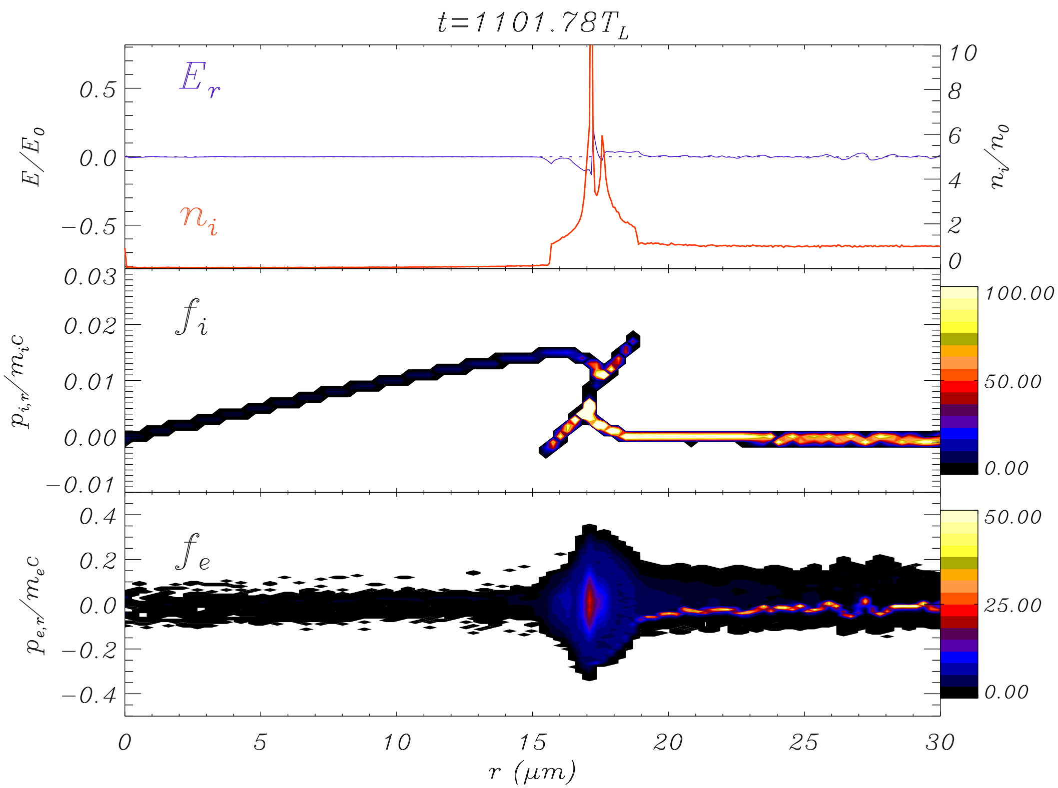

After breaking the ion spectrum “splits”: only faster ions are injected outside the channel

Ion dynamics after breaking

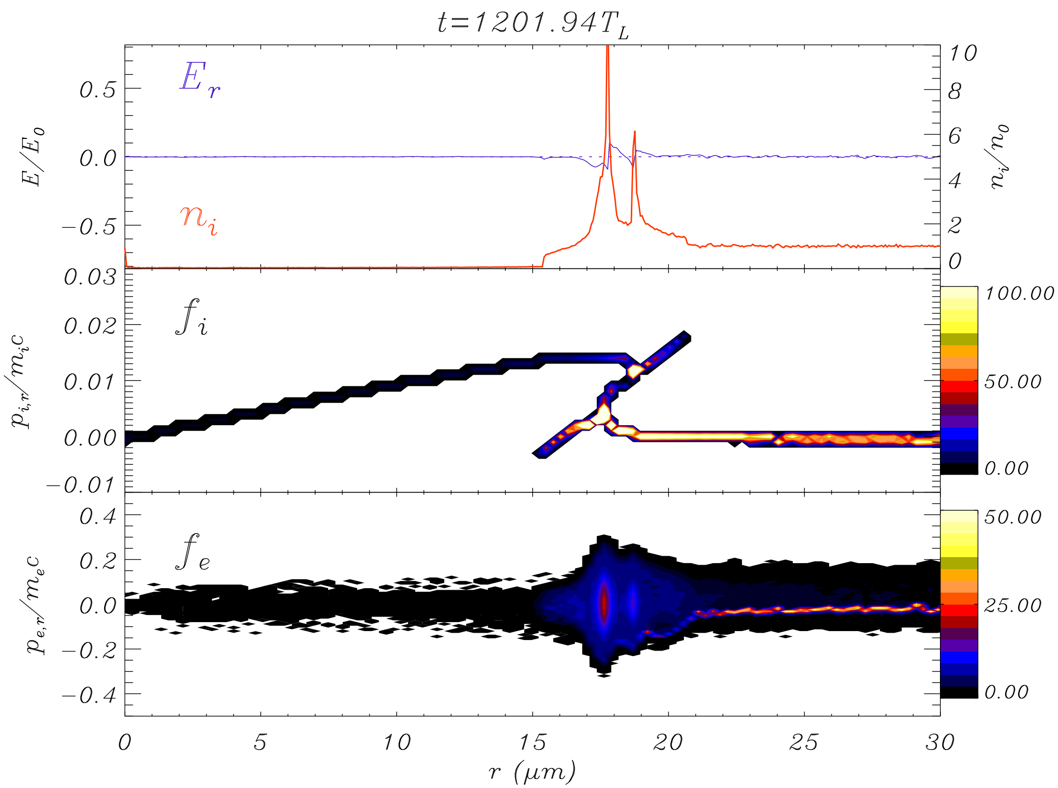

After breaking the ion spectrum "splits": only faster ions are injected outside the channel

Ion dynamics after breaking

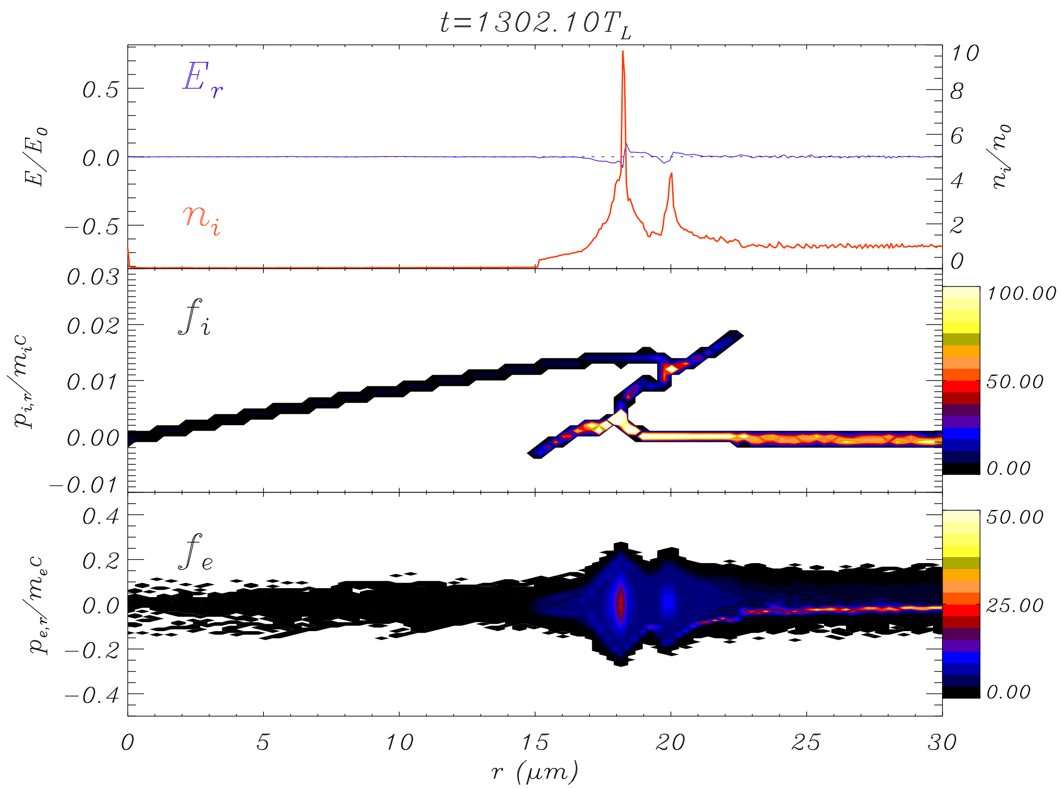

After breaking the ion spectrum "splits": only faster ions are injected outside the channel

Low-energy ions are "reflected" from the inward field and return towards the axis

Ion dynamics after breaking

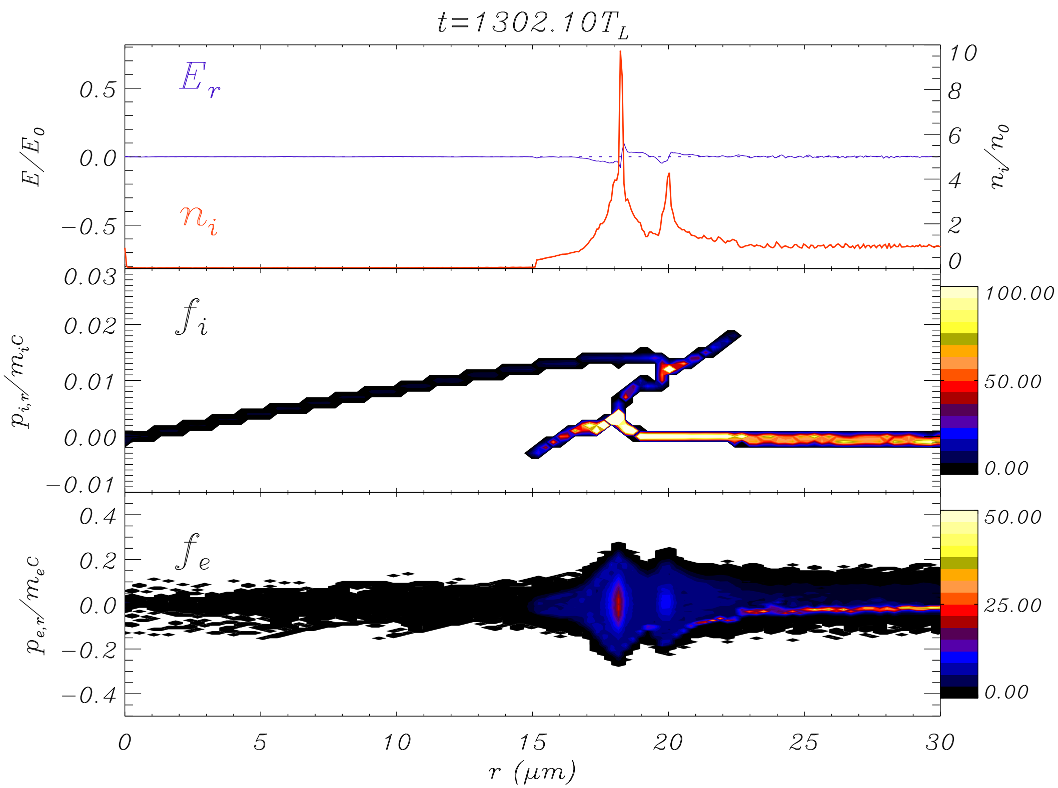

After breaking the ion spectrum “splits”: only faster ions are injected outside the channel

Low-energy ions are “reflected” from the inward field and return towards the axis

Ion dynamics after breaking

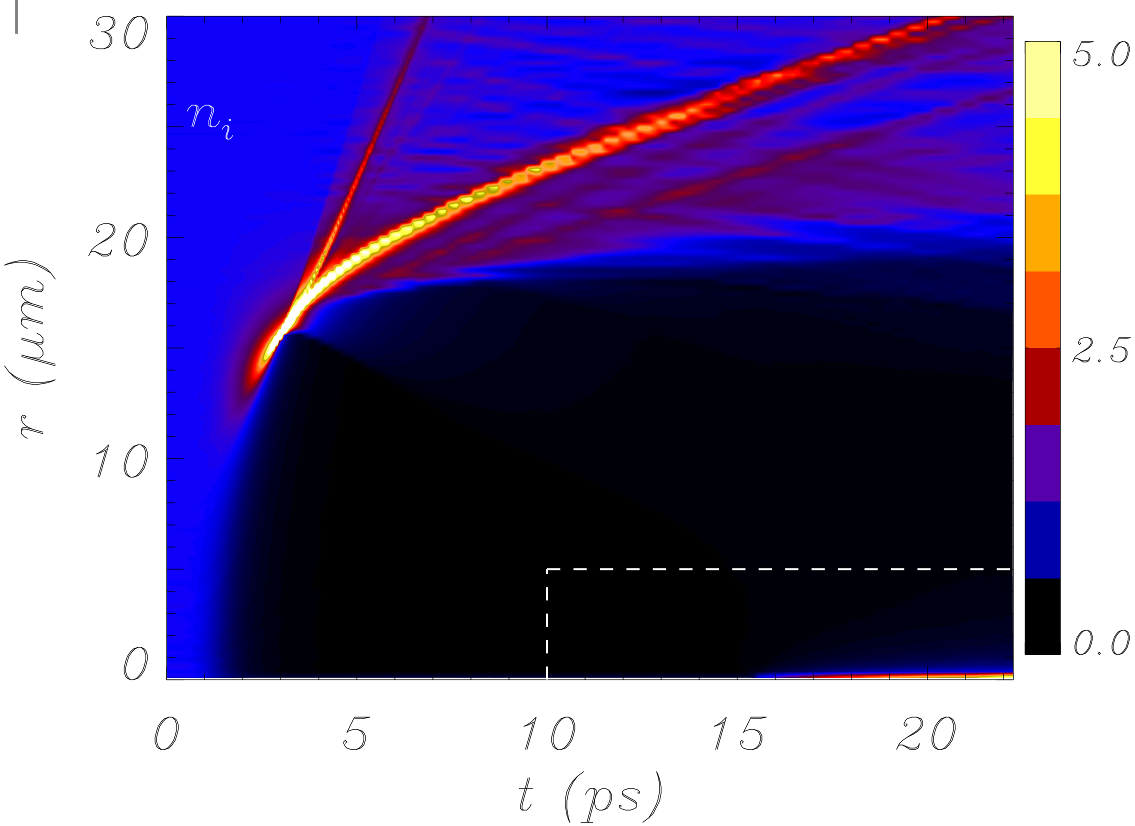

After breaking the ion spectrum "splits": only faster ions are injected outside the channel

Low-energy ions are "reflected" from the inward field and return towards the axis

A thin filament of plasma is generated on the axis at late times

Experimental indication: see M. Borghesi et al, PRL **78**, 879 (1997)

Ion dynamics after breaking

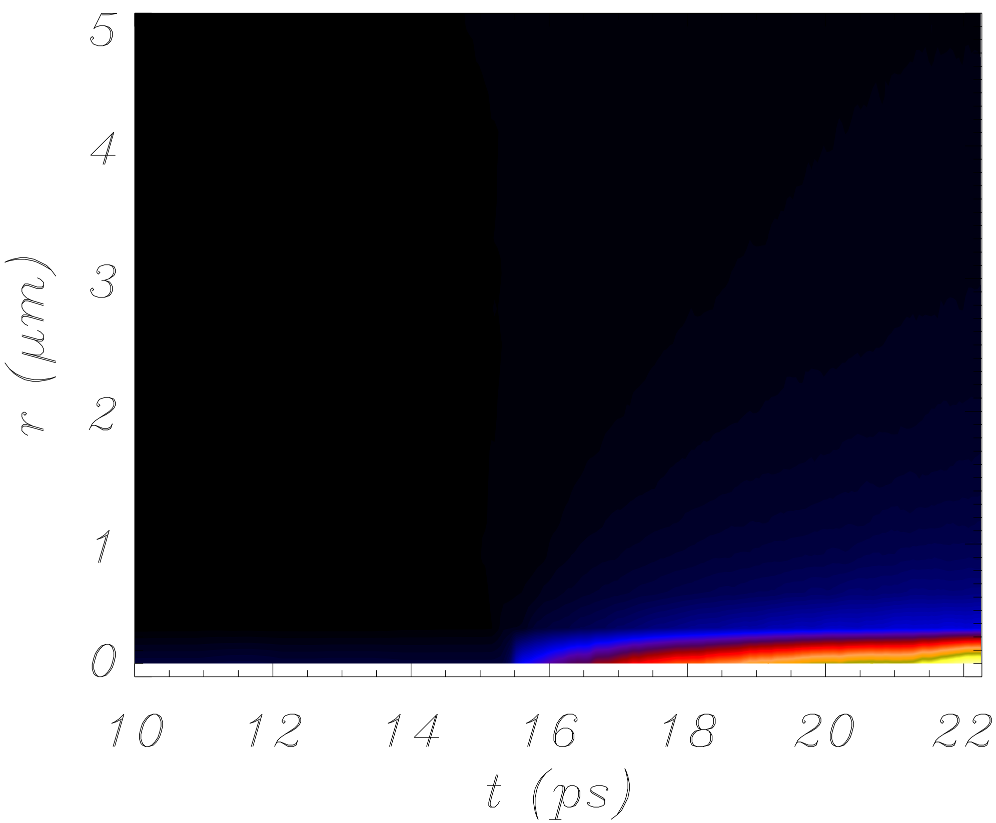

After breaking the ion spectrum "splits": only faster ions are injected outside the channel

Low-energy ions are "reflected" from the inward field and return towards the axis

A thin filament of plasma is generated on the axis at late times

Experimental indication: see M. Borghesi et al, PRL **78**, 879 (1997)

Conclusions of Part 1

Conclusions of Part 1

- A “minimal” 1D electrostatic, ponderomotive, kinetic model has been used to interpretate experimental results in the charge-displacement self-channeling regime of laser propagation in underdense plasmas

Conclusions of Part 1

- A “minimal” 1D electrostatic, ponderomotive, kinetic model has been used to interpretate experimental results in the charge-displacement self-channeling regime of laser propagation in underdense plasmas
- Simulations gave an insight into ion dynamics and electric field generation

Conclusions of Part 1

- A “minimal” 1D electrostatic, ponderomotive, kinetic model has been used to interpretate experimental results in the charge-displacement self-channeling regime of laser propagation in underdense plasmas
- Simulations gave an insight into ion dynamics and electric field generation
- Hydrodynamical breaking of the ion fluid leads to non-trivial effects (electric field “echo”, ion reflection . . .)

PART 2: LONGITUDINAL ION ACCELERATION BY CIRCULARLY POLARIZED LASER PULSES IN AN OVERDENSE PLASMA

1D simulation example of ion acceleration

1D simulation example of ion acceleration

1D PIC simulation, 26 cycles pulse, normal incidence, linear polarization, $a = 16.0$, $n_{e0}/n_c = 10$.

($\lambda = 1\mu$m $\rightarrow I = 3.5 \times 10^{20}$ W/cm^2, $\tau_L = 86$ fs, $n_e = 10^{22}$ cm^{-3}.)

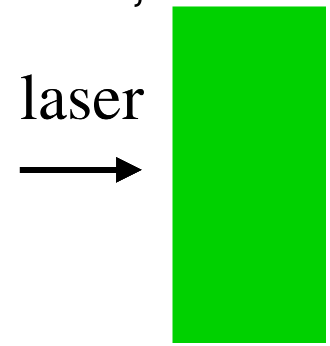

1D simulation example of ion acceleration

1D PIC simulation, 26 cycles pulse, normal incidence, linear polarization, $a = 16.0$, $n_{e0}/n_c = 10$.
($\lambda = 1\mu$m $\rightarrow I = 3.5 \times 10^{20}$ W/cm^2, $\tau_L = 86$ fs,
$n_e = 10^{22}$ cm^{-3}.)

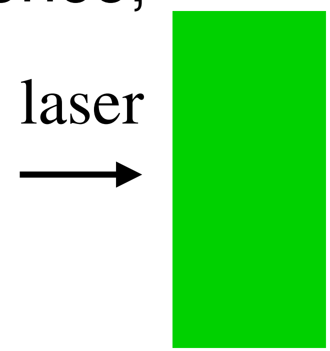

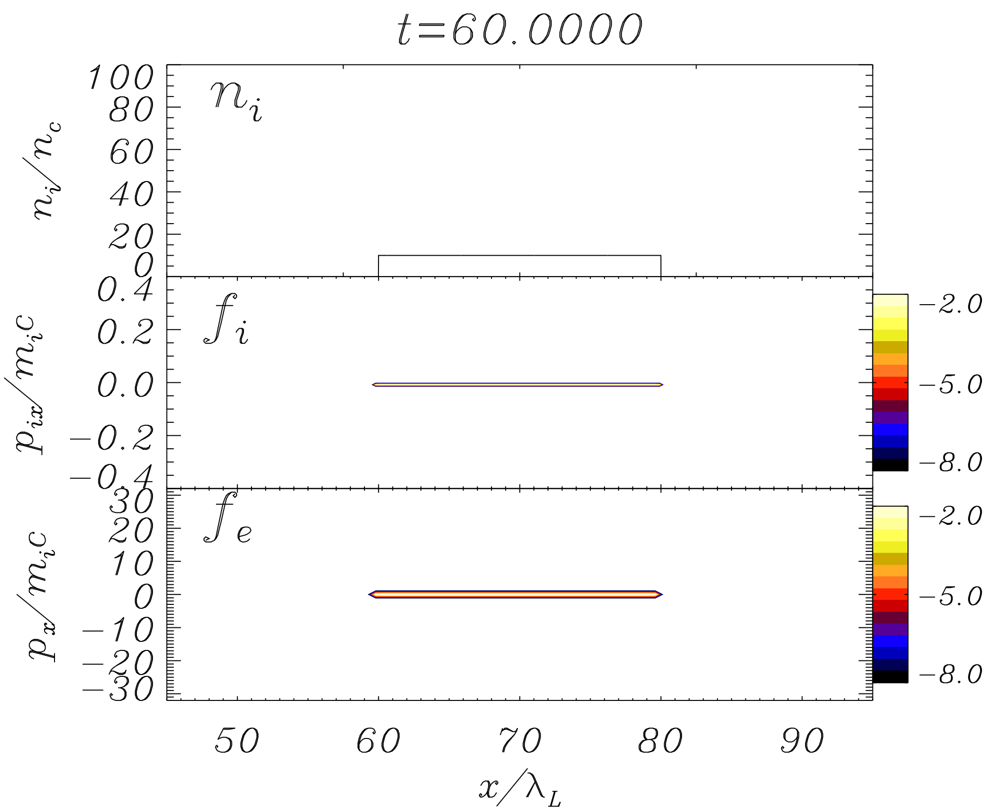

1D simulation example of ion acceleration

1D PIC simulation, 26 cycles pulse, normal incidence, linear polarization, $a = 16.0$, $n_{e0}/n_c = 10$.

($\lambda = 1\mu$m $\rightarrow I = 3.5 \times 10^{20}$ W/cm^2, $\tau_L = 86$ fs, $n_e = 10^{22}$ cm^{-3}.)

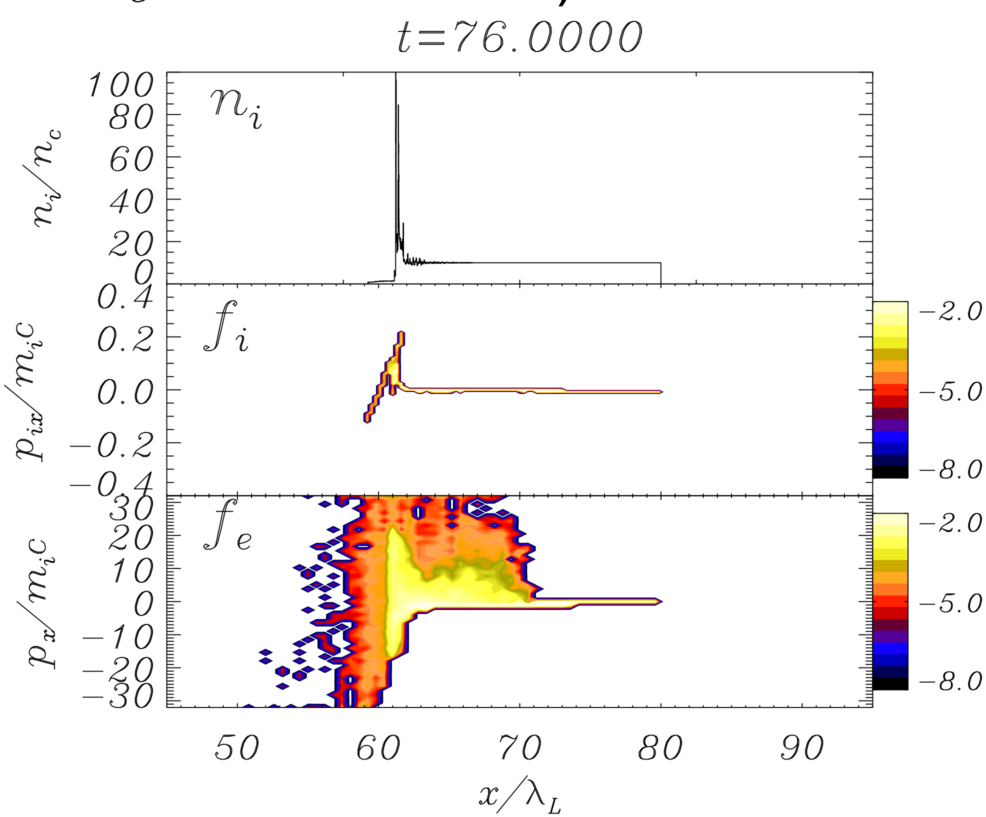

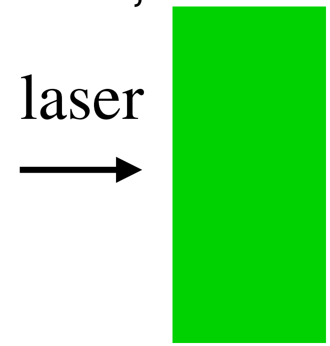

1D simulation example of ion acceleration

1D PIC simulation, 26 cycles pulse, normal incidence, linear polarization, $a = 16.0$, $n_{e0}/n_c = 10$.

($\lambda = 1\mu$m $\rightarrow I = 3.5 \times 10^{20}$ W/cm^2, $\tau_L = 86$ fs, $n_e = 10^{22}$ cm^{-3}.)

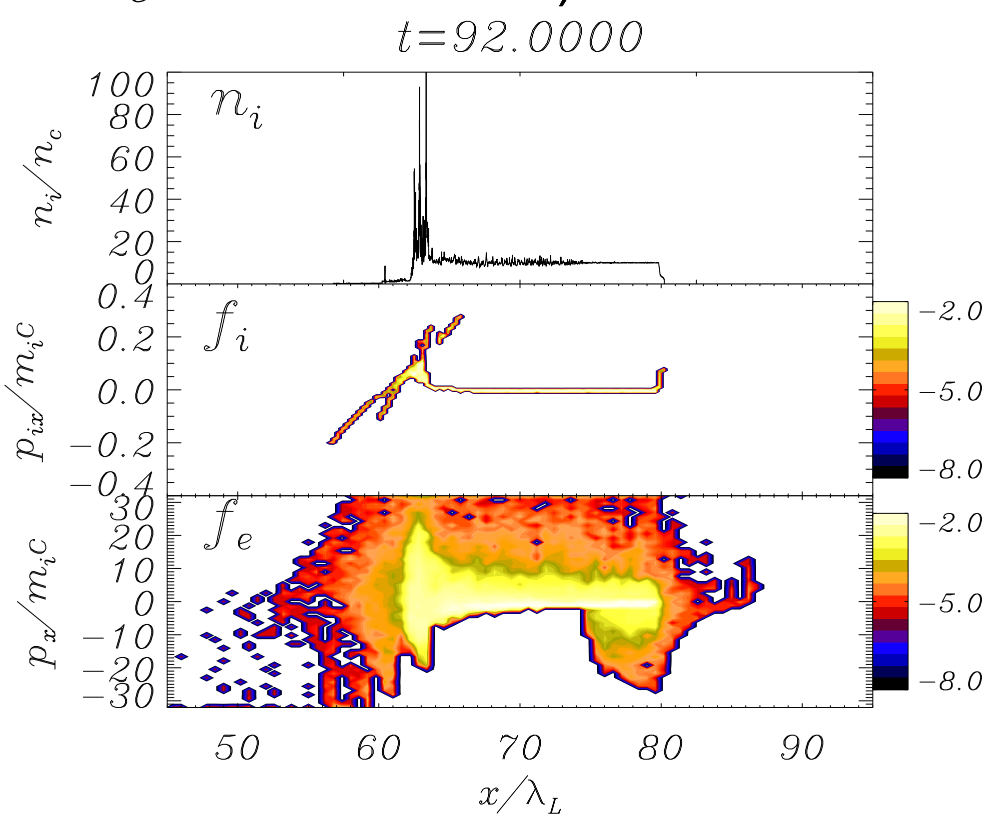

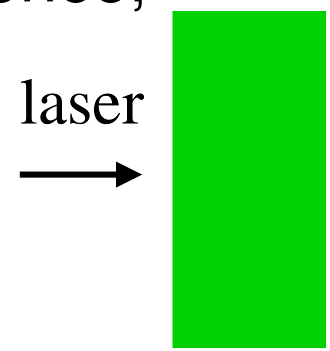

1D simulation example of ion acceleration

1D PIC simulation, 26 cycles pulse, normal incidence, linear polarization, $a = 16.0$, $n_{e0}/n_c = 10$.

($\lambda = 1\mu$m $\rightarrow I = 3.5 \times 10^{20}$ W/cm^2, $\tau_L = 86$ fs, $n_e = 10^{22}$ cm^{-3}.)

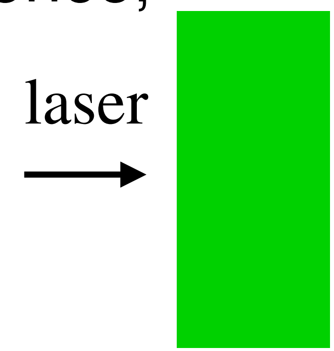

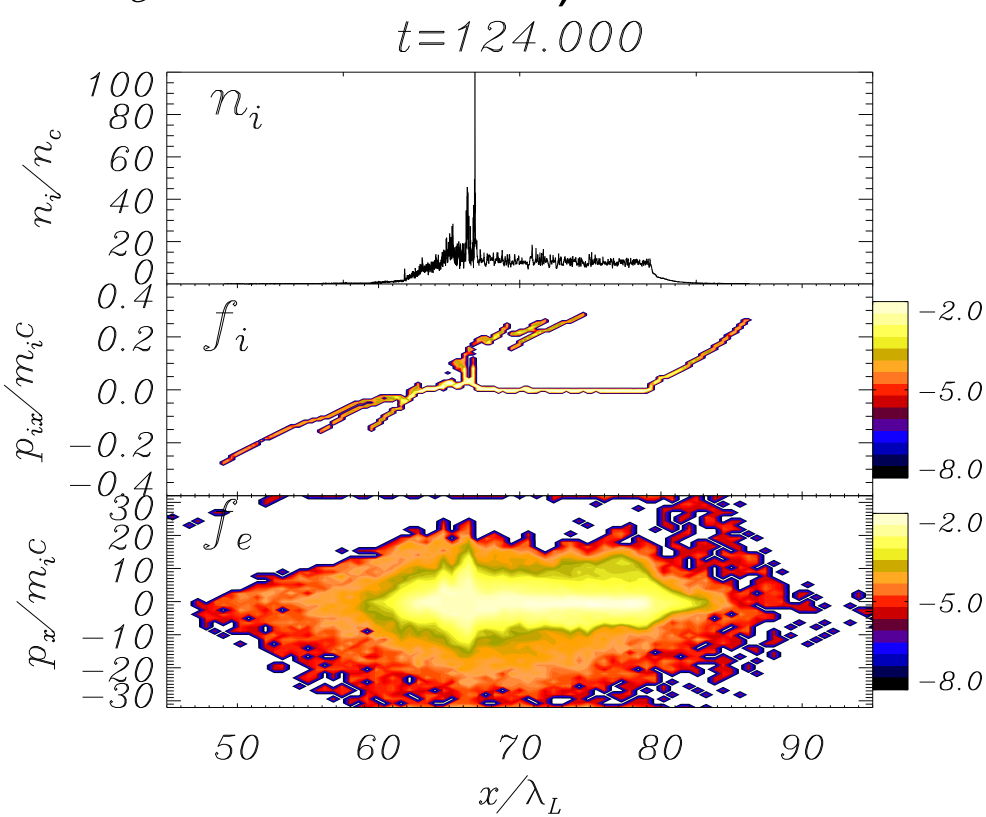

polyLab

1D simulation example of ion acceleration

1D PIC simulation, 26 cycles pulse, normal incidence, linear polarization, $a = 16.0$, $n_{e0}/n_c = 10$.
($\lambda = 1\mu$m $\rightarrow I = 3.5 \times 10^{20}$ W/cm^2, $\tau_L = 86$ fs, $n_e = 10^{22}$ cm^{-3}.)

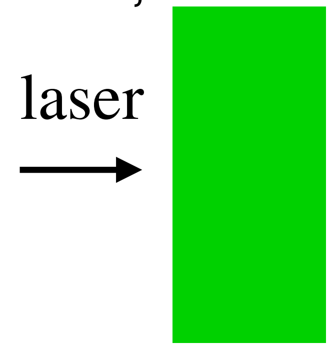

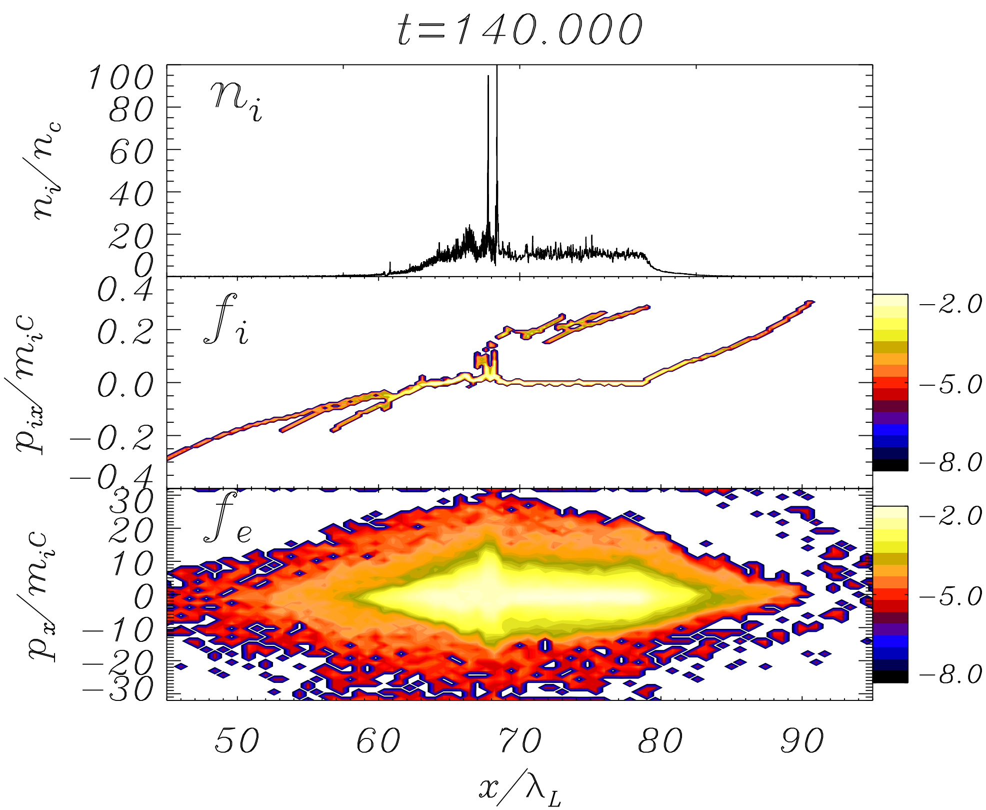

1D simulation example of ion acceleration

1D PIC simulation, 26 cycles pulse, normal incidence, linear polarization, $a = 16.0$, $n_{e0}/n_c = 10$.
($\lambda = 1\mu$m $\rightarrow I = 3.5 \times 10^{20}$ W/cm^2, $\tau_L = 86$ fs, $n_e = 10^{22}$ cm^{-3}.)

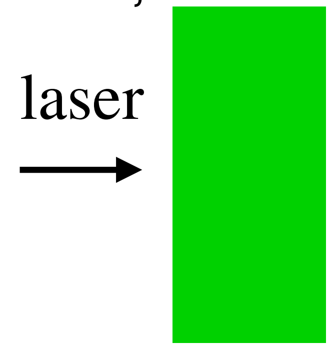

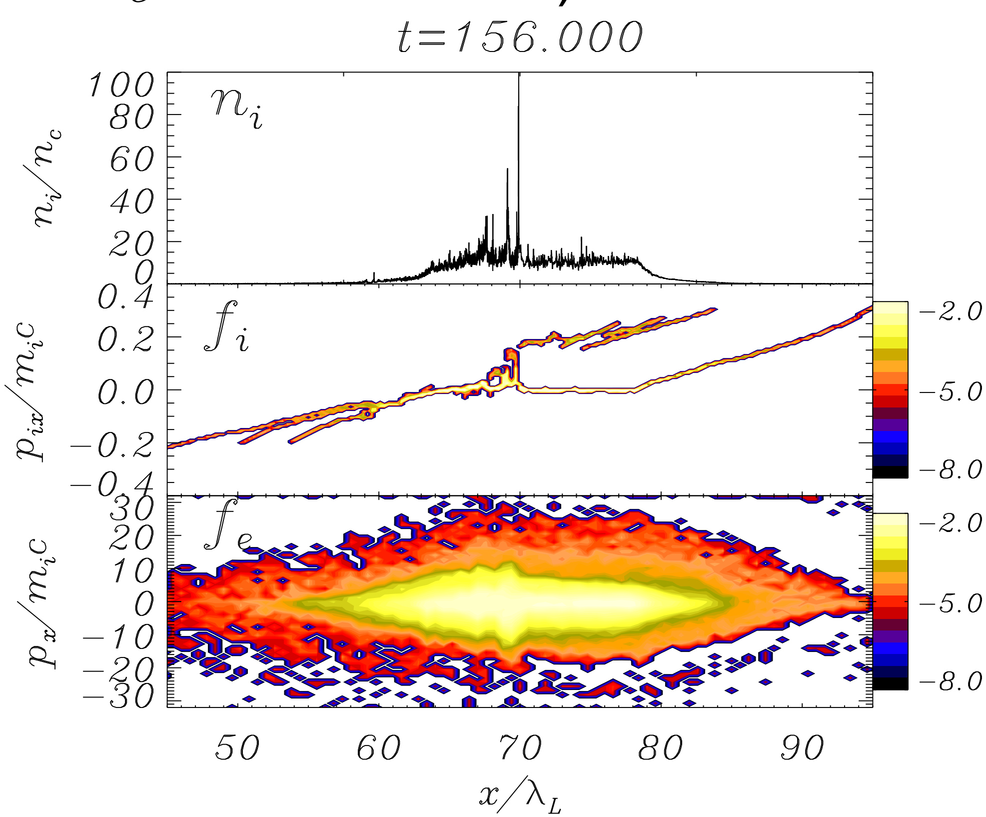

1D simulation example of ion acceleration

1D PIC simulation, 26 cycles pulse, normal incidence, linear polarization, $a = 16.0$, $n_{e0}/n_c = 10$.
($\lambda = 1\mu$m $\rightarrow I = 3.5 \times 10^{20}$ W/cm^2, $\tau_L = 86$ fs, $n_e = 10^{22}$ cm^{-3}.)

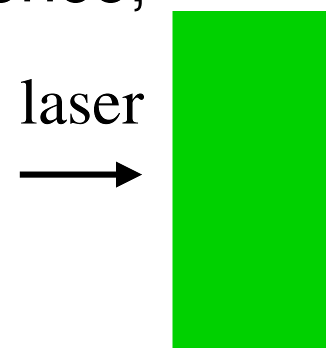

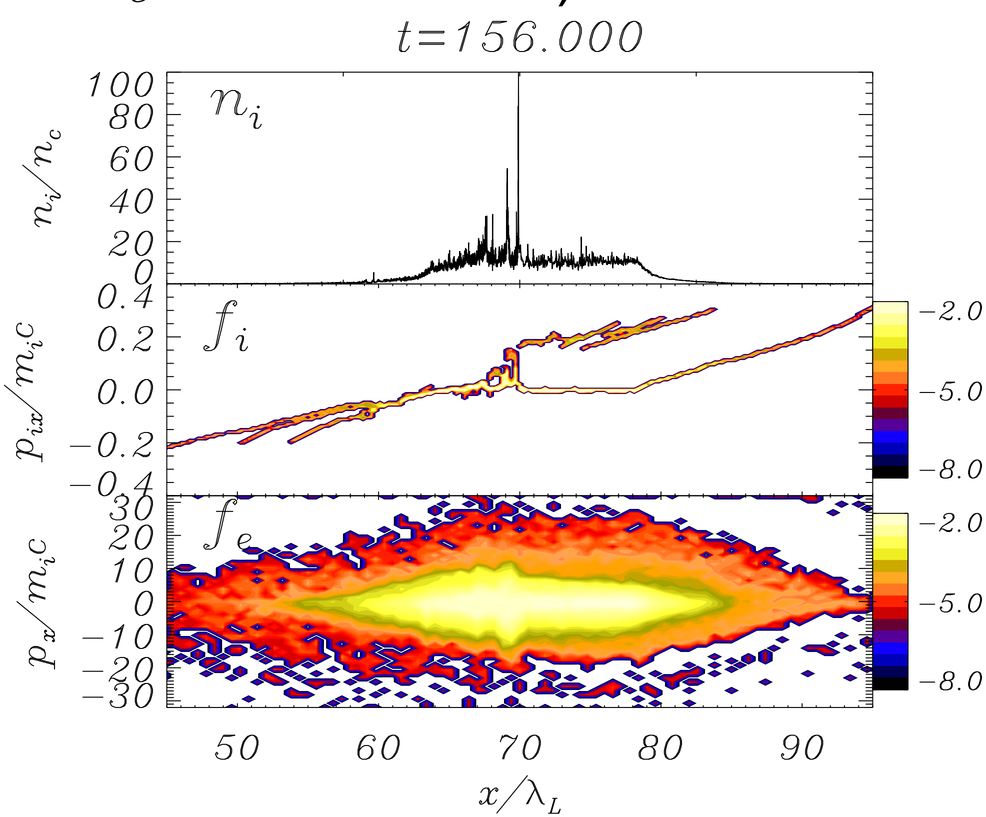

Three groups of MeV ions: two from “sheath” acceleration (from front and rear sides), one from the front – “shock” acceleration?

[Silva et al, PRL **95**, 195002 (2004)]

1D simulation example of ion acceleration

1D PIC simulation, 26 cycles pulse, normal incidence, linear polarization, $a = 16.0$, $n_{e0}/n_c = 10$.
($\lambda = 1\mu$m $\rightarrow I = 3.5 \times 10^{20}$ W/cm^2, $\tau_L = 86$ fs, $n_e = 10^{22}$ cm^{-3}.)

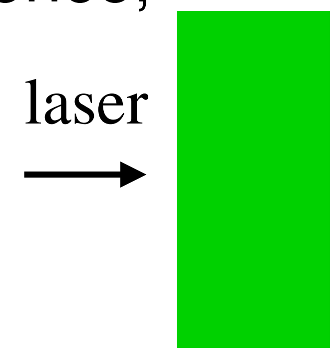

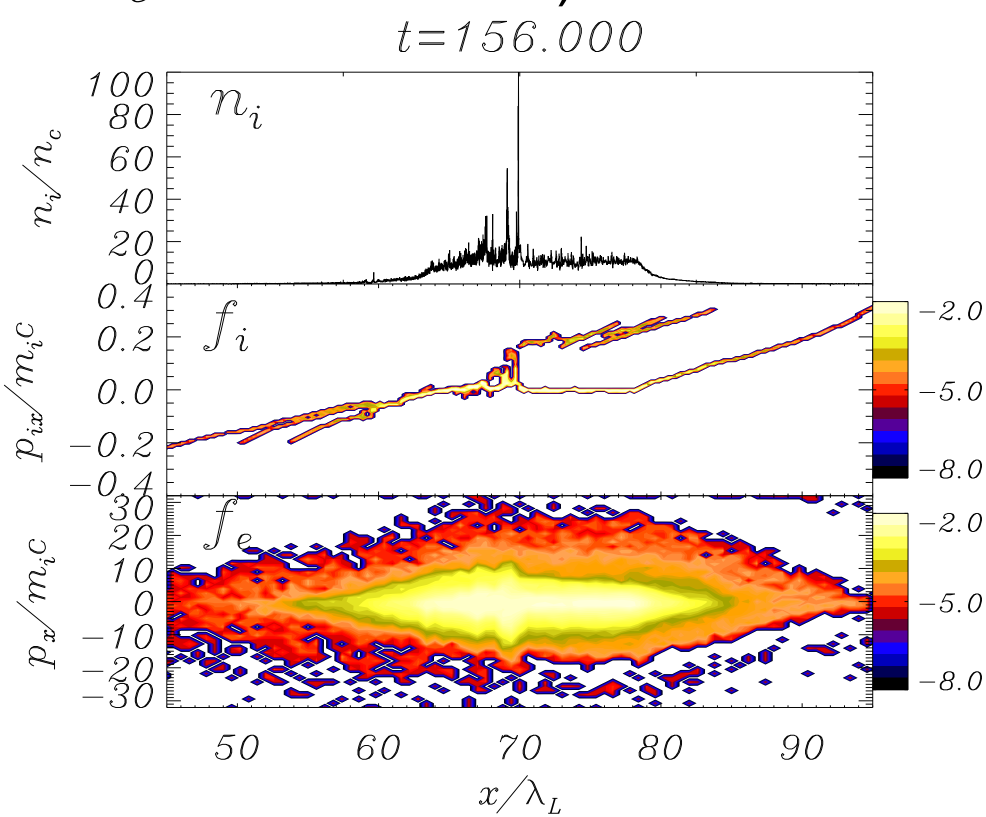

Three groups of MeV ions: two from "sheath" acceleration (from front and rear sides), one from the front – "shock" acceleration?

[Silva et al, PRL **95**, 195002 (2004)]

Electrons are heated up to several tens of MeV

Switch fast electrons off

- Fast electron generation at a steep laser-plasma interface requires an oscillating force across the boundary.

Switch fast electrons off

- Fast electron generation at a steep laser-plasma interface requires an oscillating force across the boundary.
- For normal incidence, it is the $2\omega_L$ component of the $\mathbf{v} \times \mathbf{B}$ force.

Switch fast electrons off

- Fast electron generation at a steep laser-plasma interface requires an oscillating force across the boundary.
- For normal incidence, it is the $2\omega_L$ component of the $\mathbf{v} \times \mathbf{B}$ force.
- For circular polarization, the $2\omega_L$ component vanishes; only the secular ($0\omega_L$) component remains

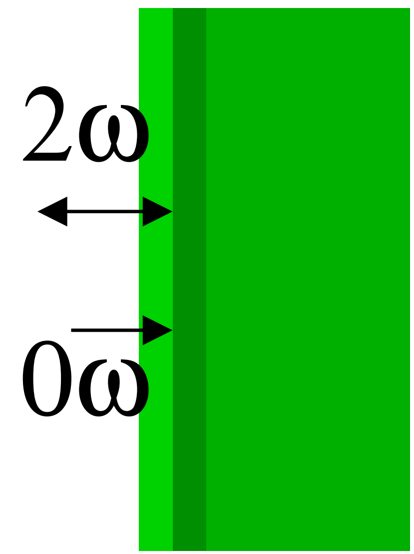

Switch fast electrons off

- Fast electron generation at a steep laser-plasma interface requires an oscillating force across the boundary.
- For normal incidence, it is the $2\omega_L$ component of the $\mathbf{v} \times \mathbf{B}$ force.
- For circular polarization, the $2\omega_L$ component vanishes; only the secular ($0\omega_L$) component remains

$\Rightarrow$ The laser plasma interaction is dominated by radiation pressure (rather than by fast electron generation and related effects)

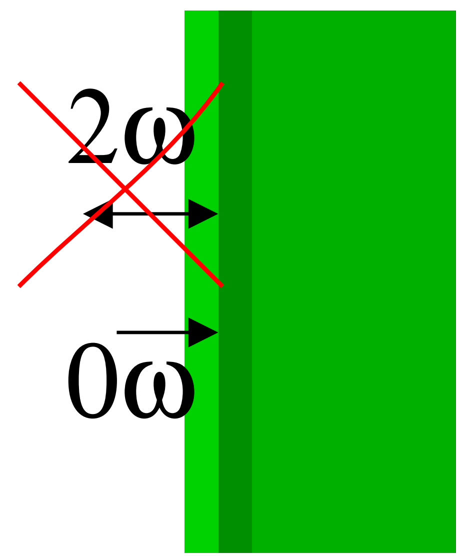

Circular polarization

Circular polarization

1D PIC simulation, circular polarization
$a = 11.3 \Rightarrow$ same energy of the linear polarization case;
other parameters are the same

T. V. Liseikina and A. Macchi, arXiv:0705.4019, Appl. Phys. Lett. (in press).

Circular polarization

1D PIC simulation, circular polarization
$a = 11.3 \Rightarrow$ same energy of the linear polarization case;
other parameters are the same

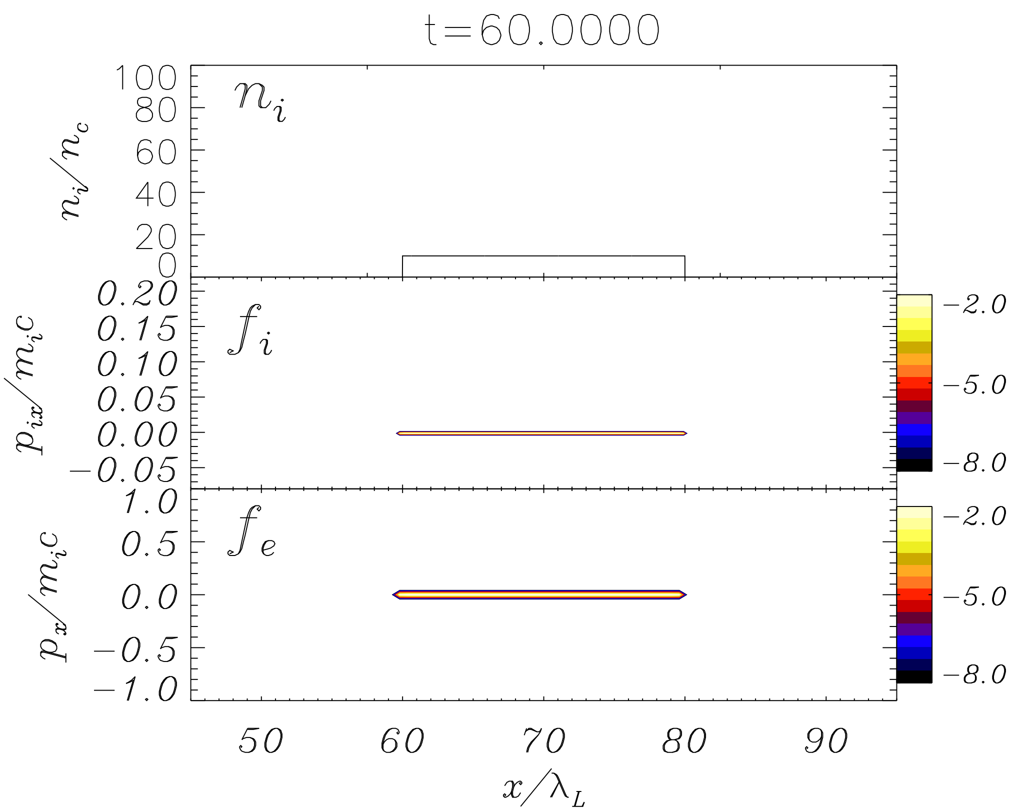

T. V. Liseikina and A. Macchi, arXiv:0705.4019, Appl. Phys. Lett. (in press).

Circular polarization

1D PIC simulation, circular polarization
$a = 11.3 \Rightarrow$ same energy of the linear polarization case; other parameters are the same

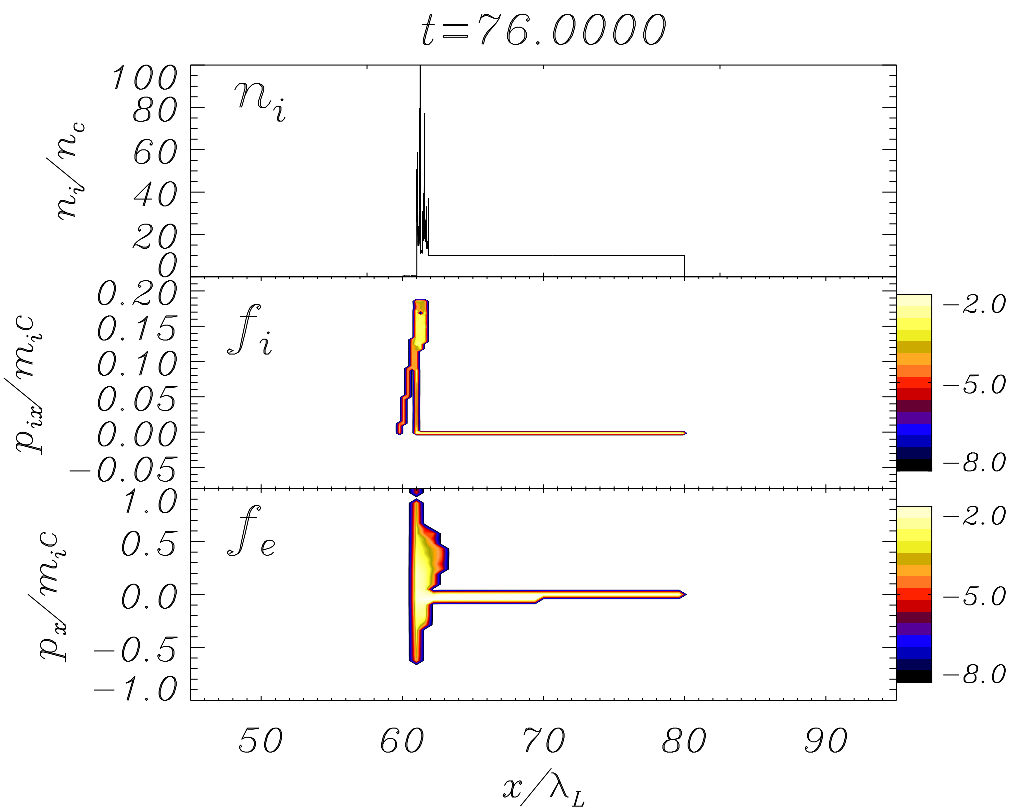

T. V. Liseikina and A. Macchi, arXiv:0705.4019, Appl. Phys. Lett. (in press).

Circular polarization

1D PIC simulation, circular polarization
$a = 11.3 \Rightarrow$ same energy of the linear polarization case; other parameters are the same

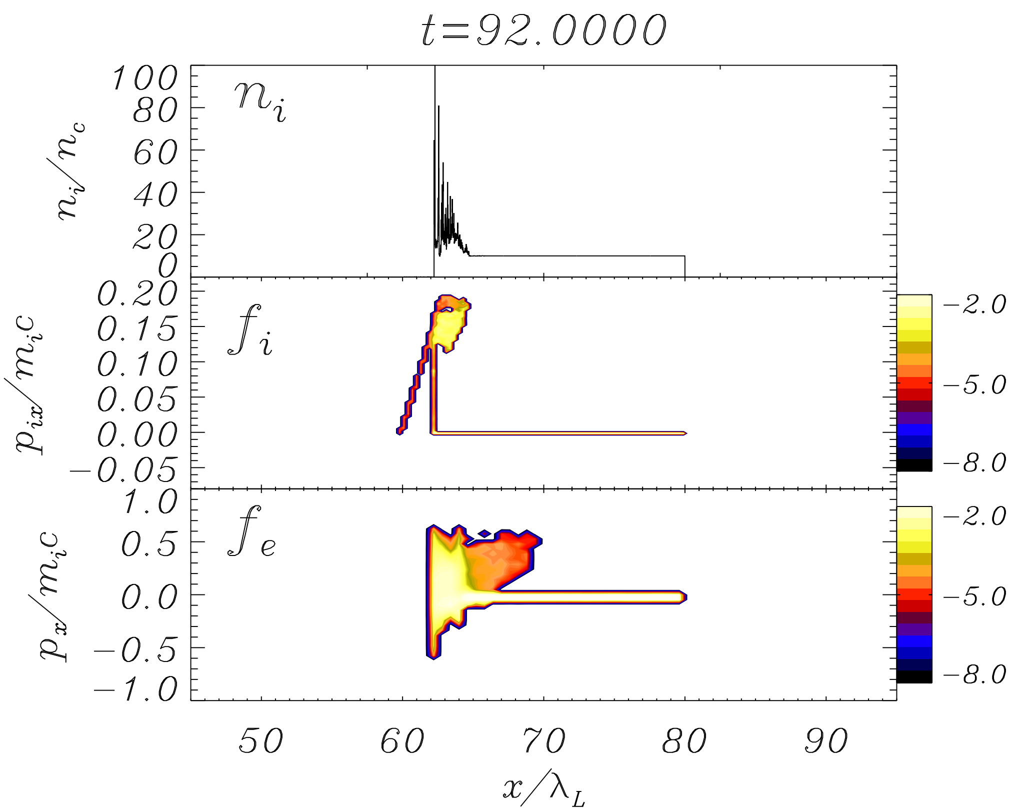

T. V. Liseikina and A. Macchi, arXiv:0705.4019, Appl. Phys. Lett. (in press).

Circular polarization

1D PIC simulation, circular polarization

$a = 11.3 \Rightarrow$ same energy of the linear polarization case; other parameters are the same

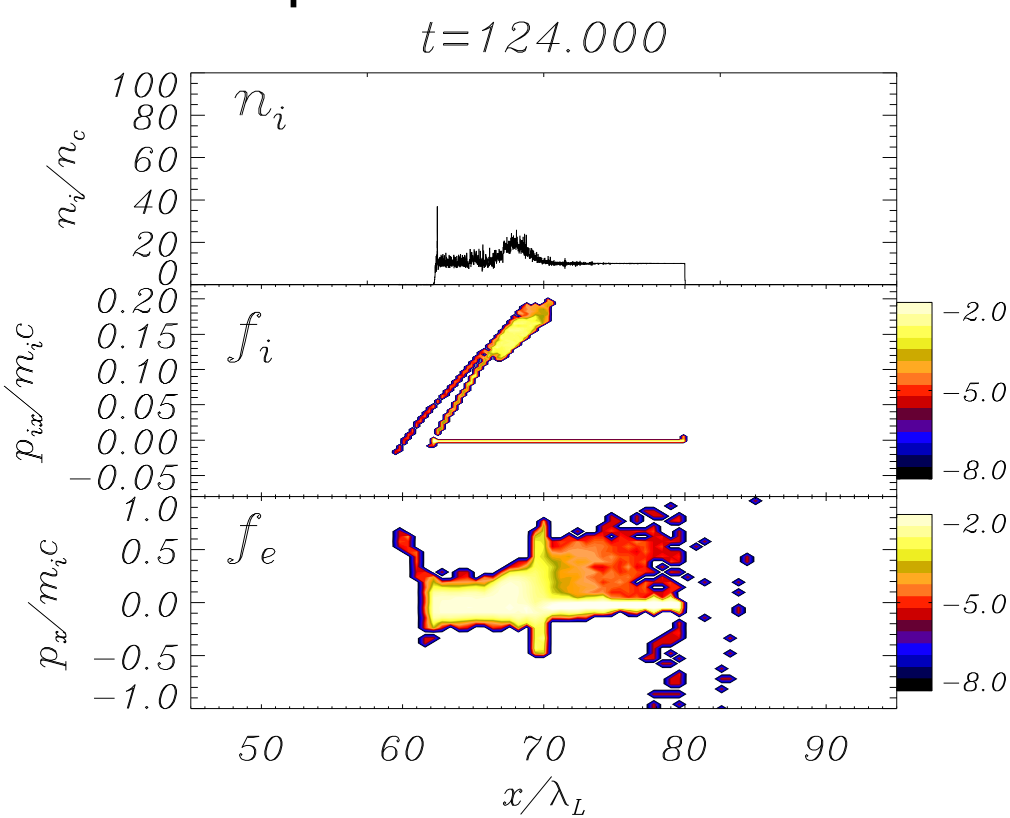

T. V. Liseikina and A. Macchi, arXiv:0705.4019, Appl. Phys. Lett. (in press).

Circular polarization

1D PIC simulation, circular polarization
$a = 11.3 \Rightarrow$ same energy of the linear polarization case; other parameters are the same

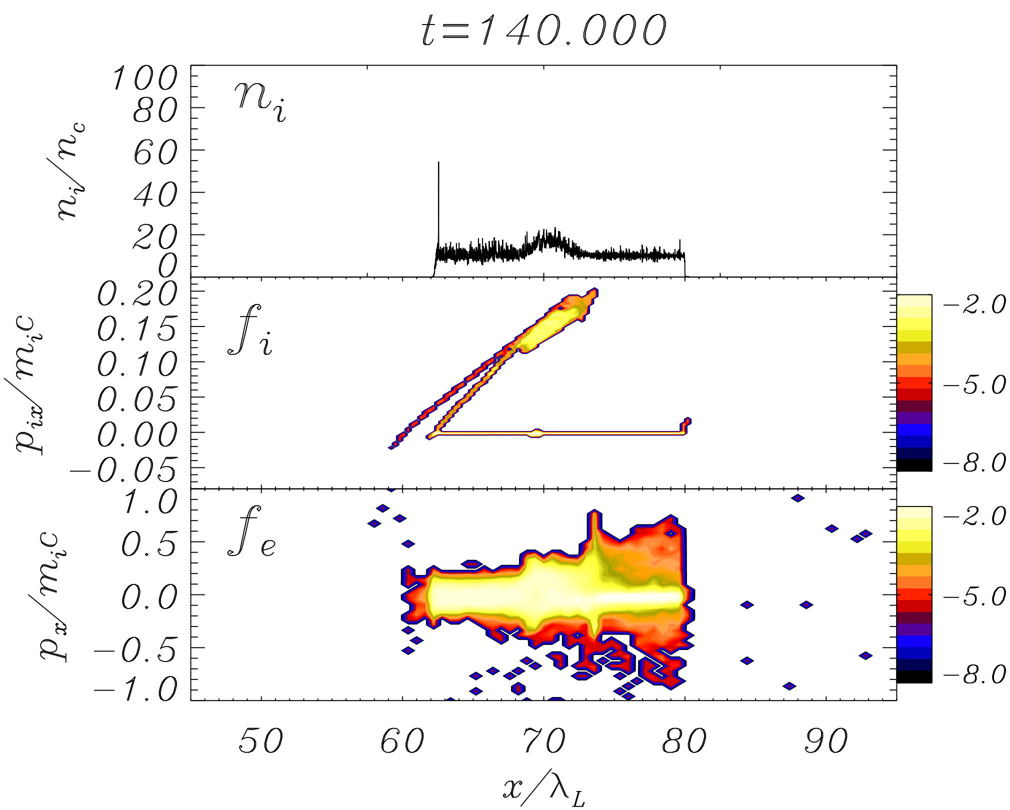

T. V. Liseikina and A. Macchi, arXiv:0705.4019, Appl. Phys. Lett. (in press).

Circular polarization

1D PIC simulation, circular polarization
$a = 11.3 \Rightarrow$ same energy of the linear polarization case;
other parameters are the same

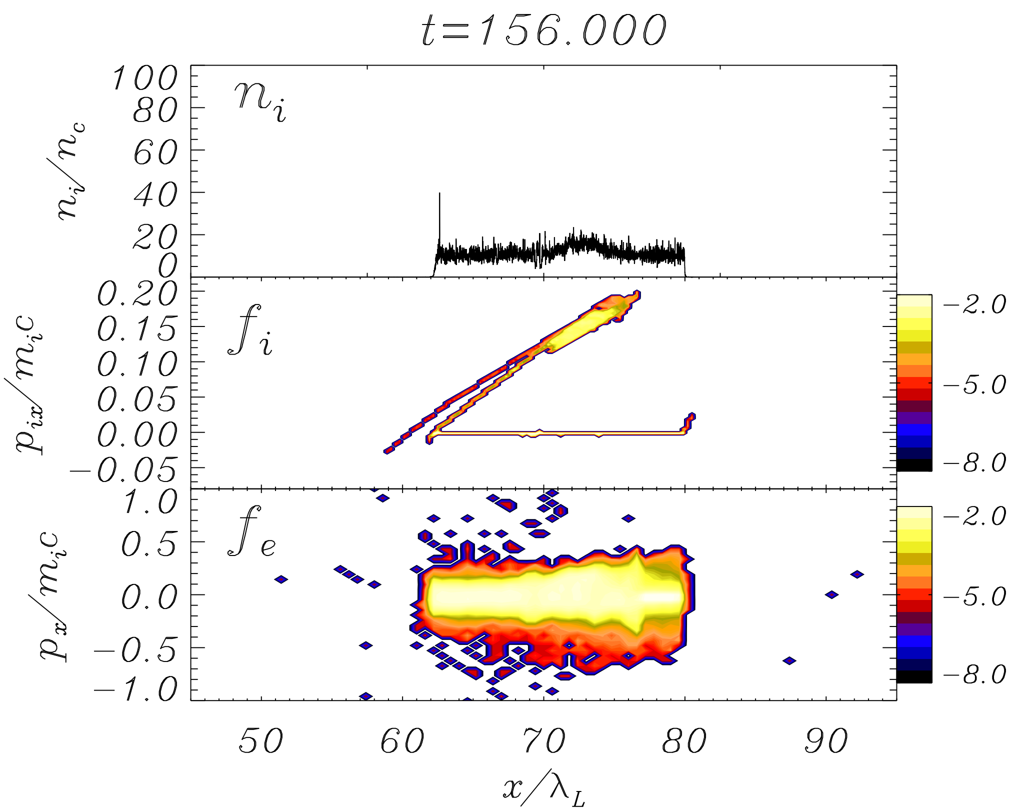

T. V. Liseikina and A. Macchi, arXiv:0705.4019, Appl. Phys. Lett. (in press).

Circular polarization

1D PIC simulation, circular polarization
$a = 11.3 \Rightarrow$ same energy of the linear polarization case;
other parameters are the same

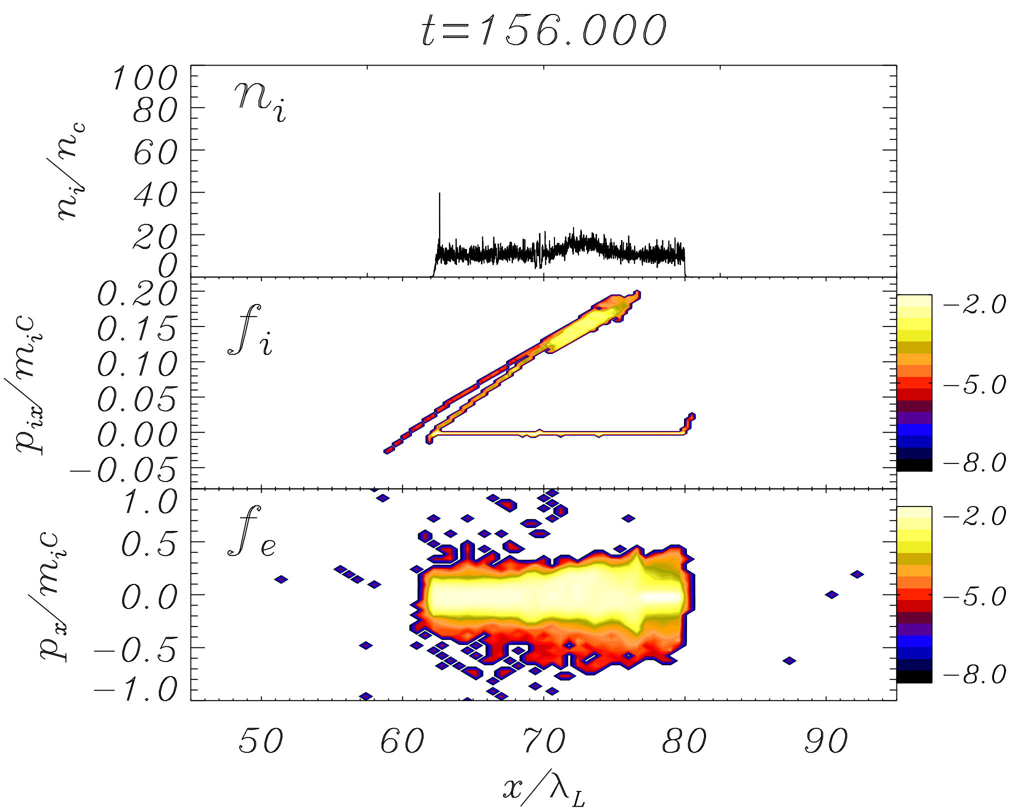

Only one group of MeV ions accelerated at the front side

T. V. Liseikina and A. Macchi, arXiv:0705.4019, Appl. Phys. Lett. (in press).

Circular polarization

1D PIC simulation, circular polarization
$a = 11.3 \Rightarrow$ same energy of the linear polarization case; other parameters are the same

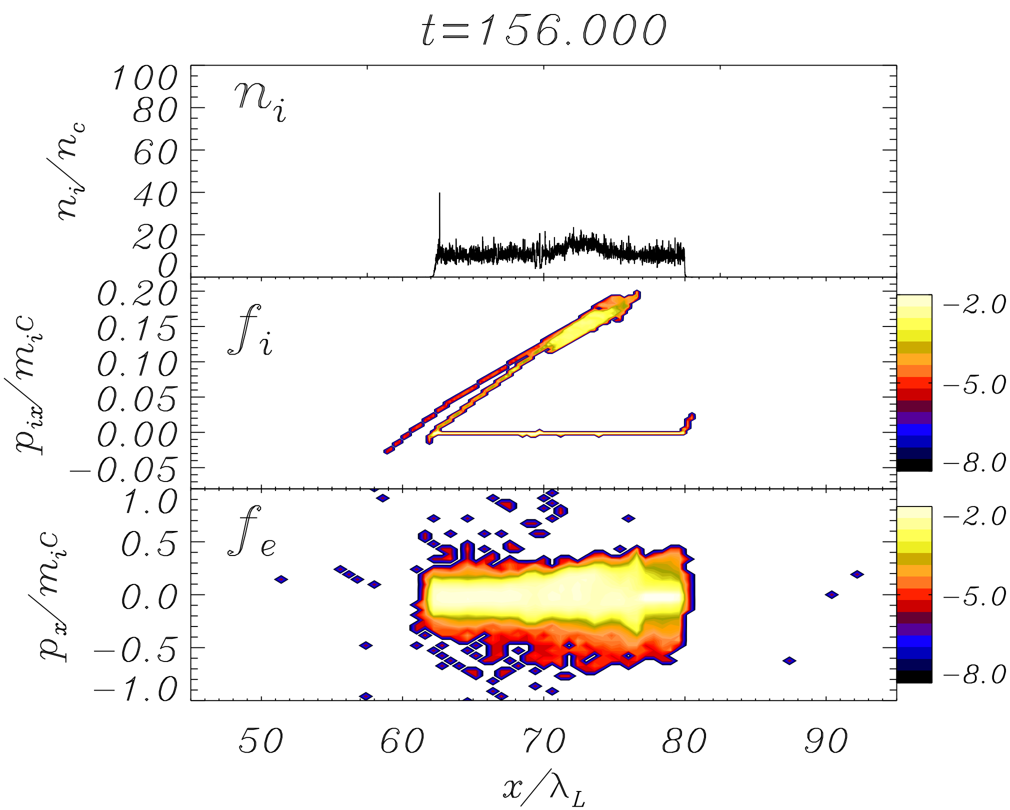

Only one group of MeV ions accelerated at the front side

Electron energy is below 1 MeV; almost no “fast” electrons!

T. V. Liseikina and A. Macchi, arXiv:0705.4019, Appl. Phys. Lett. (in press).

Absorption efficiency: circular vs linear

Absorption efficiency: circular vs linear

Ion acceleration with circular polarization promises high efficiency: 13.7% absorption for the simulation shown.
Absorption into electrons is negligible

T. V. Liseikina and A.Macchi, arXiv:0705.4019, Appl. Phys. Lett. (in press).

Absorption efficiency: circular vs linear

Ion acceleration with circular polarization promises high efficiency: 13.7% absorption for the simulation shown.
Absorption into electrons is negligible

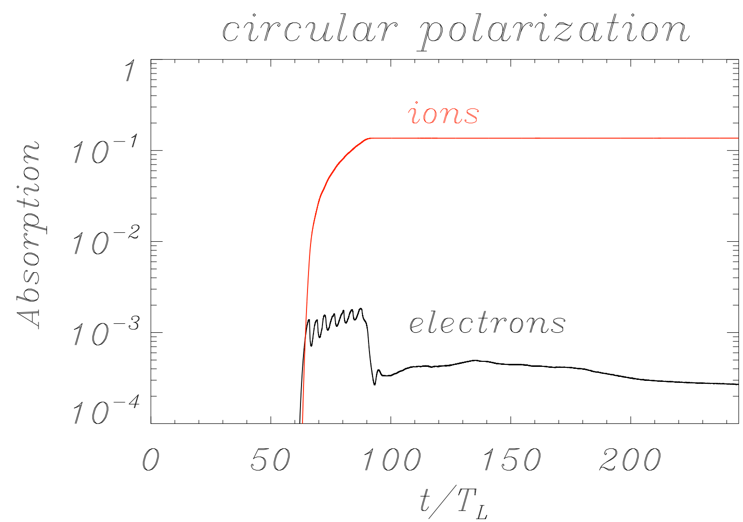

T. V. Liseikina and A.Macchi, arXiv:0705.4019, Appl. Phys. Lett. (in press).

Absorption efficiency: circular vs linear

Ion acceleration with circular polarization promises high efficiency: 13.7% absorption for the simulation shown.
Absorption into electrons is negligible

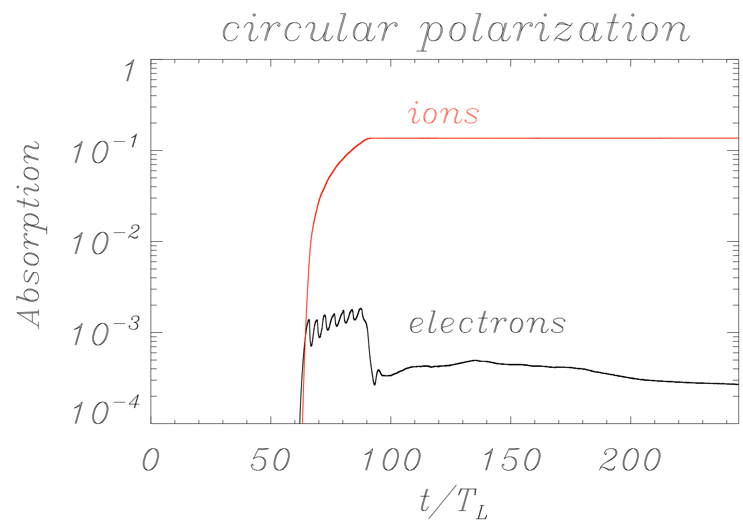

The simulation for same energy, linear polarization shows comparable absorption, but reached later, dependent on target thickness, and into several ion populations

T. V. Liseikina and A.Macchi, arXiv:0705.4019, Appl. Phys. Lett. (in press).

Absorption efficiency: circular vs linear

Ion acceleration with circular polarization promises high efficiency: 13.7% absorption for the simulation shown.
Absorption into electrons is negligible

The simulation for same energy, linear polarization shows comparable absorption, but reached later, dependent on target thickness, and into several ion populations

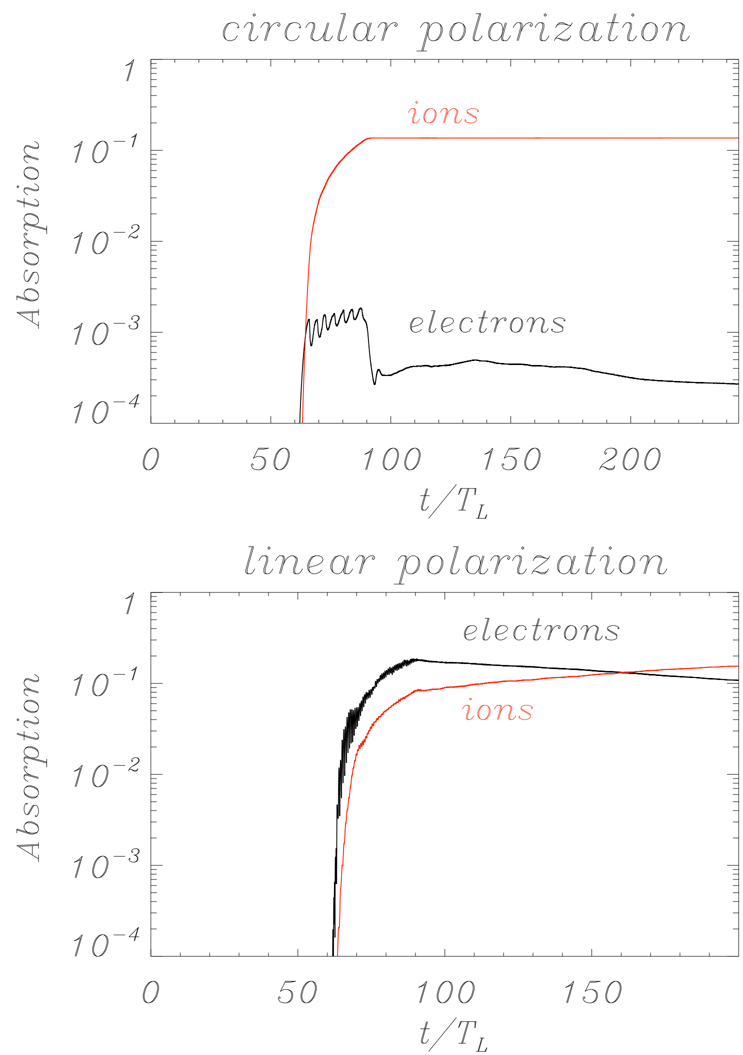

T. V. Liseikina and A.Macchi, arXiv:0705.4019, Appl. Phys. Lett. (in press).

Energy spectrum: circular vs linear

Energy spectrum: circular vs linear

Linear polarization: higher peak energies, but a thermal-like spectrum already in 1D.

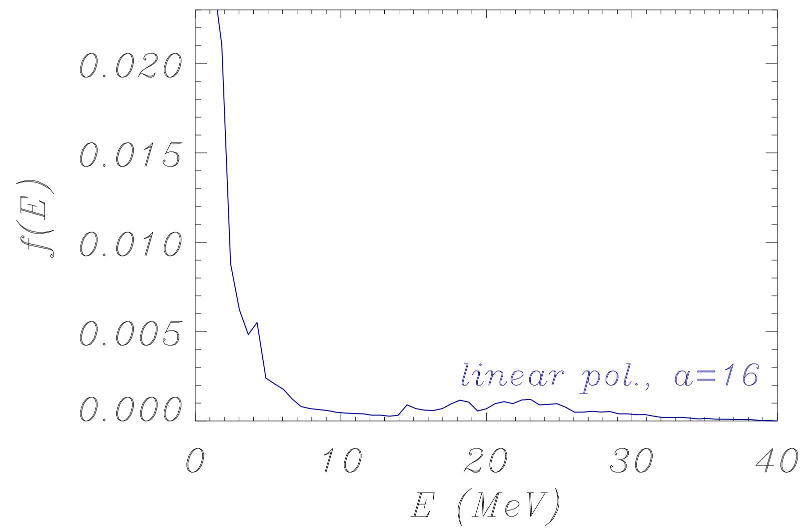

T. V. Liseikina and A.Macchi, arXiv:0705.4019, Appl. Phys. Lett. (in press).

Energy spectrum: circular vs linear

Linear polarization: higher peak energies, but a thermal-like spectrum already in 1D.

Circular polarization: lower peak energies, but a peaked, highly non-thermal spectrum.

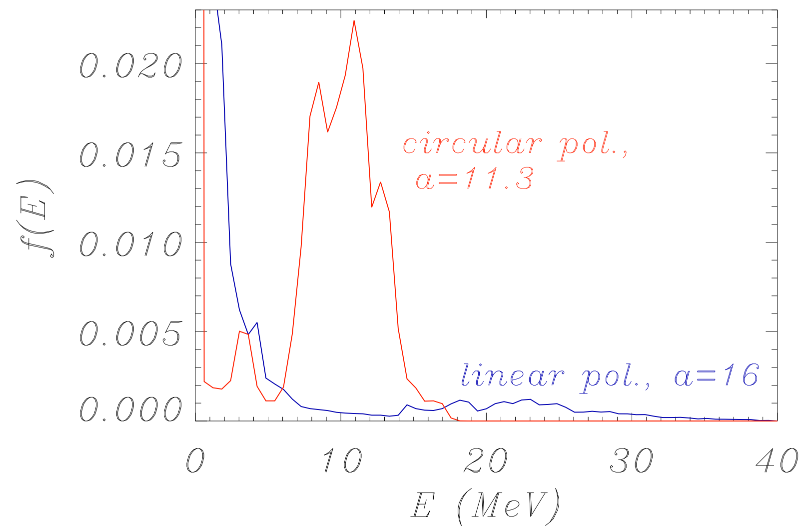

T. V. Liseikina and A.Macchi, arXiv:0705.4019, Appl. Phys. Lett. (in press).

Energy spectrum: circular vs linear

Linear polarization: higher peak energies, but a thermal-like spectrum already in 1D.

Circular polarization: lower peak energies, but a peaked, highly non-thermal spectrum.

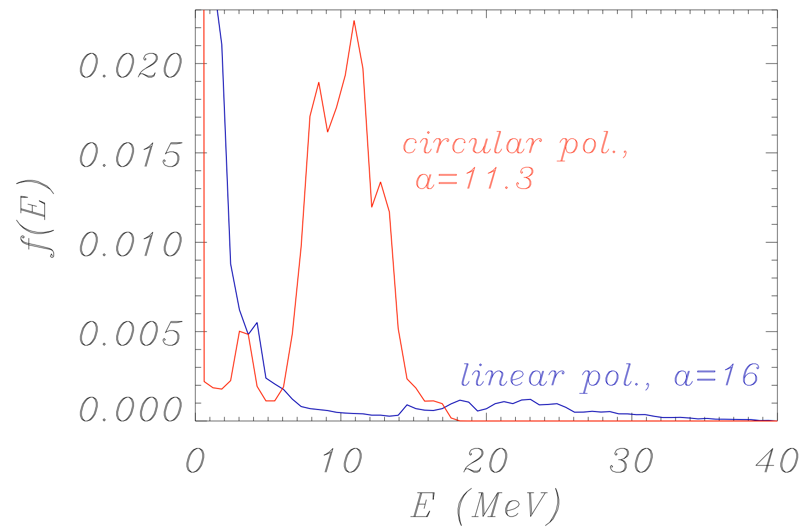

2D simulations confirm 1D results an show energy-dependent angular spread with low divergence

T. V. Liseikina and A.Macchi, arXiv:0705.4019, Appl. Phys. Lett. (in press).

Energy spectrum: circular vs linear

Linear polarization: higher peak energies, but a thermal-like spectrum already in 1D.

Circular polarization: lower peak energies, but a peaked, highly non-thermal spectrum.

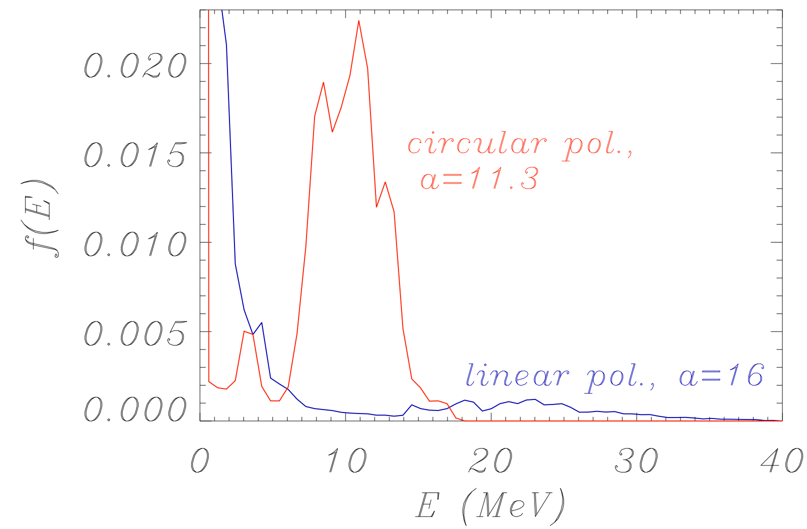

2D simulations confirm 1D results an show energy-dependent angular spread with low divergence

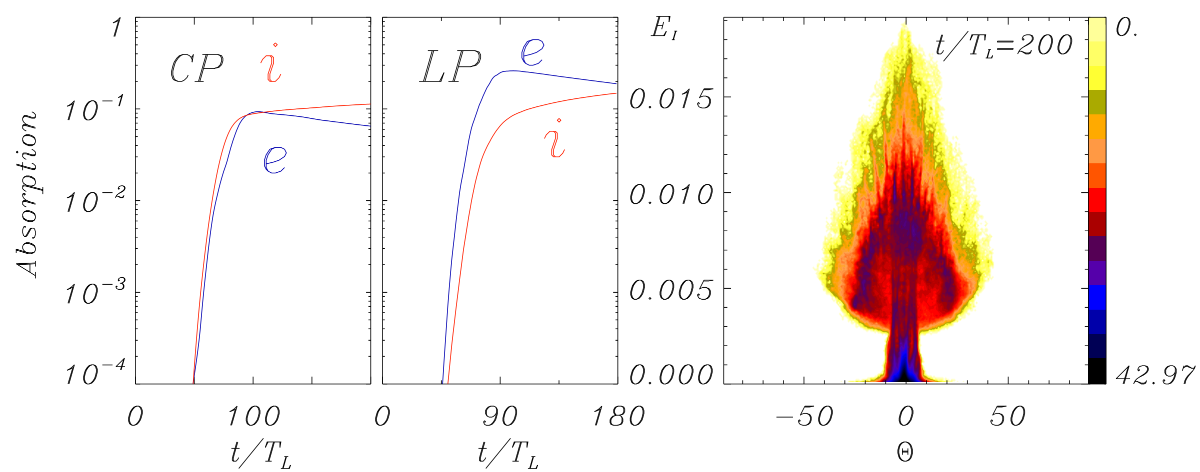

T. V. Liseikina and A.Macchi, arXiv:0705.4019, Appl. Phys. Lett. (in press).

Ion bunch acceleration

Ion bunch acceleration

Circular polarization, but weaker ($a = 2.0$) and shorter (20 fs) pulse now: $n_{e0}/n_c = 5$

Ion bunch acceleration

Circular polarization, but weaker ($a = 2.0$) and shorter (20 fs) pulse now: $n_{e0}/n_c = 5$

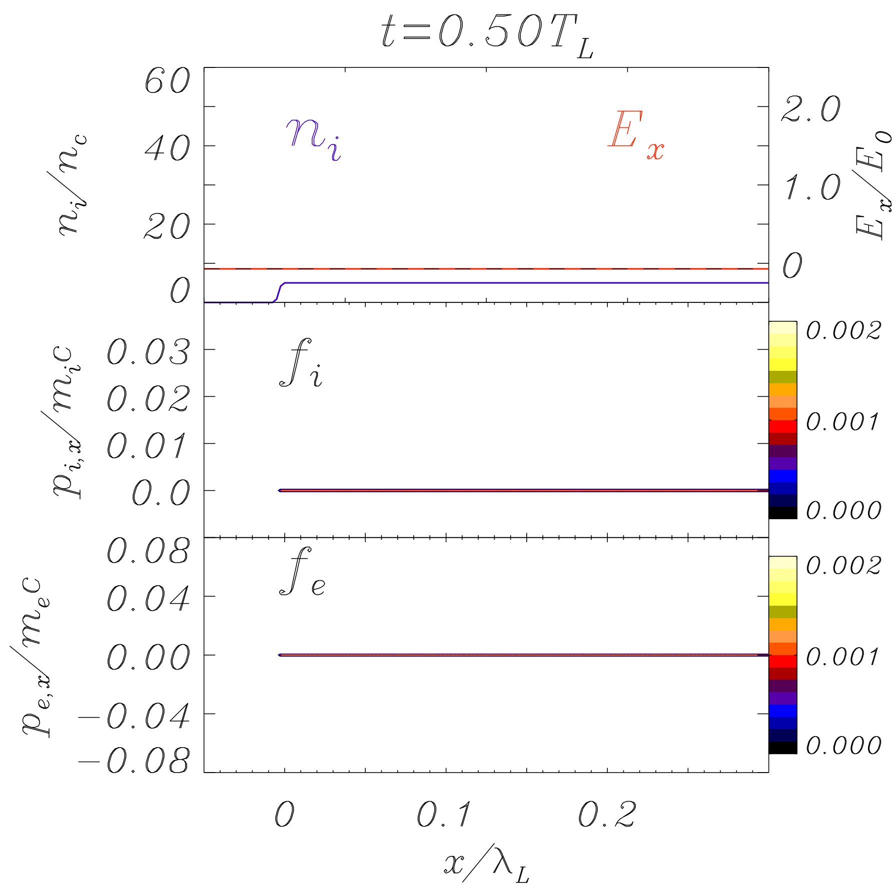

Ion bunch acceleration

Circular polarization, but weaker ($a = 2.0$) and shorter (20 fs) pulse now: $n_{e0}/n_c = 5$

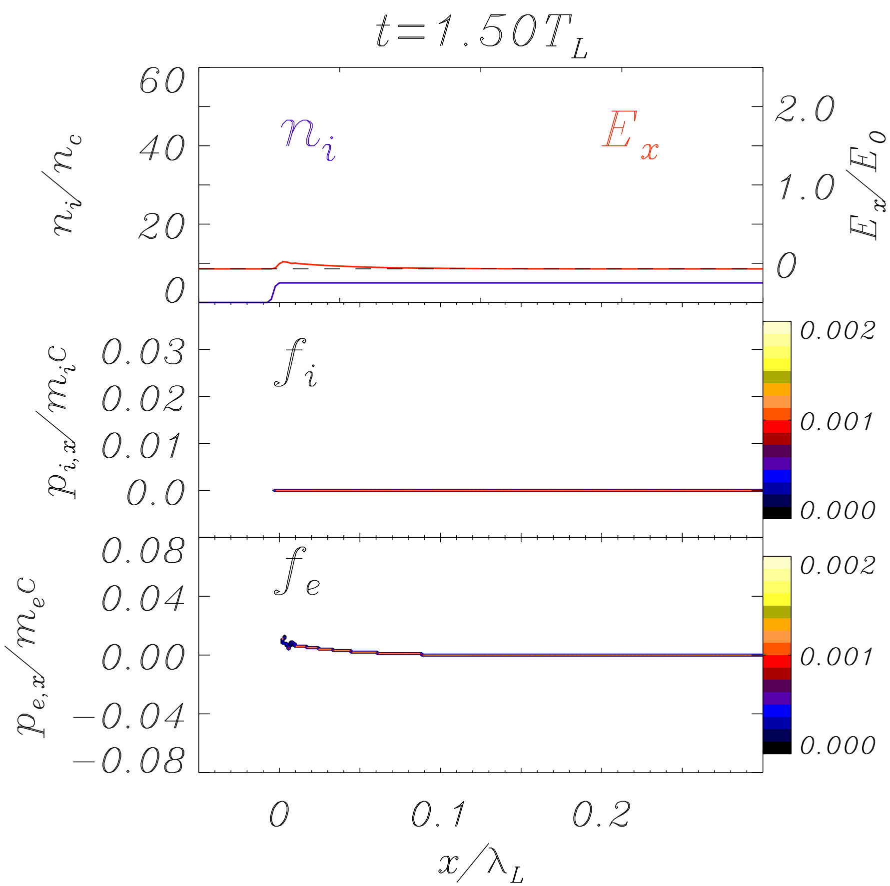

Ion bunch acceleration

Circular polarization, but weaker ($a = 2.0$) and shorter (20 fs) pulse now: $n_{e0}/n_c = 5$

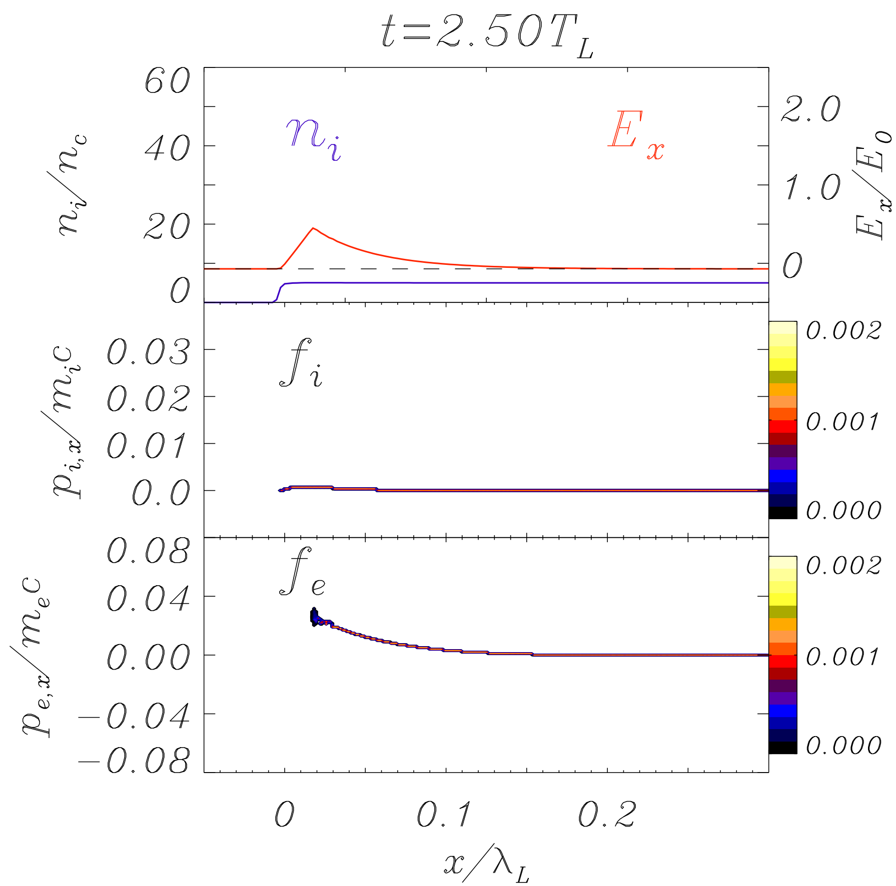

Ion bunch acceleration

Circular polarization, but weaker ($a = 2.0$) and shorter (20 fs) pulse now: $n_{e0}/n_c = 5$

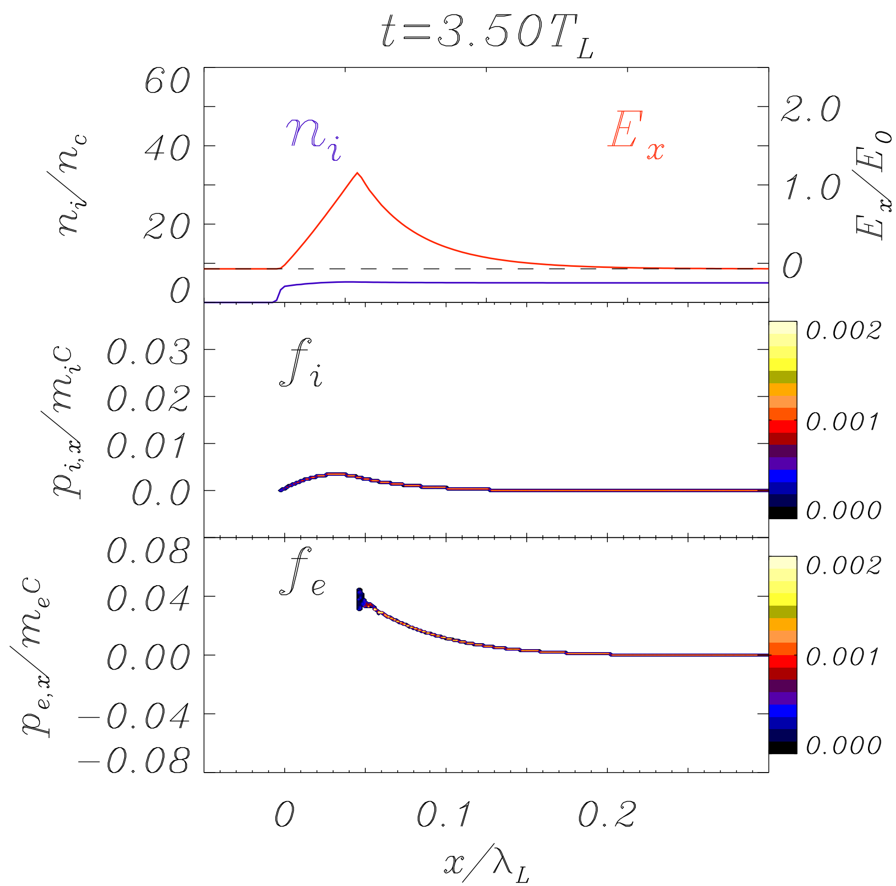

Ion bunch acceleration

Circular polarization, but weaker ($a = 2.0$) and shorter (20 fs) pulse now: $n_{e0}/n_c = 5$

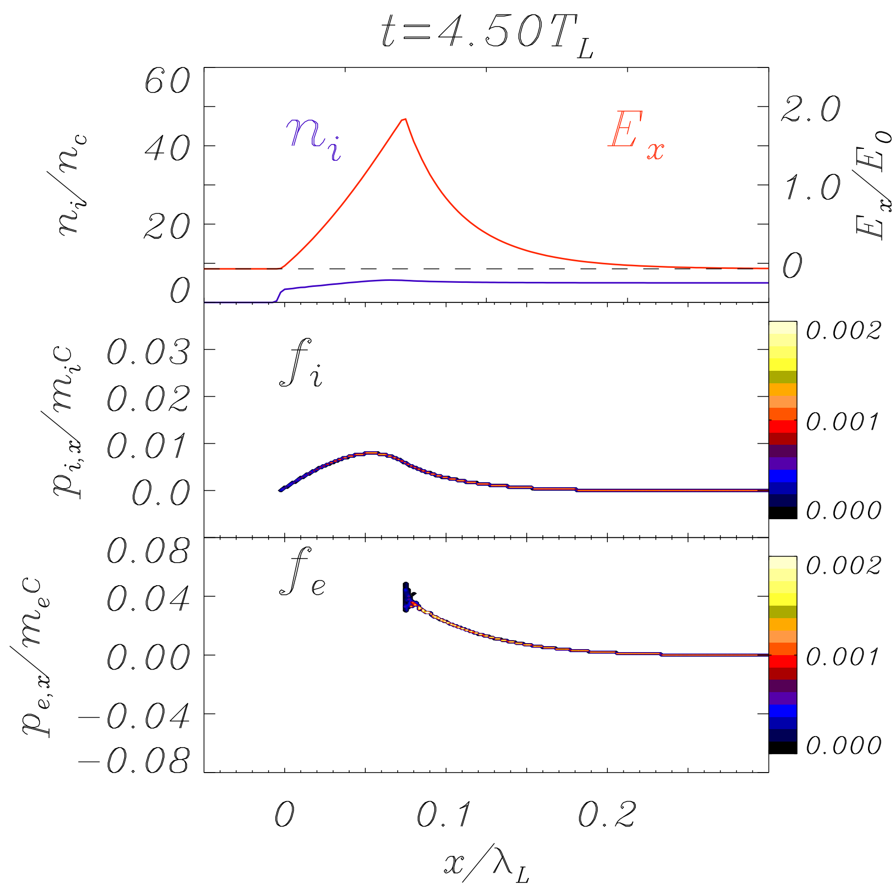

Ion bunch acceleration

Circular polarization, but weaker ($a = 2.0$) and shorter (20 fs) pulse now: $n_{e0}/n_c = 5$

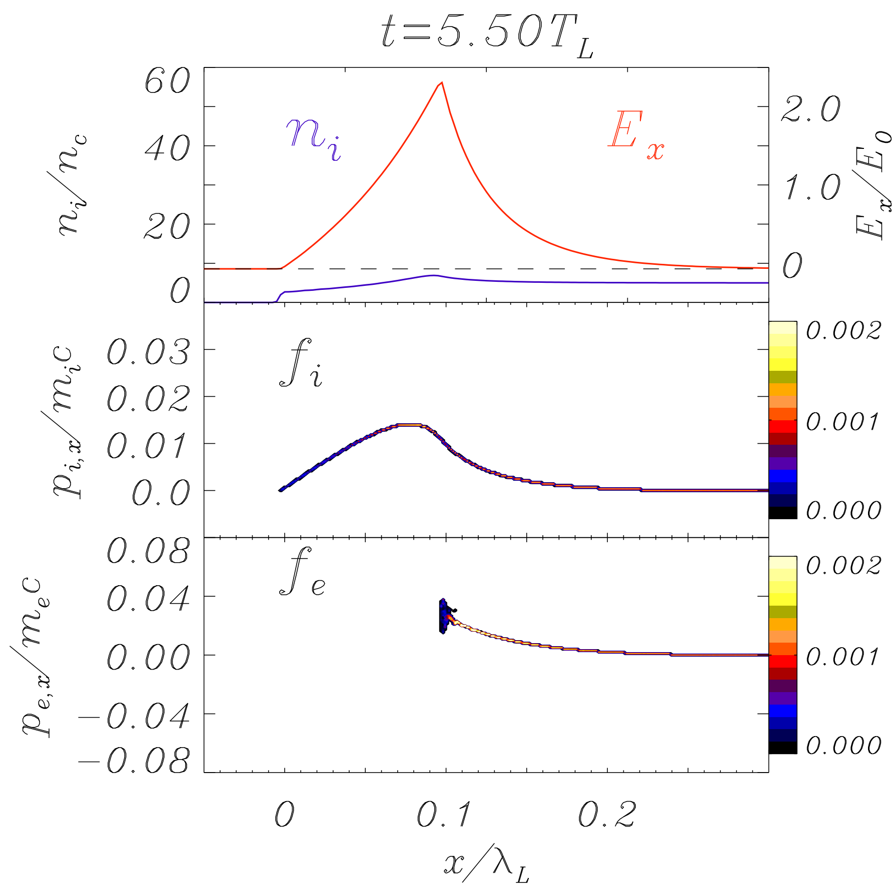

Electrostatic field E_x accelerates ions

Ion bunch acceleration

Circular polarization, but weaker ($a = 2.0$) and shorter (20 fs) pulse now: $n_{e0}/n_c = 5$

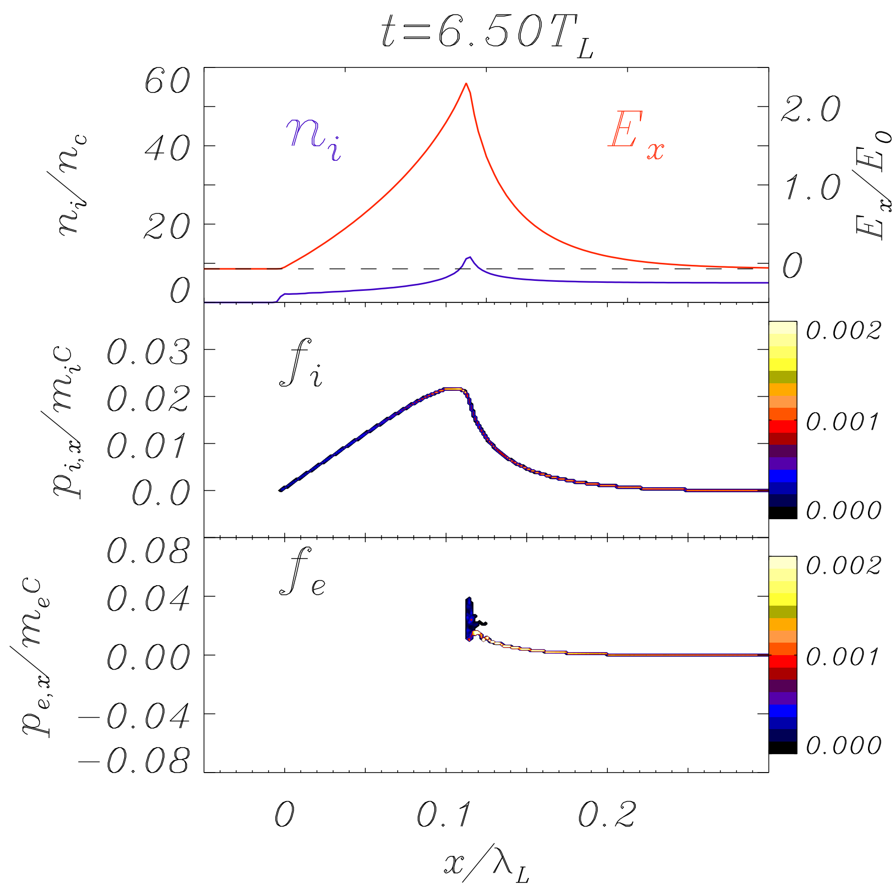

Electrostatic field E_x accelerates ions

Ion bunch acceleration

Circular polarization, but weaker ($a = 2.0$) and shorter (20 fs) pulse now: $n_{e0}/n_c = 5$

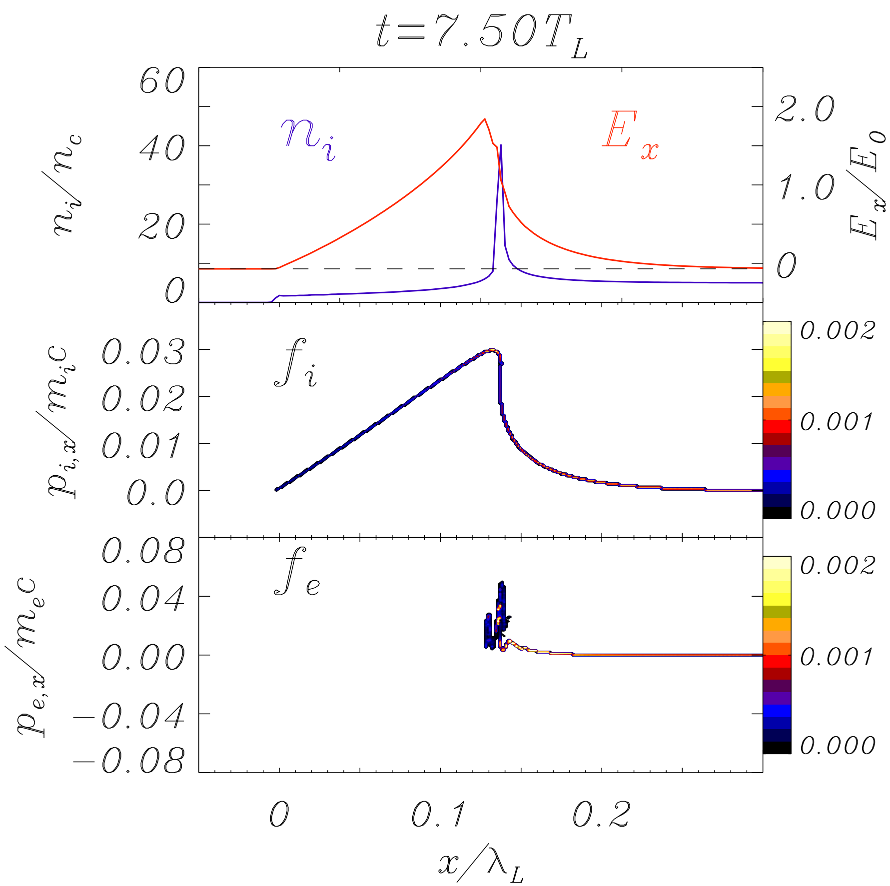

Electrostatic field E_x accelerates ions

Density spiking and breaking of the ion fluid

Ion bunch acceleration

Circular polarization, but weaker ($a = 2.0$) and shorter (20 fs) pulse now: $n_{e0}/n_c = 5$

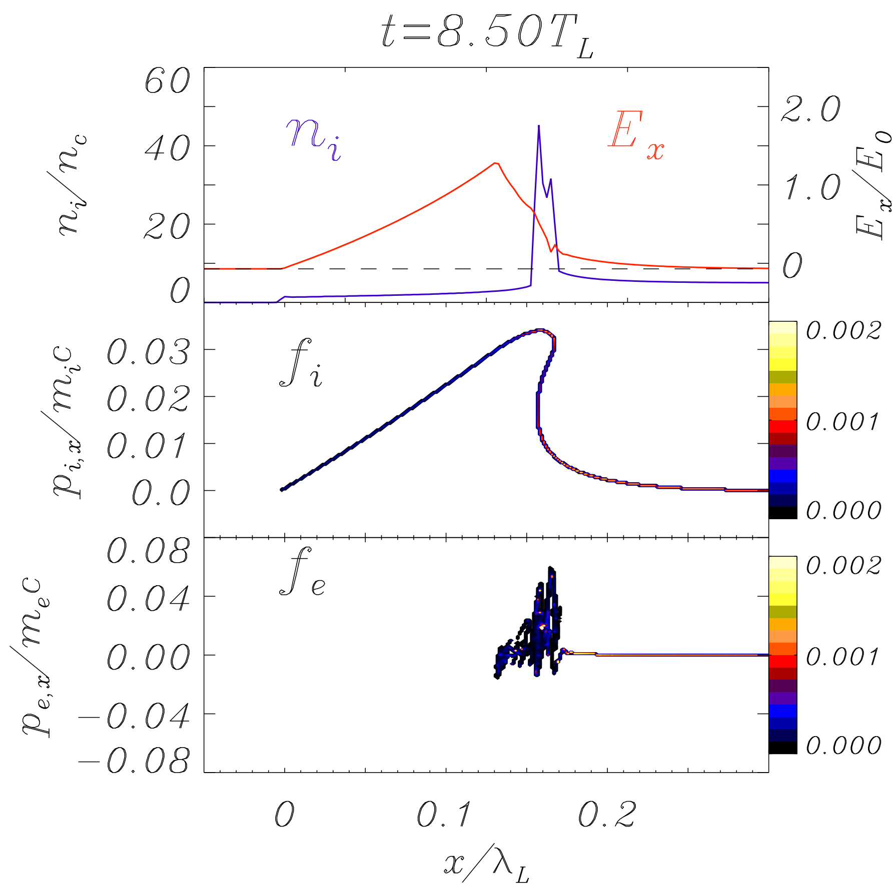

Electrostatic field E_x accelerates ions

Density spiking and breaking of the ion fluid

Production of a single ion bunch with narrow energy spectrum

Ion bunch acceleration

Circular polarization, but weaker ($a = 2.0$) and shorter (20 fs) pulse now: $n_{e0}/n_c = 5$

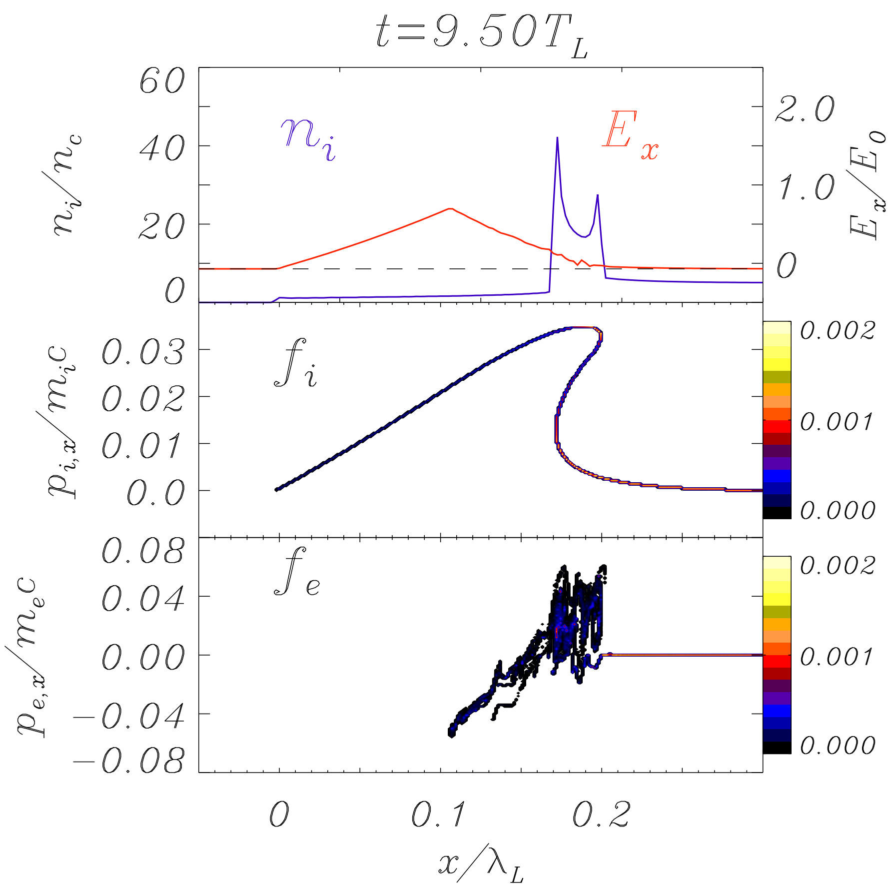

Electrostatic field E_x accelerates ions

Density spiking and breaking of the ion fluid

Production of a single ion bunch with narrow energy spectrum

Ion bunch acceleration

Circular polarization, but weaker ($a = 2.0$) and shorter (20 fs) pulse now: $n_{e0}/n_c = 5$

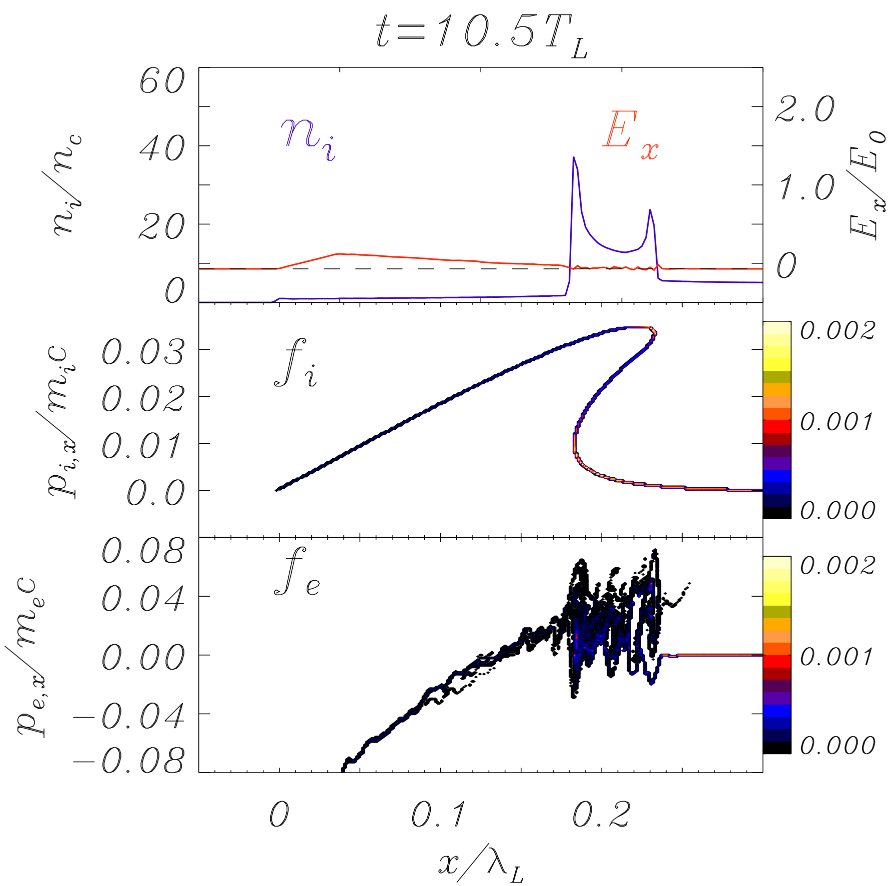

Electrostatic field E_x accelerates ions

Density spiking and breaking of the ion fluid

Production of a single ion bunch with narrow energy spectrum

Highly reminiscent of the radial dynamics in the underdense plasma case!

(Another) simple model

(Another) simple model

Assumption: quasi-equilibrium between electrostatic field and ponderomotive force (both *Lagrangian* constants).
Ions are accelerated by the electrostatic field until breaking.

(Another) simple model

Assumption: quasi-equilibrium between electrostatic field and ponderomotive force (both *Lagrangian* constants).
Ions are accelerated by the electrostatic field until breaking.

- We take simple profiles . . .

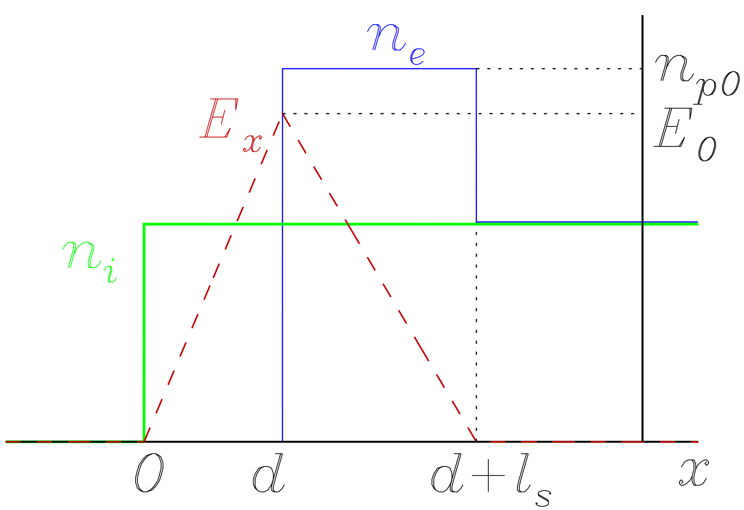

(Another) simple model

Assumption: quasi-equilibrium between electrostatic field and ponderomotive force (both *Lagrangian* constants).
Ions are accelerated by the electrostatic field until breaking.

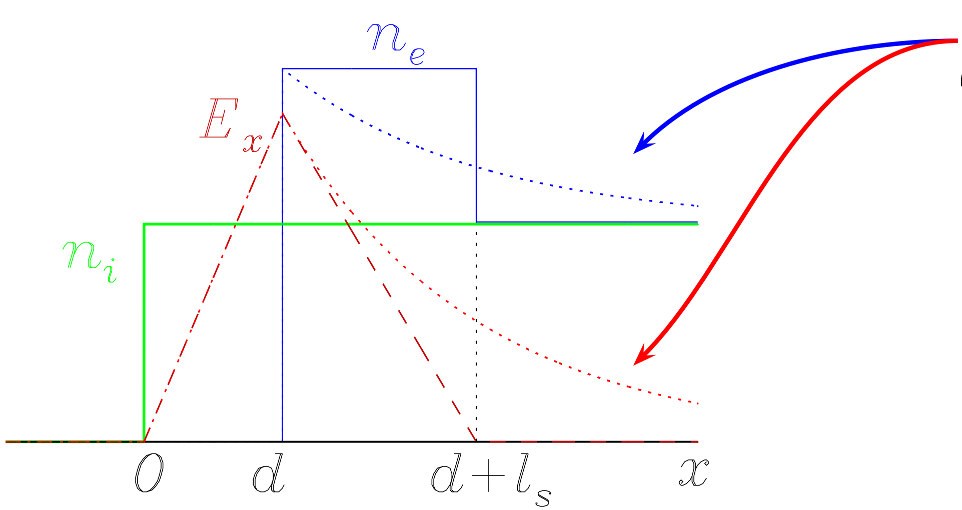

- We take simple profiles ...

... which crudely approximate "realistic" ones

(Another) simple model

Assumption: quasi-equilibrium between electrostatic field and ponderomotive force (both *Lagrangian* constants).
Ions are accelerated by the electrostatic field until breaking.

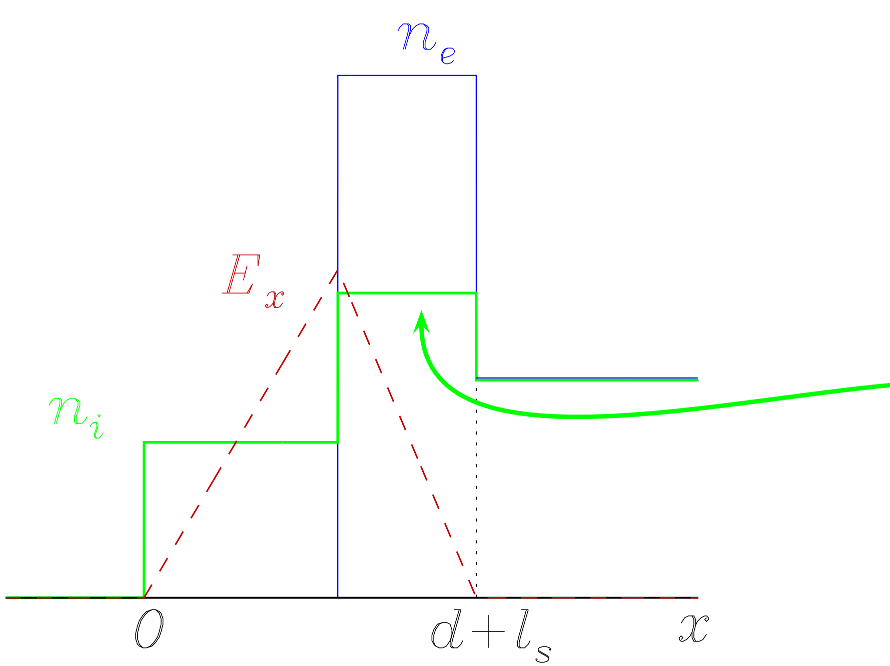

- We take simple profiles . . .

  . . . which crudely approximate "realistic" ones
- ion profile is compressed

(Another) simple model

Assumption: quasi-equilibrium between electrostatic field and ponderomotive force (both *Lagrangian* constants).
Ions are accelerated by the electrostatic field until breaking.

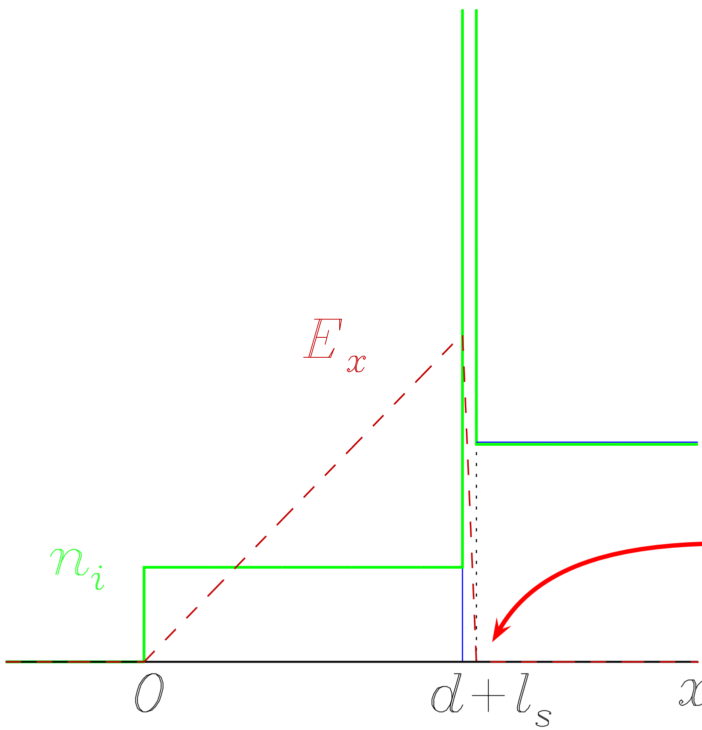

- We take simple profiles . . .

  . . . which crudely approximate "realistic" ones
- ion profile is compressed
- "breaking" at the time when all ions reach the evanescence point

Model predictions

Model predictions

- Input parameters d, E_0, n_{p0} are related by the Poisson equation and the constraints of charge conservation and total radiation pressure $P_{rad} \simeq 2I_L/c$:

Model predictions

- Input parameters d, E_0, n_{p0} are related by the Poisson equation and the constraints of charge conservation and total radiation pressure $P_{rad} \simeq 2I_L/c$:

$$E_0 = 4\pi e n_0 d\,, \qquad n_0(d+l_s) = n_{p0} l_s\,, \qquad \frac{1}{2} e E_0 n_{p0} l_s \simeq \frac{2}{c} I_L$$

Model predictions

- Input parameters d, E_0, n_{p0} are related by the Poisson equation and the constraints of charge conservation and total radiation pressure $P_{rad} \simeq 2I_L/c$:

$$E_0 = 4\pi e n_0 d\,, \qquad n_0(d + l_s) = n_{p0} l_s\,, \qquad \frac{1}{2} e E_0 n_{p0} l_s \simeq \frac{2}{c} I_L$$

- Equations of motion are easily solved to yield maximum ion velocity and breaking time, assuming $l_s \simeq c/\omega_p$:

Model predictions

- Input parameters d, E_0, n_{p0} are related by the Poisson equation and the constraints of charge conservation and total radiation pressure $P_{rad} \simeq 2I_L/c$:

$$E_0 = 4\pi e n_0 d \,, \qquad n_0(d + l_s) = n_{p0} l_s \,, \qquad \frac{1}{2} e E_0 n_{p0} l_s \simeq \frac{2}{c} I_L$$

- Equations of motion are easily solved to yield maximum ion velocity and breaking time, assuming $l_s \simeq c/\omega_p$:

$$v_m = 2c\sqrt{\frac{Z}{A}\frac{m_e}{m_p}\frac{n_c}{n_e}}a_L \qquad \tau_i \simeq T_L \frac{1}{2\pi a_L}\sqrt{\frac{A}{Z}\frac{m_p}{m_e}} \,.$$

Model predictions

- Input parameters d, E_0, n_{p0} are related by the Poisson equation and the constraints of charge conservation and total radiation pressure $P_{rad} \simeq 2I_L/c$:

$$E_0 = 4\pi e n_0 d \,, \qquad n_0(d+l_s) = n_{p0} l_s \,, \qquad \frac{1}{2} e E_0 n_{p0} l_s \simeq \frac{2}{c} I_L$$

- Equations of motion are easily solved to yield maximum ion velocity and breaking time, assuming $l_s \simeq c/\omega_p$:

$$v_m = 2c\sqrt{\frac{Z}{A}\frac{m_e}{m_p}\frac{n_c}{n_e}} a_L \qquad \tau_i \simeq T_L \frac{1}{2\pi a_L}\sqrt{\frac{A}{Z}\frac{m_p}{m_e}} \,.$$

- The average ion front velocity $v_f = v_m/2$ is the “hole boring” speed.

Model predictions

- Input parameters d, E_0, n_{p0} are related by the Poisson equation and the constraints of charge conservation and total radiation pressure $P_{rad} \simeq 2I_L/c$:

$$E_0 = 4\pi e n_0 d\,, \qquad n_0(d+l_s) = n_{p0} l_s\,, \qquad \frac{1}{2} e E_0 n_{p0} l_s \simeq \frac{2}{c} I_L$$

- Equations of motion are easily solved to yield maximum ion velocity and breaking time, assuming $l_s \simeq c/\omega_p$:

$$v_m = 2c\sqrt{\frac{Z}{A}\frac{m_e}{m_p}\frac{n_c}{n_e}}a_L \qquad \tau_i \simeq T_L \frac{1}{2\pi a_L}\sqrt{\frac{A}{Z}\frac{m_p}{m_e}}\,.$$

- The average ion front velocity $v_f = v_m/2$ is the “hole boring” speed.

  Similar predictions, but different physics with respect to the “shock” acceleration picture

Conclusions of Part 2

Conclusions of Part 2

- The use of circular polarization leads to a new regime of "radiation-pressure-dominated" ion acceleration

Conclusions of Part 2

- The use of circular polarization leads to a new regime of "radiation-pressure-dominated" ion acceleration
- Ion acceleration features may be interesting for specific applications (creation of warm dense matter?)

Conclusions of Part 2

- The use of circular polarization leads to a new regime of “radiation-pressure-dominated” ion acceleration
- Ion acceleration features may be interesting for specific applications (creation of warm dense matter?)
- Other recent works suggest that using very thin targets extremely high energies may be produced

  (see Zhang et al, Phys. Plasmas **14**, 073101 (2007); Robinson et al, arXiv:0708.2050)

Conclusions of Part 2

- The use of circular polarization leads to a new regime of "radiation-pressure-dominated" ion acceleration
- Ion acceleration features may be interesting for specific applications (creation of warm dense matter?)
- Other recent works suggest that using very thin targets extremely high energies may be produced

  (see Zhang et al, Phys. Plasmas **14**, 073101 (2007); Robinson et al, arXiv:0708.2050)
- Ion acceleration in this regime can be illustrated by a simple model, which accounts for ion "bunch" fomation via hydrodynamical breaking

A general conclusion . . .

A general conclusion . . .

- During a stay in Darmstadt (end of 1999), Prof. Peter Mulser suggested me to work on a problem of breaking of (electron) plasma waves driven by laser-plasma interactions

A general conclusion . . .

- During a stay in Darmstadt (end of 1999), Prof. Peter Mulser suggested me to work on a problem of breaking of (electron) plasma waves driven by laser-plasma interactions
- This work has never been finalized :-(

A general conclusion . . .

- During a stay in Darmstadt (end of 1999), Prof. Peter Mulser suggested me to work on a problem of breaking of (electron) plasma waves driven by laser-plasma interactions
- This work has never been finalized :-(
- It was my destiny to eventually realize that hydrodynamical breaking is a very basic and important phenomenon in laser-plasma interaction, although in a different context

A general conclusion . . .

- During a stay in Darmstadt (end of 1999), Prof. Peter Mulser suggested me to work on a problem of breaking of (electron) plasma waves driven by laser-plasma interactions
- This work has never been finalized :-(
- It was my destiny to eventually realize that hydrodynamical breaking is a very basic and important phenomenon in laser-plasma interaction, although in a different context